# Regulation of intracellular trafficking

# by UNC-50 and the GARP complex

# in *C. elegans*

**PhD Thesis**

In partial fulfilment of the requirements

for the degree "Doctor of Philosophy (PhD)"

in the Neuroscience Program

at the Georg August University Göttingen,

Faculty of Biology

**Submitted by**

**Ling Luo**

**Born in**

Xin Yu, China

**2010**

**Thesis committee:**

Prof. Dr. Erwin Neher,      Max Planck Institute for Biophysical Chemistry

Dr. Stefan Eimer,      European Neuroscience Institute

Prof. Dr. Fred Wouters,      Physiology, Göttingen University

**Declaration**


I hereby declare that the PhD thesis entitled, "Regulation of intracellular trafficking by UNC-50 and the GARP complex in *C. elegans*", was written independently and with no other sources and aids than quoted.



Göttingen, 4th June, 2010



------------------------------------------

       Ling Luo

# List of contents

# Acknowledgements

First, I would like to thank my supervisor Dr. Stefan Eimer for giving me the opportunity to work in his lab. I would not have finished my PhD project without his patient supervision during the last four years, as well as his continuous support and encouragement during my difficult times.

I also thank my thesis committee members Professor Erwin Neher and Professor Fred Wouters for their useful advices and support for my project.

I thank all colleagues in my lab for sharing the wonderful four years with me: Marija, Nikhil, Christian, Nora, Mandy, and Maike. Working with you guys is a great experience. I thank Jan for your nice EM pictures, Katrin and Sabine for your excellent technique assistance to my experiments.

I would like to thank all the classmates from the Neuroscience Program. It was excellent to have one year of master course with you guys. Special thanks go to Chen Ye, who shared the flat and life with me for the last three years, and Bao Jin, who often prepare delicious dishes for us during the weekends. Friendships with you guys are never forgettable.

I would like to thank Professor Michael Hörner and Sandra Drube from the Neuroscience program coordination office for their endless support during my master and PhD years.

Last but not least, I would not have survived the four years of PhD without the support of my family. Love, understanding and encouragement from my wife Yanan always keep me motivated, no matter we live together or not. My lovely daughter Maobei is my ultimate source of happiness. Every time I think of your bubbly face and babbling, all those negative emotions disappear immediately.

# I Abbreviation list

ACh – acetylcholine

nAChR – nicotinic acetylcholine receptor

AD – Alzheimer's disease

ADAM – a disintegrin and metalloprotease

AP – adaptor protein

ARF – ADP-ribosylation factor

ARL – ARF-like

BAR domain – Bin/Amphiphysin/Rvs domain

BWM – body wall muscle

CCV – clathrin-coated vesicle

CI-MPR – cation-independent mannose-6-phosphate receptor

COG complex – conserved oligomeric Golgi complex

CPY – carboxypeptidase Y

DI domain – disintegrin domain

DIC – differential interference contrast

DTC – distal tip cell

DTT – Dithiothreitol

EGTA – ethylene glycol tetraacetic acid

EHD – Eps-15 homology domain

epsinR – epsin-related

ER – endoplasmic reticulum

ERAD – ER-associated degradation

ERGIC – ER-Golgi intermediate compartment

GABA – gamma-amino butyric acid

GAP – GTPase activating protein

GARP complex– Golgi associated retrograde protein complex

GEF – guanine nucleotide exchange factor

GGA – *Golgi*-associated, *Gamma*-adaptin homology, *ARF* binding proteins

HPF EM – high pressure freeze electron microscopy

IPTG – isopropyl β-D-thiogalactopyranoside

KIF – kinesin superfamily

MP domain – metalloprotease domain

MPR – mannose 6-phosphate receptor

MuSK – muscle-specific tyrosine kinase

MVB – multivesicular body

NDPase – nucleoside diphosphatase

NGM – nematode growth medium

NMJ – neuromuscular junction

PLAC domain – protease and lacunin domain

PVC – prevacuolar compartment

PX domain – phox domain

PtdIns(3,5)$P_2$ – phosphatidylinositol 3,5-biphosphate

RTK – receptor tyrosine kinase

SNARE – soluble NSF attachment protein receptor

SNX – sorting nexin

TGN – trans-Golgi network

TM domain – transmembrane domain

# II Summary

Fast synaptic transmission at the neuromuscular junctions (NMJs) in *C. elegans* is mediated by the neurotransmitter acetylcholine which activates ligand-gated ion channels of the nicotinic acetylcholine receptor (nAChR) family at the postsynaptic membrane. UNC-50 is a conserved integral Golgi membrane protein that has been shown to be critical for the plasma membrane transport of a specific AChR. However, the function of UNC-50 during AChR transport is not known yet. In this study, we use synthetic lethality analysis to genetically map the function of UNC-50. We show that mutations in *unc-50* are lethal specifically in combination with mutations in factors that are involved in retrograde transport from endosomes to Golgi, like the Golgi associated retrograde protein (GARP) complex. This indicates that UNC-50 is also involved in retrograde transport from endosomes to Golgi. Furthermore, in *unc-50* mutants we found defective gonad morphology which is caused by the aberrant migration of the gonadal distal tip cell (DTC). This defect is caused by the mistrafficking of the metalloprotease MIG-17. MIG-17 is normally secreted from the body wall muscles and anchored at the gonadal basement membrane to direct the migration of DTCs. This suggests that MIG-17, like the AChR, is mistrafficked in *unc-50* mutants at the Golgi-endosomal interface.

In order to understand the process of retrograde trafficking from endosomes to the Golgi, we functionally characterized the GARP complex in *C. elegans*. We show that the GARP complex has four subunits: VPS-52, VPS-53, VPS-54 and a novel metazoan subunit VPS-51. GARP mutants are viable but show lysosomal defects. We demonstrate that GARP subunits bind a specific set of Golgi SNAREs, suggesting that the GARP complex supports tethering to multiple Golgi domains.

# III Introduction

## 2.1 Neurotransmission at the *C. elegans* neuromuscular junction

Fast excitatory synaptic transmission at the neuromuscular junction (NMJ) in nematode *C. elegans* is mediated by the neurotransmitter acetylcholine (ACh), while inhibitory neurotransmission at the NMJ is mediated by the neurotransmitter gamma-amino butyric acid (GABA). *C. elegans* is a nice model system for studying protein functions on regulating synaptic transmission, because it has a relatively simple and well-described cell organization of motor system (Figure 1). A typical NMJ in *C. elegans* is shown in Figure 2. The body wall muscle sends muscle arms to contact both cholinergic and GABAergic motor neuron axons, forming functional synapses, NMJs. There are both excitatory and inhibitory innervations for the NMJs. The excitatory transmission is mediated by nicotinic acetylcholine receptors (nAChRs) and the inhibitory transmission is mediated by $GABA_A$ receptors (Figure 3). *C. elegans* move forward and backward by propagating sine waves along their bodies. This is achieved by constantly alternating contraction and relaxation of the body wall muscles. For example, cholinergic motor neurons activate the ventral body wall muscles by releasing acetylcholine, while they simultaneously activate inhibitory GABAergic motor neurons that project axons to the dorsal body wall muscles, leading to their relaxation (Figure 4) (Walrond and Stretton, 1985a; Walrond and Stretton, 1985b). Thus, by contracting body wall muscles on one side and relaxing body wall muscles on the other side, the worms can achieve the sine wave locomotion.

**A**



**B**
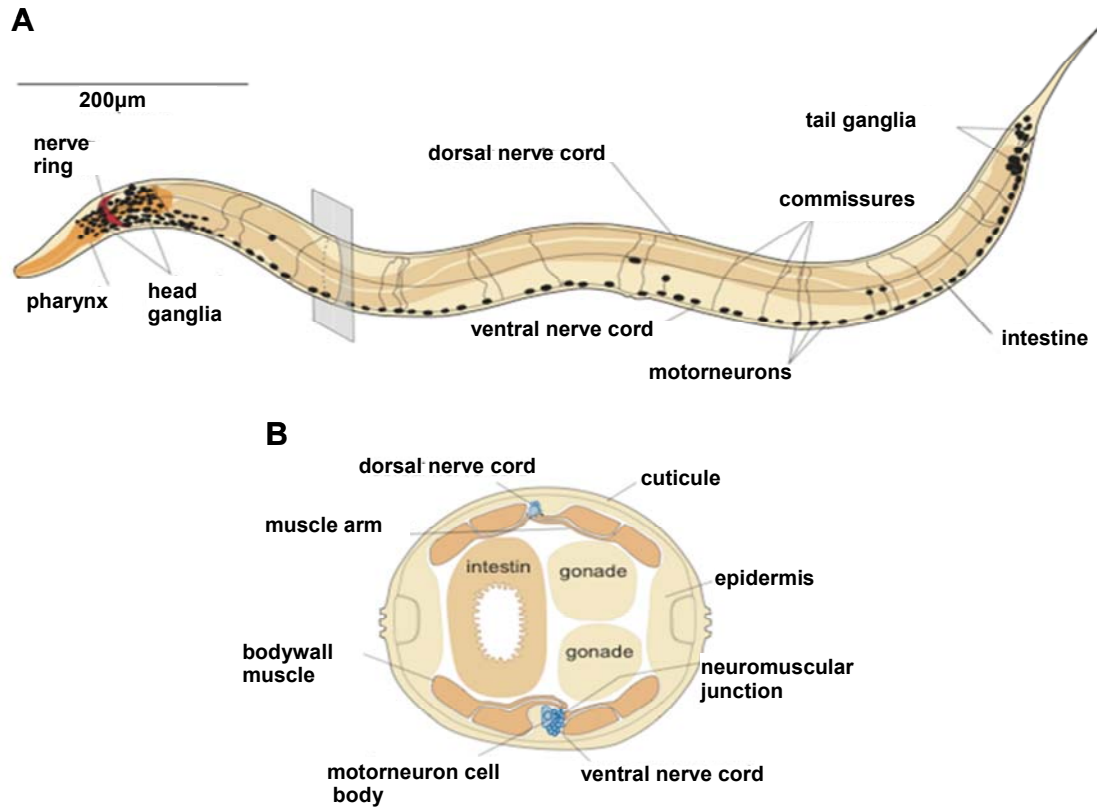


**Figure 1. Cell organization of the motor system in *C. elegans***

(A) The ventral nerve cord contains cell bodies of the motor neurons. The motor neurons send processes to the dorsal side of the body, forming the dorsal nerve cord, which stretches along the body and forms synapses with the dorsal body wall muscles.

(B) The body wall muscles line as quadrants along the dorsal and ventral side of the worm. The body wall muscles send muscle arms to the nerve cords to form functional synapses-the neuromuscular junctions (NMJs).
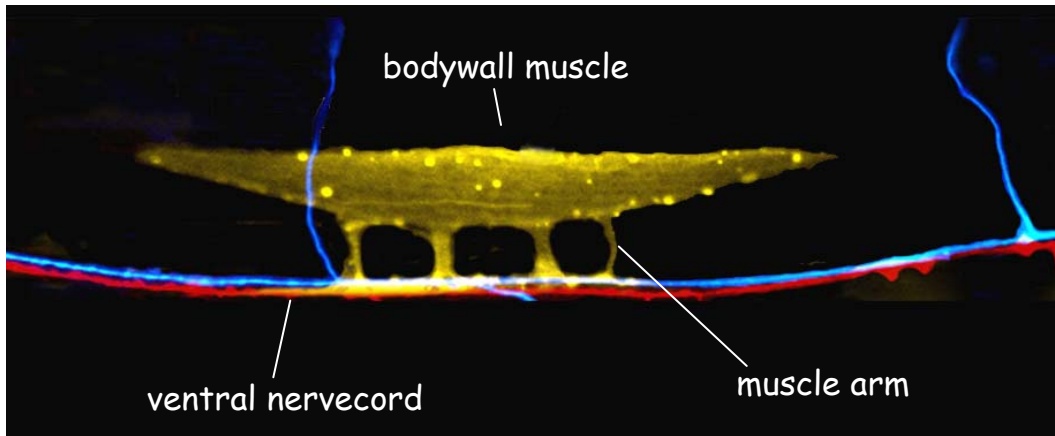
**Figure 2. NMJ in *C. elegans***

Body wall muscles send muscle arms to contact nerve cords. Both cholinergic (red lines) and GABAergic (blue lines) innervations on body wall muscles are shown. (Modified from Scott J. Dixon and Peter J. Roy's picture)
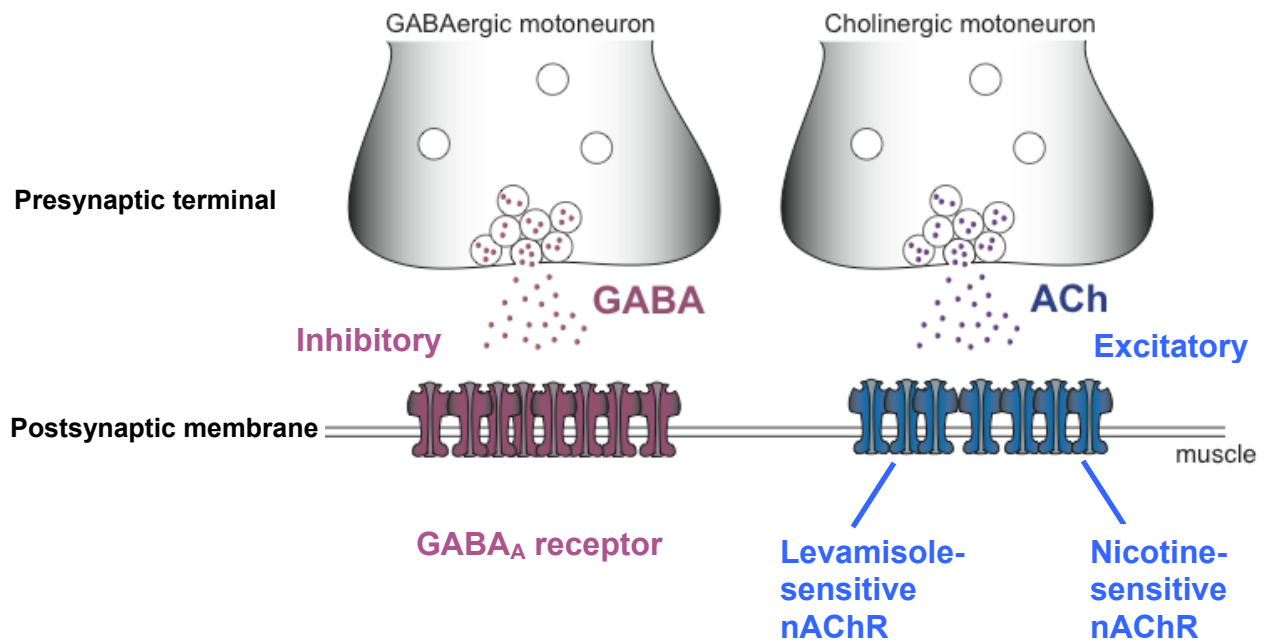


**Figure 3. Molecular architecture of *C. elegans* NMJ**

At the NMJ, inhibitory GABAergic transmission is mediated by $GABA_A$ receptor. Excitatory cholinergic innervations are mediated by two types of nicotinic acetylcholine receptors (nAChRs): levamisole-sensitive nAChRs and nicotine-sensitive nAChRs.
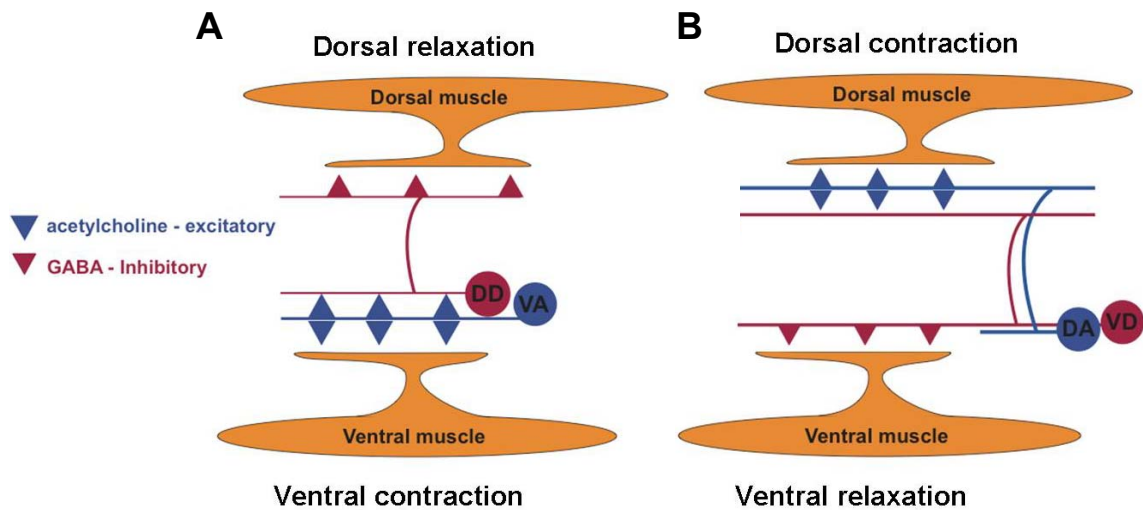
**Figure 4. Neuronal control of locomotion in *C. elegans***

*C. elegans* move in a sine wave manner. This is achieved by cycles of two-step actions: A) Cholinergic motor neurons activate the ventral body wall muscles by releasing acetylcholine, while they simultaneously activate inhibitory GABAergic motor neurons that relax the dorsal body wall muscles. B) Cholinergic motor neurons activate the dorsal body wall muscles by releasing acetylcholine, while they simultaneously activate inhibitory GABAergic motor neurons that relax the ventral body wall muscles.

## 2.2 Two types of nAChRs at the *C. elegans* NMJ

Cholinergic transmission at the *C. elegans* NMJ is mediated by two types of nAChRs at the postsynaptic membrane: one type of nAChR can be selectively activated by the anthelmintic drug levamisole, while the other type of receptor can be selectively activated by the nAChR agonist nicotine. The levamisole-sensitive nAChRs are heteropentamers composed of α-subunits UNC-38, UNC-63 and non-α subunits UNC-29, LEV-1 (Figure 5A) (Culetto et al., 2004; Fleming et al., 1997; Richmond and Jorgensen, 1999). In contrast, the nicotine-sensitive

nAChRs are homopentamers that consist of five α7-like subunits encoded by *acr-16* (Francis et al., 2005; Touroutine et al., 2005) (Figure 5A). Levamisole receptor subunits UNC-29, UNC-38, UNC-63 and LEV-1 were initially found in a genetic screen for mutants that are resistant to cholinergic agonist levamisole (Culetto et al., 2004; Fleming et al., 1997; Lewis et al., 1980b). "*unc*" stands for uncoordinated locomotion phenotype, since deletion of nAChRs impairs neurotransmission from the motor neurons to the body wall muscles, thus causing under-excitation of the muscles (Lewis et al., 1980b). The two types of receptors are pharmacologically different. The levamisole-sensitive nAChR contains two ACh binding sites, while the nicotine-sensitive nAChR contains five ACh binding sites (Figure 5A). Both receptor types can also be distinguished by their electrophysiological properties. When evoked with ACh, nicotine-sensitive receptor currents exhibit much larger amplitude and faster desensitization than levamisole-sensitive receptor currents (Figure 5B) (Touroutine et al., 2005).

**A**



**Levamisole-sensitive nAChR**          **Nicotine-sensitive nAChR**
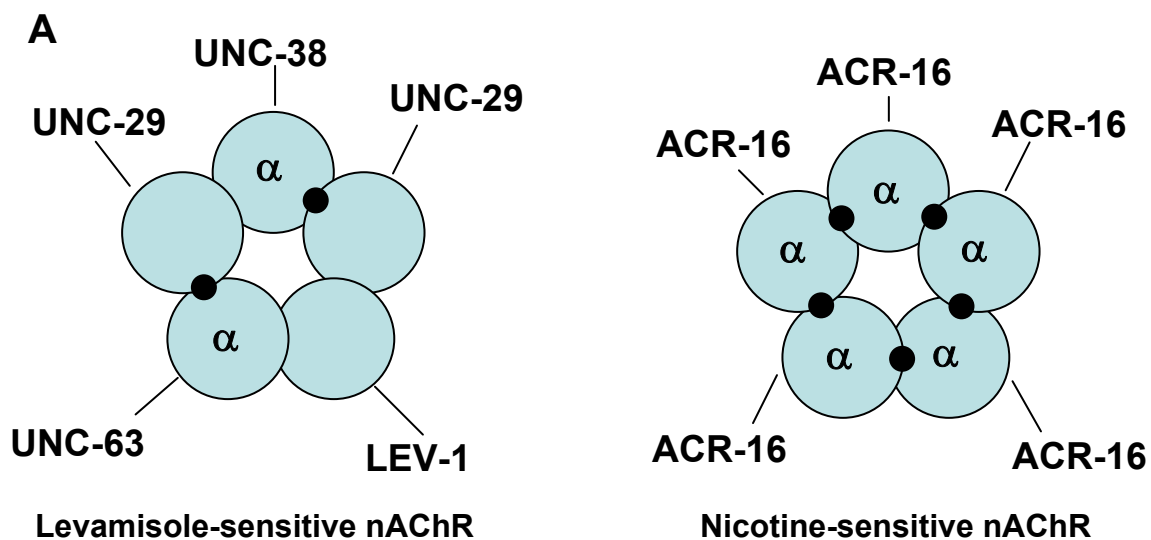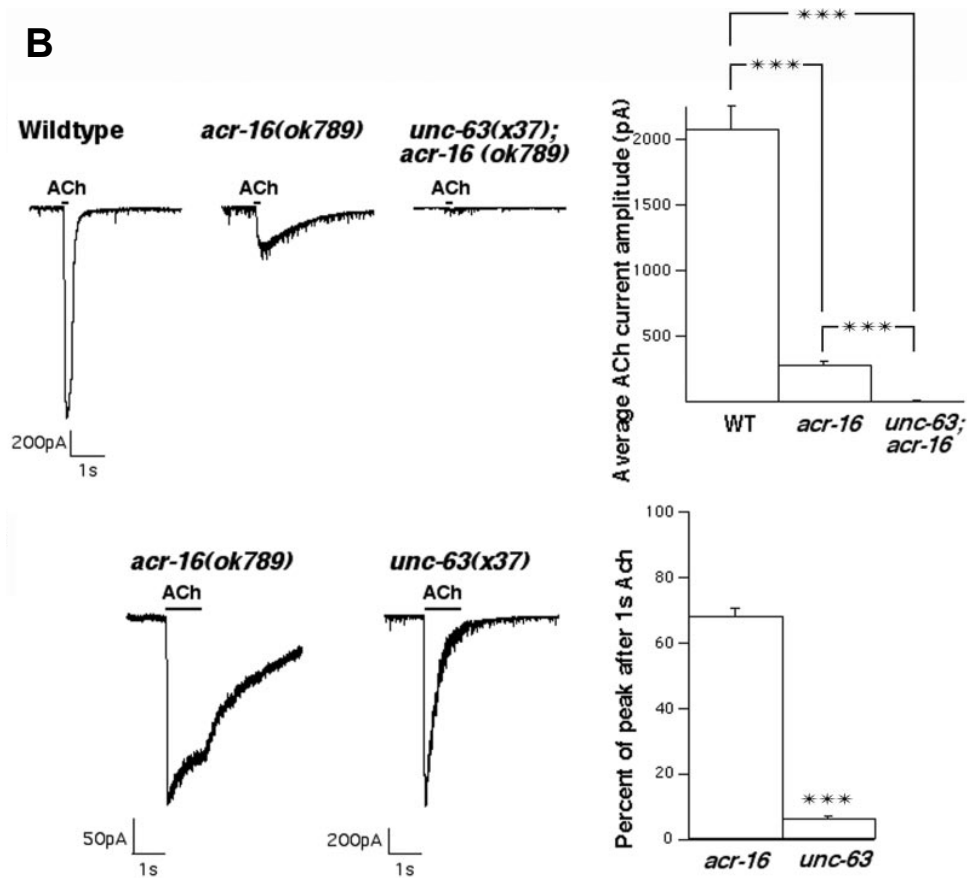
**Figure 5. Different characteristics of the two types of nAChRs at the *C. elegans* NMJ**

(A) Levamisole-sensitive nAChRs are heteropentamers consisting of UNC-38, UNC-63, UNC-29 and LEV-1. Nicotine-sensitive nAChRs are homopentamers composed of five ACR-16 subunits. α subunit indicates subunit that bind ACh molecules. Levamisole-sensitive nAChR has two ACh binding sites, while ACR-16 receptor has five ACh binding sites.

(B) Upper panel: ACR-16 receptor mediated currents count for 80% of the total ACh current amplitude, while the levamisole receptors conduct the rest 20%. The muscle ACh current in *unc-63*(*x37*);*acr-16*(*ok789*) double mutants was completely eliminated. Lower panel: Levamisole-sensitive nAChR mediated currents exhibited desensitization at a much slower rate than the nicotine-sensitive nAChR mediated currents. (Touroutine et al., 2005)

## 2.3 nAChRs are involved in various cell functions

Although G-protein coupled muscarinic-type acetylcholine receptors and acetylcholine-gated chloride channels were also reported (Culotti and Klein, 1983; Putrenko et al., 2005), the majority of acetylcholine receptors are pentameric ligand-gated cation channels. nAChRs belong to a large superfamily of Cys-loop ion channel receptors, which also include GABA, glycine and serotonin (5-HT) receptors (Corringer et al., 2000). The structure of nAChR has been determined. nAChR is assembled from a ring of five homologous subunits and divided into three distinct domains: a large N-terminal extracellular ligand binding domain, a membrane spanning pore, and a smaller intracellular domain (Figure 6) (Unwin, 2005). nAChR subunits that contain two cysteine residues at positions analogous to Cys192 and Cys193 in the Torpedo α-subunit, have been classified as α-type subunits (Millar and Gotti, 2009). Although α-subunits are supposed to be agonist binding subunits, recent studies showed that nicotinic agonists bind at the interfaces between an α and non-α subunit. Therefore, both α and non-α subunits contribute to agonist binding sites (Sine, 2002). A total of 17 distinct nAChRs subunits were identified in vertebrates and they are predominantly expressed in neurons and muscles. The α1, β1, γ, δ, and ε subunits were found in vertebrate muscle, while α2-α10, β2-β4 are normally found in neurons (Albuquerque et al., 2009). Although some nAChR subunits, like the α7 subunit, can form homopentameric receptors, most nAChRs are heteropentamers composed of both α and non-α subunits (Millar and Gotti, 2009).
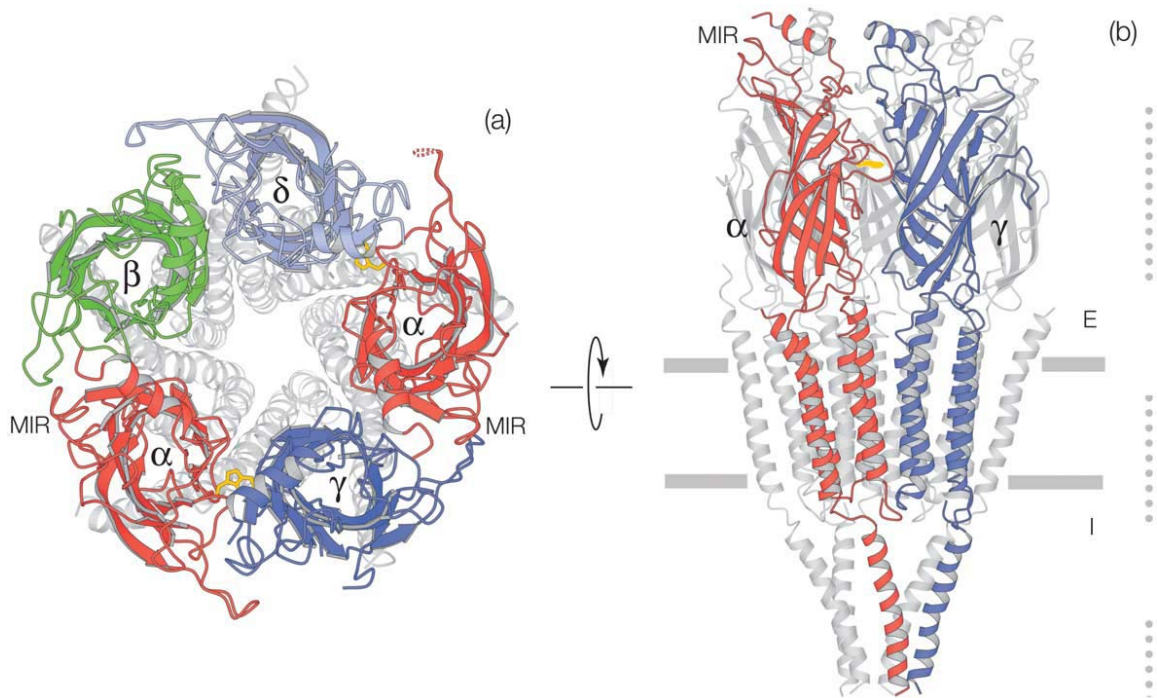
**Figure 6. Structure of nAChR**

A typical muscle nAChR contains five subunits: two α-subunits and β,γ,δ-subunits. There are two acetylcholine binding sites in the nAChR. One lays between α-subunit and γ-subunit, the other lays between α-subunit and δ-subunit. Each subunit can be divided into three functional domains: a large N-terminal extracellular ligand binding domain, a membrane spanning pore, and a smaller intracellular domain. (Unwin, 2005)

In the peripheral nervous system, nAChRs are mainly distributed on the NMJs, where they activate muscles. nAChRs are also ubiquitously expressed in the central nervous system (Albuquerque et al., 1997; Tribollet et al., 2004). In hippocampus, α7 subunit containing nAChRs are highly expressed (Seguela et al., 1993; Zarei et al., 1999). Hippocampal nAChRs are present at presynaptic sites, as well as somatic and dendritic sites (Zarei et al., 1999). In hippocampus, activation of nAChRs has been shown to facilitate the release of several neurotransmitters such as glutamate, GABA, and norepinephrine (Gray et al.,

1996). The facilitation involves nAChR mediated increases in presynaptic calcium concentration, which is achieved by high calcium permeability of α7 nAChRs or through depolarization and activation of voltage gated calcium channels (Wonnacott, 1997). Synaptic plasticity underlining learning and memory is also regulated by nAChRs, which facilitate excitatory neurotransmitter release with a coincident postsynaptic stimulus (Ji et al., 2001).

In mammals, nAChRs have also been found to be expressed in non-neuronal cells, where they control multiple cell functions such as apoptosis, adhesion, migration, proliferation, secretion, and survival (Gotti and Clementi, 2004; Wessler et al., 2003).

Many diseases are associated with impaired functions of nAChRs. In myasthenia gravis, nAChRs at the postsynaptic NMJs are blocked by autoimmune antibodies, leading to muscle degeneration and fatiguability (Conti-Fine et al., 2006). The first sign of the Alzheimer's disease (AD) is a decrease of α7 nAChRs in the brain (Nordberg, 1994). Degeneration of the cholinergic neurons of the basal forebrain accompanied by cognitive deficits is one of the hallmarks in AD (Auld et al., 2002). Cognitive impairment caused by loss of cholinergic neurotransmission is also observed in schizophrenia (Geula and Mesulam, 1995). Cholinesterase is a family of enzymes that catalyze the hydrolysis of acetylcholine into choline and acetic acid (Leuzinger and Baker, 1967). Inhibition of cholinesterase increases both the level and duration of action of acetylcholine. Thus, cholinesterase

inhibitors are often used to treat myasthenia gravis, AD and schizophrenia (Albuquerque et al., 2009; Conti-Fine et al., 2006). The Alzheimer's disease pathogenic peptide amyloid $\beta_{1-42}$ ($A\beta_{1-42}$) binds to the $\alpha7$ nicotinic nAChRs with high affinity (Wang et al., 2000a; Wang et al., 2000b). In hippocampal neurons, the $\alpha7$ nAChR activation mediates $A\beta$ induced phosphorylation of tau protein, which is another pathogen of AD (Wang et al., 2003). Deletion of $\alpha7$ nAChR leads to a protection from the dysfunction in synaptic integrity and learning and memory behavior in a mouse AD model (Dziewczapolski et al., 2009). In primate and rodent model of Parkinson's disease, uptake of nicotine shows enhanced striatal dopamine release and prevention of toxin induced degeneration of dopaminergic neurons (Albuquerque et al., 2009).

In *C. elegans,* nAChRs are required for many other cell functions and behaviors besides locomotion: egg laying (Bany et al., 2003; Kim et al., 2001), pharyngeal pumping (McKay et al., 2004; Steger and Avery, 2004), defecation cycling (Thomas, 1990), and male mating (Garcia et al., 2001; Liu and Sternberg, 1995). A nAChR homologue CUP-4 is required for efficient fluid phase endocytosis in the macrophage like cell-coelomocytes in *C. elegans* (Patton et al., 2005).

## 2.4 Assembly, transport and clustering of nAChRs

nAChRs are required for muscle function and cognition, and they are pentamers consisting of five different subunits. Subunit composition and assembly of nAChRs have to be tightly monitored. Tight control systems have to be in place

to prevent incorrectly assembled nAChRs from reaching the cell surface. Thus, it is important to understand how nAChRs are the assembled and transported to their sites of action.

nAChR subunits are synthesized, folded and assembled within the endoplasmic reticulum (ER) in a sequential and ordered manner (Green and Millar, 1995; Smith et al., 1987). Several ER-resident chaperones are facilitating this process: nonspecific chaperones like BIP and calnexin, and nAChR specific chaperone RIC-3 (Forsayeth et al., 1992; Gelman et al., 1995; Halevi et al., 2002). The ER chaperones mostly dissociate from the subunits once the receptors were assembled and matured. However, in mouse muscle cells, only about 30% of the synthesized subunits reach the cell surface, suggesting that the assembly process and quality control are tightly regulated (Merlie and Lindstrom, 1983). Once nAChR subunits are not folded or assembled correctly, they are either given the second chance to refold with the assistance of ER chaperones or rapidly degraded by the ER-associated degradation (ERAD) mechanism (Christianson and Green, 2004; Wanamaker et al., 2003). Unassembled nAChR subunits can not be transported to the cell surface due to the exposure of an evolutionarily conserved ER retention motif PL(Y/F)(F/Y)xxN in the first transmembrane (TM) domain, which is buried in the nAChR pentamers (Wang et al., 2002). A conserved motif $Arg^{313}$-$Lys^{314}$ in the large cytoplasmic loop between the third and the fourth transmembrane domain is also exposed in unassembled

α-subunits, in which the motif mediates its Golgi-ER retrograde transport by association with COPI coats (Keller et al., 2001).

After reaching the cell surface, nAChRs need to be clustered at the synaptic regions. Density of nAChRs in the synaptic region is 1000 times higher than that in the extrasynaptic membrane (Fertuck and Salpeter, 1976). The muscle-specific tyrosine kinase (MuSK) and a cytoplasmic peripheral membrane protein rapsyn are required for clustering nAChRs at the NMJs (DeChiara et al., 1996; Gautam et al., 1995). The motor neurons secret a proteoglycan named agrin, which activates the MuSK to promote nAChR clustering and stabilization (Glass et al., 1996; McMahan, 1990). In *C. elegans*, nAChRs are also clustered by extracellular interaction with a postsynaptic transmembrane protein LEV-10 (Gally et al., 2004; Gendrel et al., 2009). A muscle secreted complement-control-related protein LEV-9 also contributes to nAChRs clustering by stabilizing LEV-10 localization (Gendrel et al., 2009).

Recently, an interesting study has showed that by co-expressing five levamisole receptor subunits: LEV-1, UNC-29, UNC-38, UNC-63, and LEV-8, and three genes encoding ancillary proteins involved in assembly or trafficking of the receptors: RIC-3, UNC-50, and UNC-74, functional levamisole receptors can be heterologously reconstituted in the plasma membrane of *Xenopus laevis* oocytes. Absence of any of these eight genes would dramatically impair levamisole receptor expression and function (Boulin et al., 2008). This indicates that an

nAChR subtype specific mechanism may exist for assembly, transport and clustering of nAChRs.

## 2.5 UNC-50 is critical for levamisole receptor sorting

Although we have some knowledge about the early events during nAChR assembly and ER retention, not much is understood about nAChR cell surface transport. Recently, a protein UNC-50 was identified to be specifically required for nAChR cell surface transport in *C. elegans* (Eimer et al., 2007). *unc-50* mutants were initially isolated from the genetic screen for mutants that are resistant to the cholinergic agonist levamisole (Lewis et al., 1980a). Phenotypically, *unc-50* mutants show uncoordinated locomotion due to impaired cholinergic transmission. It was later shown that *unc-50* does not encode a nAChR subunit. Body wall muscles of *unc-50* mutants show no contraction in response to the application of levamisole (Figure 8A). However, the nicotine induced response and the GABA induced response were unaffected (Figure 8B,C) (Eimer et al., 2007). This suggests that functional levamisole-sensitive nAChRs are not present on the muscle cell surface in *unc-50* mutants. Indeed, the levamisole receptor subunit UNC-29 is not detectable in *unc-50* mutants (Figure 8D, E). Moreover, unassembled UNC-29 is retained within the cell, probably in the ER, and detectable in *unc-50* mutants by western blot (Figure 8F) (Eimer et al., 2007). This indicates that UNC-50 is required for transport of levamisole receptors to the synapse at a post-assembly step. It was shown that UNC-29 is specifically missorted to the lysosomal system and degraded in *unc-*

*50* mutants (Figure 8E) (Eimer et al., 2007). This suggests that a nAChR subtype-specific transport route to the synapses may exist. UNC-50 is cell-autonomously required in body wall muscles for transporting levamisole receptors to the cell surface, indicating that UNC-50 is a muscle cell specific factor for levamisole receptor cell surface expression (Eimer et al., 2007). UNC-50 is a highly conserved transmembrane protein (Figure 7). Its yeast homologue Gmh1p and human homologue GMH1 interact with the yeast Sec7 domain containing ARF (ADP-ribosylation factor)-GEFs (guanine nucleotide exchange factors) Gea1p and Gea2p (Chantalat et al., 2003; Eimer et al., 2007). Since UNC-50 is localized to the Golgi and ARF-GEFs are highly conserved regulators of membrane dynamics and protein sorting at the TGN, UNC-50 may have essential functions in protein trafficking at the Golgi-endosomal interface.
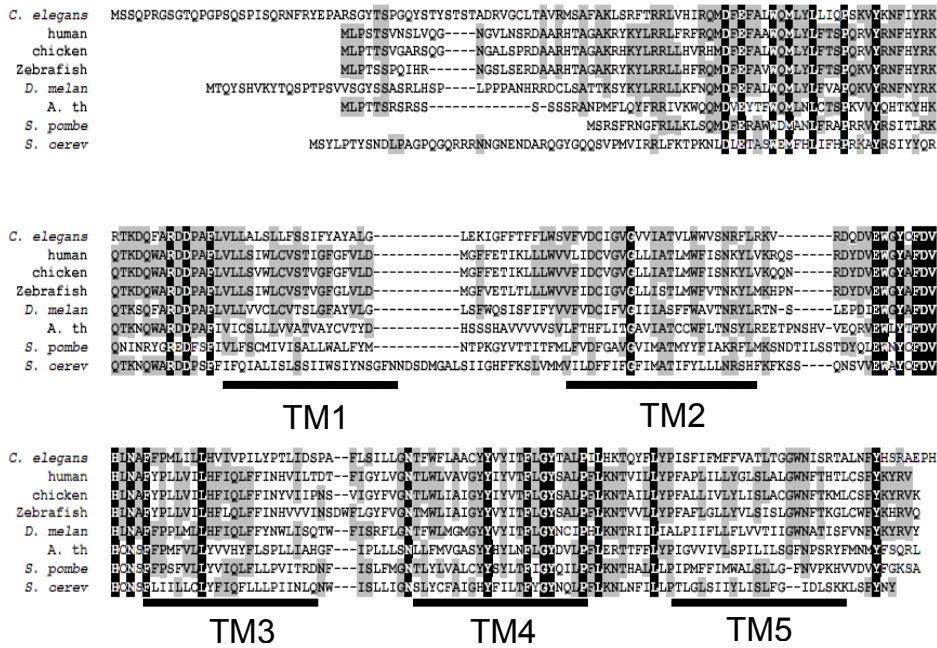
```
C. elegans  MSSQPRGSGTQPGPSQSPISQRNFRYEPARSGYTSPGQYSTYSTSTADRVGCLTAVRMSAFAKLSRFTRRLVHIRQMDFEFALTQLYLLIQGSKVYKNFIYRK
     human  MLPSTSVNSLVQG----NGVLNSRDAARHTAGAKRYKYLRRLFRFRQMDFEFAATQLYLFTSPQRVYRNFHYRK
   chicken  MLPTTSVGARSQG----NGALSPRDAARHTAGAKRHKYLRRLLHVRHMDFEFALTQLYLFTSPQRVYRNFHYRK
 Zebrafish  MLPTSSPQIHR------NGSLSERDAARHTAGAKRYKYLRRLLHFRQMDFEFAVWQLYLFTSPQRVYRNFNYRK
  D. melan  MTQYSHVKYTQSPTPSVVSGYSSASRLHSP----LPPPANHRRDCLSATTKSYKYLRRLLKFNQMDFEFALTQLYLFVAPQKVYRNFNYRK
     A. th  MLPTTSRSRSS-------------S-SSSRANPMFLQYFRRIVKWQQMDVPYTFWQLNLCTSPKVVYQHTKYHK
  S. pombe  MSRSFRNGFRLLKLSQMDFERAWDWANLFRALRRVYRSITLRK
  S. cerev  MSYLPTYSNDLPAGPQGQRRRNNGNENDARQGYGQQSVPMVIRRLFKTPKNLDLRTASYEWFHLIFHLRKAYRSIYYQR


C. elegans  RTKDQFARDDPABLVLLALSLLFSSIFYAYALG-----------LEKIGFFTFFLWSVFVDCIGVGVVIATVLWWVSNRFLRKV-------RDQDVEWGYQFDV
     human  QTKDQWARDDPABLVLLSIWLCVSTIGFGFVLD-----------MGFFETIKLLLWVVLIDCVGVGLLIATLMWFISNKYLVKRQS-----RDYDVEWGYAFDV
   chicken  QTKDQWARDDPABLVLLSVWLCVSTVGFGFVLD-----------MGFFETIKLLLWVVFIDCVGVGLLIATLMWFISNKYLVKQQN-----RDYDVEWGYAFDV
 Zebrafish  QTKDQWARDDPABLVLLSIWLCVSTVGFGLVLD-----------MGFVETLTLLLWVVFIDCIGVGLLISTLMWFVTNKYLMKHPN-----RDYDVEWGYAFDV
  D. melan  QTKSQFARDDPABLVLLVVCLCVTSLGFAYVLG-----------LSFWQSISFIFYVVFVDCIFVGIIIASFFWAVTNRYLRTN-S-----LEPDIEWGYAFDV
     A. th  QTKNQWARDDPABIVICSLLLVVATVAYCVTYD-----------HSSSHAVVVVVSVLFTHFLITGAVIATCCWFLTNSYLREETPNSHV-VEQRVEWLYTFDV
  S. pombe  QNINRYGRDFSEIVLFSCMIVISALLWALFYM-----------NTPKGYVTTITFMLFVDFGAVGVIMATMYYFIAKRFLMKSNDTILSSTDYQLEWNYQFDV
  S. cerev  QTKNQWARDDPSEFIFQIALISLSSIIWSIYNSGFNNDSDMGALSIIGHFFKSLVMMVILDFFIPGFIMATIFYLLLNRSHFKFKSS----QNSVVERAYQFDV
                      _____                        _____
                             TM1                                         TM2


C. elegans  HLNAEFPMLILTHVIVPILYPTLIDSPA--FLSILLGNTFWFLAACYYVYITELGYTALPLUHKTQYFLYPISFIFMFFVATLTGGWNISRTALNFYHSRAEPH
     human  HLNAEYPLLVILHFIQLFFINHVILTDT--FIGYLVGNTLWLVAVGYYIYVTELGYSALPELKNTVILLYPFAPLILLYGLSLALGWNFTHTLCSFYKYRV
   chicken  HLNAEYPLLVILHFIQLFFINYVIIPNS--VIGYFVGNTLWLIAIGYYIYVTELGYSALPELKNTAILLYPFALLIVLYLISLACGWNFTKMLCSFYKYRVK
 Zebrafish  HLNAEYPLLVILHFIQLFFINHVVVINSDWFLGYFVGNTMWLIAIGYYVYITELGYSALPELKNTVVLLYPFAFLGLLYVLSISLGWNFTKGLCWFMKHRVQ
  D. melan  HLNAEFPPLMLIHFIQLFFYNWLISQTW--FISRFLGNTFWLMGMGYYVYITELGYNCIPELKNTRIILIALPIIFLLFLVVTIIGWNATISFVNFYKYRVY
     A. th  HQNSGFPMFVILYVVHYFLSPLLIAHGF---IPLLLSNLLFMVGASYYHYLNGLGYDVLPELRTTFFLYPIGVVIVLSPILILSGFNPSRYFMNMYFSQRL
  S. pombe  HQNSGEPSFVLIYVIQLFLLPVITRDNF---ISLFMGNTLYLVALCYYSYLTELGYQILPELKNTHALLLPIPMFFIMWALSLLG-FNVPKHVVDWYFGKSA
  S. cerev  HQNSELIILLQLYFIQFLLLPIINLQNW---ISLLIGNSLYCFAIGHFEILTEYGYNQLPELKNLNFILLPTLGLSIIYLISLFG--IDLSKKLSFLNY
                 _____        _____       _____
                        TM3                     TM4                   TM5
```

**Figure 7. UNC-50 is an evolutionary conserved integral membrane protein**

Depicted is the clustalX alignment of UNC-50 with its orthologs from yeast to humans. The locations of the five predicted transmembrane (TM) regions are indicated. N-terminal of UNC-50 lays at the cytosolic side and C-terminal lays in the luminal side. Residues conserved between all species are highlighted in black and conserved residues between most species in gray. (Eimer et al., 2007)
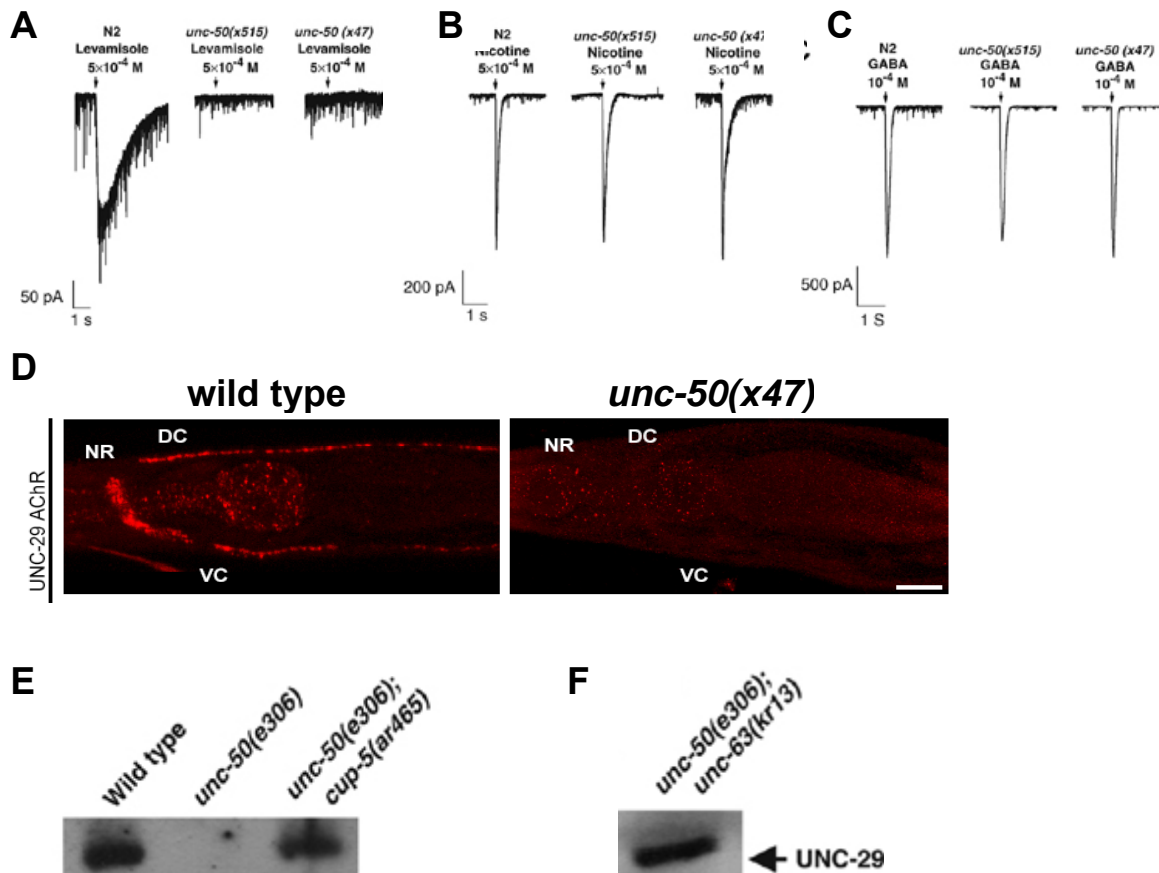
**Figure 8. UNC-50 is specifically required for levamisole receptor function in *C. elegans* (Modified from Eimer et al. 2007)**

(A) Levamisole evoked muscle current is totally abolished in *unc-50* mutants.

(B) Nicotine induced current is unaffected in *unc-50* mutants.

(C) GABA induced current is not affected in *unc-50* mutants.

(D) In *unc-50(x47)* mutant, levamisole receptor subunit UNC-29 can not be detected in the nerve ring by immunostaining.

(E) UNC-29 can not be detected by western blot in *unc-50(e306)* single mutant. But UNC-29 re-appears in *unc-50(e306);cup-5(ar465)*, indicating that UNC-29 is degraded by the lysosomal system in *unc-50(e306)* mutant. CUP-5 is required for the formation of lysosomes from endosomal–lysosomal hybrid organelles (Treusch et al., 2004).

(F) UNC-29 re-appears in *unc-50(e306);unc-63(kr13)* double mutant, indicating that UNC-50 functions after levamisole receptor assembly.

## 2.6 An overview of the secretory pathways in eukaryotic cells

Eukaryotic cells are highly specialized and compartmentalized systems, generating different intracellular micro-environments. Each compartment has specific functions, based on different protein and lipid compositions. These compartments have to exchange proteins and lipids continuously to maintain their integrity. Thus, protein and lipid transport between cellular compartments is essential. In eukaryotic cells, the majority of the proteins are synthesized in the endoplasmic reticulum (ER) and transported to their respective destinations via the secretory pathway. These proteins include secreted proteins, membrane proteins and lysosomal/vacuolar proteins.

The entry point of the secretory pathway is the ER. In the ER, there are two independent quality control systems that target unfolded and misfolded proteins: the unfolded-protein-response (UPR) system and the ER-associated-degradation (ERAD) system (Friedlander et al., 2000; Jarosch et al., 2003). Misfolded or unfolded proteins are translocated into the cytoplasm , polyubiquitinated , and subjected to proteasome-mediated proteolysis (Jarosch et al., 2003).

Proteins that have passed ER quality control are exported from the ER by COPII vesicles (Barlowe et al., 1994). On their route to the Golgi, proteins exiting the ER pass through the ER-Golgi intermediate compartment (ERGIC), the marker of which is the lectin ERGIC-53 (Appenzeller-Herzog and Hauri, 2006). The ERGIC is supposed to be an interface between COPII and COPI mediated transport,

since it has markers specific for both COPII and COPI vesicles (Scales et al., 1997). The ERGIC is also thought to be the location where the first sorting steps take place, based on the fact that COPII and COPI markers are localized to distinct regions, and that ERGIC-53 and anterograde cargo show different behavior (Ben-Tekaya et al., 2005; Martinez-Menarguez et al., 1999). Exit from ERGIC to the cis-Golgi is COPI independent, as structures with anterograde cargo leaving the ERGIC are COPI negative and significantly larger than the typical COPI vesicles (Martinez-Menarguez et al., 1999; Presley et al., 1997; Scales et al., 1997).

The next step in the secretory pathway is the transport through the Golgi apparatus, which is mediated by COPI vesicles (Ladinsky et al., 1999). A Golgi stack consists of four to six cisternae, which differ in protein and lipid composition, and form a gradient from the cis-side to the trans-side. However, how secretory cargo traverses the Golgi and how Golgi resident proteins localize to different compartments of the organelle are not completely understood. One of the explanations is the cisternal maturation model: cisternae assemble at the cis-Golgi, progress through the stack while carrying the secretory cargo forward, and then ultimately disintegrate at the TGN stage by forming transport carriers. Resident Golgi proteins are recycled from late cisternae to early cisternae, driving maturation of younger cisternae (Glick and Malhotra, 1998; Pelham, 1998). The next station is the TGN, which is a primary cargo-sorting site. At the TGN, transport is mainly mediated by clathrin-coated vesicles (CCVs), which

contain three core components: small GTPases, adaptor proteins and the scaffold protein clathrin. CCVs sort cargo by adaptor proteins and carry them to different destinations such as plasma membrane, endosomes and lysosomes (Figure 9).
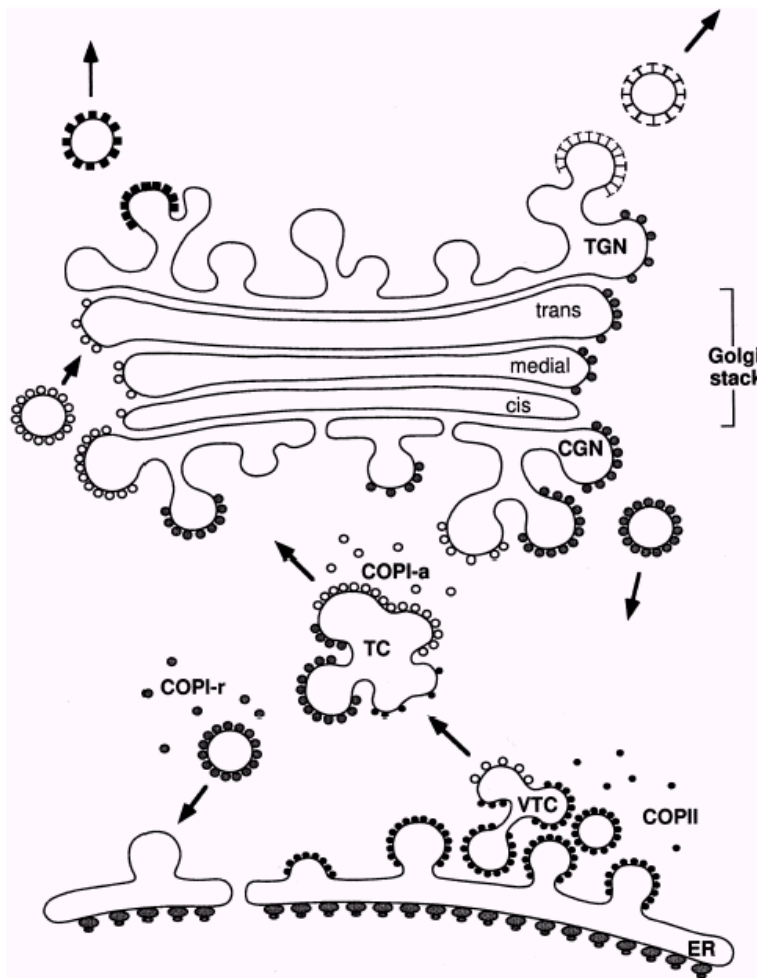


**Figure 9. Model of eukaryotic secretory pathway**

COPII-coated vesicles form a VTC (vesicular-tubular cluster) close to the ER. COPI and COPII vesicles fuse to form transport complex (TC) or ER-Golgi intermediate compartment (ERGIC). The TC moves towards the cis-face of the Golgi complex where it builds up the cis-Golgi network (CGN). COPI can bud vesicles from membranes of the TCs and Golgi complex that move in either the anterograde (COPI-a) or retrograde (COPI-r) direction. (Lowe and Kreis, 1998)

Meanwhile, there is also retrograde transport, in which proteins and lipids are transported back from the endosomes to the Golgi (Figure 10). Retrograde transport is crucial for a diverse range of cellular functions. Retrograde transport and anterograde transport are inter-dependent. Yeast vacuolar hydrolase receptor Vps10p and mammalian mannose 6-phosphate receptors (MPRs) are constantly recycled from endosomes to the trans-Golgi network (TGN). Newly synthesized acid hydrolase precursor proteins are captured by Vps10p or MPRs at the TGN and transported to endosomes. Once they reach endosomes, the acidic environment of the endosomal lumens dissociates the cargo from the receptors (Munier-Lehmann et al., 1996). After that, the hydrolase precursors are transported to the late endosomes and lysosomes, while the receptors are recycled back to the TGN. Another example of retrograde cargo is the Wnt transporter, Wntless. Proper secretion of the morphogen Wnt requires recycling Wntless from endosome to Golgi (Belenkaya et al., 2008; Coudreuse et al., 2006; Franch-Marro et al., 2008; Pan et al., 2008; Port et al., 2008; Prasad and Clark, 2006; Yang et al., 2008). The retrograde endosome to Golgi transport system is also important for cellular entry of some pathogens and viruses. After binding to cell surface receptors, Shiga toxin is endocytosed to early endosomes and transported to the ER via the TGN/Golgi apparatus (Johannes and Popoff, 2008; Sandvig and van Deurs, 2005).

Retrograde trafficking is also mediated by transport vesicles. Formation of retrograde transport vesicles is tightly regulated. First, the cargo have to be
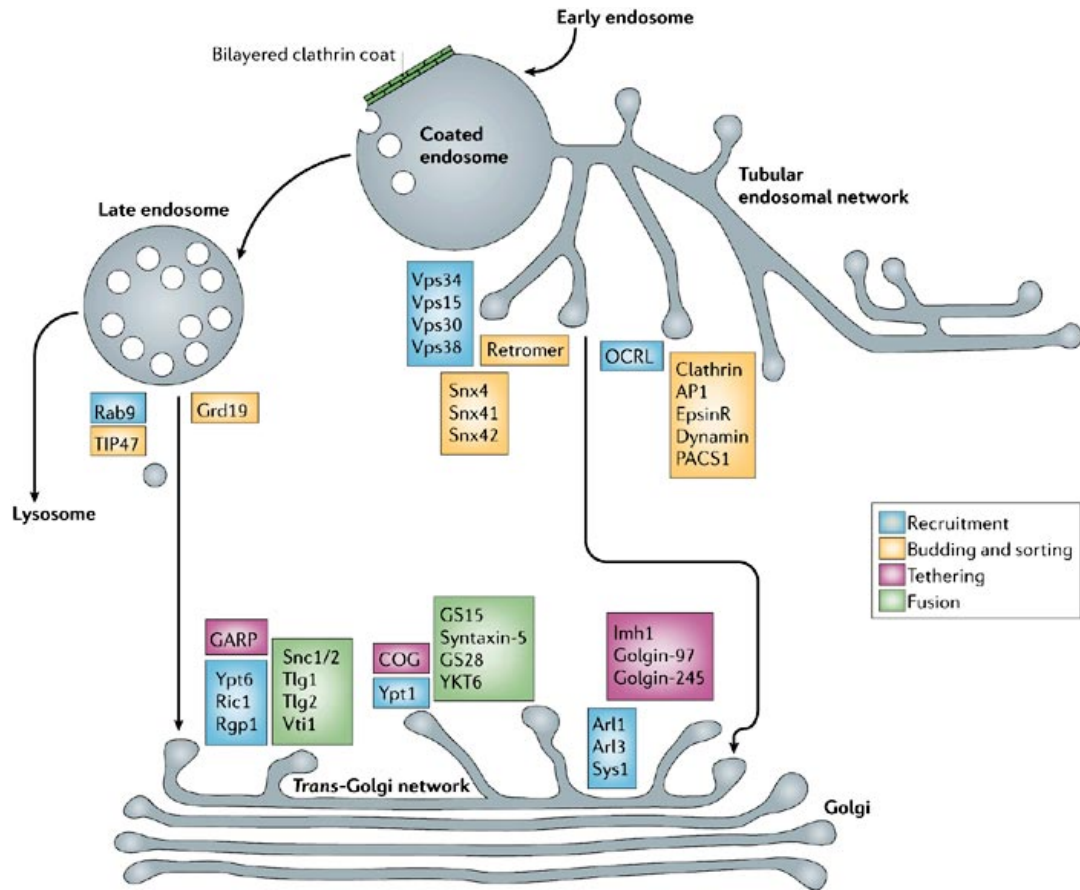
**Figure 10. Components of the molecular machinery that mediates retrograde transport from endosomes to the *trans*-Golgi network**

Retrograde transport starts from a coated endosome, which is an intermediate in the maturation between early and late endosomes. The coated endosome is connected to a vast tubular endosomal network, and from there some proteins are transported to the TGN. Other cargo remain in the vacuolar part as the coated endosome matures to the late endosome, and then they are transported to the TGN by vesicles. Parallel pathways seem to exist from both the coated endosome and the late endosome to the TGN. All of the machinery components are color coded according to their function in membrane recruitment, budding and sorting, tethering or fusion. Components are grouped on the basis of their functional or physical interactions. (Bonifacino and Rojas, 2006)

recruited to a specialized microdomain on the endosomal membrane. The retromer Vps26-Vps29-Vps35 core complex is required for recognizing retrograde cargo like Vps10p and cation-independent mannose-6-phosphate receptor (CI-MPR). Then, this microdomain has to be curved to form a tubular structure. The retromer SNX (sorting nexin) subunit induces membrane curvature change by its BAR (Bin/Amphiphysin/Rvs) domain, and that leads to retrograde tubule formation. Finally, scission of the coated vesicles happened with the assistance of dynamin (Nicoziani et al., 2000). The transport vesicles leave the original compartment and move towards the target compartment.

The fusion of transport vesicles with the destination compartment is executed by the SNARE (soluble N-ethylmaleimide-sensitive factor attachment protein receptor) proteins, which exist at both the vesicles and target membranes (Jahn and Scheller, 2006). Although SNARE proteins are sufficient to execute membrane fusion in purified membrane fusion assays *in vitro*, cells require additional factors for efficient vesicular membrane trafficking *in vivo* (Lang and Jahn, 2008). In particular, it is still not clear how specificity is achieved during the membrane transport. A set of additional factors helps to make the match by tethering transport vesicles to the acceptor membrane. These factors also confer specificity for the fusion process by bringing the SNARE proteins in close proximity to allow efficient SNARE pairing. Tethering factors can be divided into two groups: i) long coiled-coil proteins and ii) multi-subunit tethering complexes. Long coiled-coil proteins are recruited to acceptor membrane mostly by small

GTPases and mark the identity of domains on subcellular compartments (Short et al., 2005). Multimeric tethering complexes are also bound by small GTPases in their active, GTP bound form, and cooperate with the long coiled-coil proteins to tether vesicles to the acceptor membrane (Whyte and Munro, 2002). Three of these multisubunit tethering complexes share similarities in their domain architecture and are composed of multimers of fourfold-symmetric components: the exocyst, the conserved oligomeric Golgi (COG) complex and the Golgi associated retrograde protein (GARP) complex (Whyte and Munro, 2002). The exocyst, which contains eight subunits, is required for tethering of vesicles to the plasma membrane and localizes mainly to sites of polarized growth (Hsu et al., 2004). In contrast, the COG and the GARP complexes are thought to function mainly in retrograde transport from endosome to Golgi (Conboy and Cyert, 2000; Conibear et al., 2003; Conibear and Stevens, 2000; Reggiori et al., 2003; Siniossoglou and Pelham, 2002).

## 2.7 Goal of the study

In *unc-50* mutants, levamisole receptor subunit UNC-29 is selectively missorted to the lysosomes and degraded. Levamisole evoked postsynaptic response is totally abolished in *unc-50* mutants. Thus, failure of forming functional levamisole receptors leads to an uncoordinated movement phenotype and resistance to levamisole. UNC-50 is highly conserved through species. UNC-50 and its yeast homologue Gmh1p and human homologue GMH1 all interact with the yeast Sec7 domain containing ARF-GEFs Gea1p, which is a highly conserved regulator of membrane dynamics and protein trafficking (Chantalat et al., 2003; Eimer et al., 2007). Thus, UNC-50 seems to be a general trafficking factor. However, the role of UNC-50 for regulating levamisole receptor trafficking and its general functions in the intracellular transport system are not understood yet. The goal of this study was to identify the functions of UNC-50 in intracellular transport in the nematode *C. elegans*. We found that UNC-50 has parallel or redundant role with several protein complexes. One of these complexes is a quatrefoil tethering complex, the GARP complex, which is involved in retrograde transport from endosome to Golgi. In order to characterize retrograde membrane transport from endosome to Golgi as well as the functions of UNC-50, we made the first functional characterization of the GARP complex in *C. elegans*. Besides levamisole receptors, we also looked for additional factors whose trafficking is affected in the absence of UNC-50 and investigated how their functions are regulated by UNC-50.

# III Material and Methods

## 3.1 Strains

Strains were maintained at $20^oC$ with standard NGM unless stated (Brenner, 1974). Strains used in this study:

Wild type Bristol N2 strain

Linkage group I (LG I):

*vps-51(tm4275),* NF299 *cogc-1(k179),* NF1684 *cogc-3(k181),* DH1206 *rme-8(b1023), syn-13(tm2037)*, RB662 *apb-3(ok429)*, PS529 *unc-101(sy108),*

LG II:

KN555 *vps-35(hu68), arl-3(tm1703),* VC616 *dab-1(gk291)*

LG III:

VC2202 *vps-53(ok2864), syn-16(tm1560), unc-50(x47), unc-50(x35), unc-50(ok1847)*

LG IV:

NF773 *fbl-1(k201)*, NF774 *fbl-1(k206)*

LG V:

VC985 *vps-54(ok1463),* DH1201 *rme-1(b1045)*, NF198 *mig-17(k174)*

LG X:

VC625 *vps-52(ok853),* VC2117 *rab-6.2(ok2254),* NL2013 *rsd-3(pk2013)*, NL2037 *rsd-3(pk2013)*, *klp-4(tm2114)*, *apt-9(tm3776)*, CB840 *dpy-23(e840)*, *snx-1(tm847)*


CB5600 *ccIs4251* I; *him-8(e1489)* IV

RT258 *unc-119(ed3)* III; *pwIs50 [lmp-1::GFP + unc-119(+)]*

DH1033 *sqt-1(sc103)* II; *bIs1 [vit-2::GFP + rol-6(su1006)]* X

DH1336 *bIs34 [rme-8::GFP + rol-6(su1006)]*

NP745 unc-*119(ed3)* III*; cdIs40 [pcc1::GFP::CUP-5 + unc-119(+) + myo-2::GFP]*

NP822 *unc-119(ed3)* III*; cdIs54 [pcc1::MANS::GFP + unc-119(+) + myo-2::GFP]*

NP705 *unc-119(ed3)* III*; cdIs29 [pcc1::GFP::TRAM + unc-119(+) + ttx-3::GFP]*

NP941 *unc-119(ed3)* III*; cdIs85 [pcc1::2xFYVE::GFP + unc-119(+) + myo-2::GFP]*

GS1912 *arIs37 [pmyo-3::ssGFP]* I; *dpy-20(e1282)* IV

All the strains used in this study were from CGC and Dr. Shohei Mitani. All strains have been outcrossed at least three times before analysis.

## 3.2 Molecular biology

*vps-51/B0414.8, vps-52/F08C6.3, vps-53/T05G5.8*, and *vps-54/T21C9.2* cDNAs were PCR amplified from a *C. elegans* mixed stage cDNA library (Proquest, Invitrogen) and subcloned. To express the different GARP complex subunits in *C. elegans* body wall muscle (BWM) cells under the control of the *myo-3* promoter, the respective cDNA along with a fluorescent protein tag were cloned into pPD115.62(*pmyo-3::gfp*) replacing GFP. As fluorescent protein tags either mYFP citrine, mCherry or tagRFP (Evrogen) were used. *vps-51* and *vps-53* were N-terminally tagged while *vps-52* and *vps-54* were tagged at the C-terminus.

To analyze the expression pattern of *vps-51*, *vps-52*, and *vps-53,* a 3.6kb, 470bp, and 4,5 kb promoter fragment upstream of the start ATG, respectively, was

amplified from genomic DNA and subcloned as a *HindIII* and *BamHI* fragment into *pPD115.62* (*pmyo-3::gfp*) by replacing the *myo-3* promoter. All clones were verified by sequencing.

## 3.3 Production of transgenic animals

To generate transgenic animals young adult hermaphrodites were used for microinjection of DNA mixes into the distal part of the gonads (Mello et al., 1991). Expression constructs were injected at 20 ng/µl and protein fusions at 5 ng/µl. *pttx-3::gfp* and *rol-6 (su1006)* were used as co-injection markers each at 30ng/µl. The total DNA concentration of injection mixtures was adjusted to 120ng/µl by adding *pBlueScript SKII* (Stratagene)*.

## 3.4 Co-immunoprecipitation and western blotting

*C. elegans* mixed staged worms from one 9 cm plate were rinsed off, washed and snap frozen in liquid nitrogen and kept at -80   until subsequent use. The frozen worm pellet was ground with a mortar and pestle and frozen in liquid nitrogen. While thawing, 4-5 volumes of homogenization buffer (50mM HEPES, 7.5% glycerol, 10mM NaCl, 1mM EDTA, 0.1% NP-40) and complete EDTA-free protease inhibitor (Roche) were added. The suspension was kept at 4   and centrifuged at 500G for 10 minutes. 1.5 ml of supernatant was incubated with 4µg monoclonal mouse anti-GFP (Invitrogen) for 3 hours at 4  . 10µl of protein A coated paramagnetic beads slurry (New England BioLabs) were added and incubated for 2 hours at 4  . Beads were washed 3 times with 1ml

homogenization buffer and eluted by adding 2xLaemmli buffer at 96 . Western blotting was done according to the standard method. To detect mCherry fusion proteins a polyclonal rabbit anti-DsRed (Clontech) was used at 1:1000 dilution. Secondary HRP labeled anti-mouse and anti-rabbit antibodies were purchased from Jackson/Dianova and used at 1/10000.

## 3.5 Antibody production

Antibody against VPS-51 was produced by immunizing rabbit with 1ug of purified 6xHis-tag fused fragment of VPS-51(amino acid 1-374). Antibody against VPS-54 was produced by immunizing mouse with 1ug of purified 6xHis-tag fused fragment of VPS-54(amino acid 1-293).

## 3.6 Phylogenetic analysis

Phylogenetic trees were generated based on the PFAM Vps51 (PF08700) full alignment and subsets thereof, respectively of full-length sequences selected based on phylogeny and aligned using MAFFT (Katoh et al., 2005). Trees were constructed using neighbourjoining (Frickenhaus and Beszteri, 2008; Howe et al., 2002) and Bayesian inference (Ronquist and Huelsenbeck, 2003). Motif discovery was carried out using MEME (Bailey et al., 2009).

## 3.7 TR-BSA pulse chase assay

1mg/mL TR-BSA was injected into the body cavity of the pharyngeal region of young adult worms. After recovering on the NGM plates at 20°C for 10 min, 15

min, 30 min, 45 min and 60 minutes, injected worms were mounted in 50mM sodium azide on 2% agarose pads for confocal microscopy. More than five coelomocytes of different worms show similar results with the same time spot.

## 3.8 Confocal microscopy and data analysis

Confocal microscopy images were taken on a Leica DM IRE2 inverted confocal microscope equipped with a 488nm laser and a 561nm laser. Intensity of GFP in coelomocytes was measured by ImageJ. Sizes of RME-8::GFP, CUP-5::GFP, LMP-1::GFP positive vesicles in coelomocytes were measured by XtraCOunt (developed by Christian Olendrowitz). Statistics were done with Microsoft Excel.

## 3.9 Yeast two hybrid

The Matchmaker yeast two-hybrid assay was performed according to the manufacturer's protocol (Clontech). *vps-51, -52, -53,* and *-54* were cloned into the bait and prey vectors, pGBKT7 and pGADT7 (Clontech), respectively. All *C. elegans* SNARE proteins were identified and annotated by sequence comparison (Kloepper et al., 2008), PCR amplified and subcloned into the prey vector pGADT7. The appropriate plasmid combinations were transformation into the yeast strain AH109 (Clontech) and tested for interaction on selective plates lacking histidine.

## 3.10 High pressure freezing Electron microscopy

A 100 μm deep aluminium platelet (Microscopy Services, Flintbek) was filled with *E. coli* OP 50 suspension. About 20 young adult worms were transferred into the chamber and immediately frozen using a BalTec HPM 10. Freeze substitution was carried out in a Leica EM AFS at -90 °C for 100 h in 0,1% tannic acid and another 7 h in 2 % $OsO_4$ (each w/v in dry acetone), according to Rostaing et al. 2006.

40 nm sections were cut using a Leica UC6 ultramicrotome. Ribbons of sections were transferred on Formvar-coated copper slot-grids. The grids were placed for 10 min on drops of 4 % (w/v) uranyl acetate in 75% methanol and then washed in distilled water. After air drying the grids were placed on lead citrate (Reynolds, 1963) for 2 min in a $CO_2$-free chamber, and rinsed in distilled water. Micrographs were taken with a 1024 × 1024 CCD detector (Proscan CCD HSS 512/1024; Proscan Electronic Systems, Scheuring, Germany) in a Zeiss EM 902A, operated in the bright field mode.

## 3.11 3D Reconstructions of EM images

Serial sections of neuronal cell bodies were imaged at a magnification of 12,000x Images were imported into "reconstruct" (Fiala, 2005) and aligned linearly. Vesicles were reconstructed as "sphere", all other components (nucleus, mitochondria, Golgi stacks, and further cell-inclusions) as "Boissonnat surface".

## 3.12 Analysis of DTC migration phenotypes

Samples were prepared by immobilizing young adult hermaphrodites with 50mM sodium azide and placing them on 2% agarose pads. A Zeiss Axiovert 200 microscope equipped with a 40x objective and Nomarski differential interference contrast (DIC) optics was used to exam the morphology of gonad. Both anterior and posterior arms were examined. Each strain was scored three times independently.

## 3.13 Cryo-section and immunostaining

Worms of mix stage were collected with M9 buffer and concentrated into 400uL icy blocks by freezing with liquid nitrogen. Slicing the blocks into 15-20uM thick sections with cryotome, and collect the sections on glass slices coated with poly-glycine. The samples were kept at -80 $^{o}$C until use. Thaw the slices at room temperature, and wash with PBS three times, each time 10 minutes. Block with 2% BSA in PBS for about one hour. Incubate with rabbit anti-GFP (1:1000, molecular probes) in PBS containing 1% BSA for 2 hours. Then wash once with PBS for 5 minutes. Incubate with Alexa 568 goat anti-rabbit-IgG (1:100), phalloidin (5U/mL) in PBS containing 1% BSA for 2 hours. Then incubate with DAPI (1:1000) for 10 minutes. Wash 3 times with PBS, each time for 5 minutes. Cover the sections with cover slips and the samples are ready for imaging.

Table 1.  Primers used in this study

| Primer number | Description | Primer sequence from 5' to 3' |
|---|---|---|
| oGQ 299 | forward primer outside *arl-3(tm1703)* deletion | cgt ctc tat ggt aac ata cgg gag cta gag agt |
| oGQ 300 | reverse primer outside *arl-3(tm1703)* deletion | caa ctt cct tct tat agg ttt cca ctg aaa ttg |
| oGQ301 | forward primer inside *arl-3(tm1703)* deletion | ata ctg aag cag ctg tcc tct gaa gat gtt caa |
| oGQ302 | reverse primer inside *arl-3(tm1703)* deletion | tga gag act gcc aca gag ata ttg taa atg gat |
| oGQ303 | forward primer outside *syn-16(tm1560)* deletion | cgc aca cct ttt cgc att taa taa ata tta tcg |
| oGQ304 | reverse primer outside *syn-16(tm1560)* deletion | ttg gct ttg gcg tta atc agt tga ttt taa acg |
| oGQ305 | forward primer inside *syn-16(tm1560)* deletion | aga aga cta gat gaa ctt gga gag gca cag aga |
| oGQ306 | reverse primer inside *syn-16(tm1560)* deletion | tta caa ttt agt aac aat aat aag aat cag tac |
| oGQ 311 | forward primer outside *syn-13(tm2037)* deletion | ttg atc gaa cgt cag att agc gat gca gta gat |
| oGQ 312 | reverse primer outside *syn-13(tm2037)* deletion | ata cta ctt gaa tag gcc act tat tat caa aat |
| oGQ 313 | forward primer inside *syn-13(tm2037)* deletion | aat caa tca aaa ctt cac tag aag cct gca ttt |
| oGQ 314 | reverse primer inside *syn-13(tm2037)* deletion | aag cca ctt tac aca tgc cag ttt ata tat ttt |
| oGQ 315 | forward primer outside *vps-54(ok1463)* deletion | gga tgt gtt cac agt tcc tgc caa tga tga ttt |
| oGQ 316 | reverse primer outside *vps-54(ok1463)* deletion | cta ttc aaa cat aat gtc att aag cga ctc gag |
| oGQ 317 | forward primer inside *vps-54(ok1463)* deletion | aga act ttc tgc tgt cct act tgg att gat gag |
| oGQ 318 | reverse primer inside *vps-54(ok1463)* deletion | gag tgg aat acc atc ctt cct tgt cac act tgg |
| oGQ858 | forward primer outside *apb-3(ok429)* deletion | ttc aca aaa tga taa att tgt gat agc agt ggt tag cgt ctc |
| oGQ859 | reverse primer outside *apb-3(ok429)* deletion | taa tcg agt ttc cct tca cat cga gac ctt ctt cag ttt tta |
| oGQ860 | forward primer for matching inside *apb-3(ok429)* deletion | ctg gac ttg tcc aat tga ttt ctt ctt ccg atg aga aag tcg |
| oGQ861 | reverse primer inside *apb-3(ok429)* deletion | aga tgg ttt tgg gtt agg ctt ctc ctc tgg ctc act atc atc |

| oGQ862 | forward primer outside *dab-1(gk291)* deletion | aat ccg aca ttt ttt ctt att tcc att tcg aaa gta ata aca |
|---|---|---|
| oGQ863 | reverse primer outside *dab-1(gk291)* deletion | agt gct ggc gtg atg caa tga tga ctg ctg ttg ttg gat att |
| oGQ864 | forward primer inside *dab-1(gk291)* deletion | atg tta tct ttt tgt tat cta taa cat ttt cag gaa aga gtt |
| oGQ865 | reverse primer inside *dab-1(gk291)* deletion | ttc ctt ctt gct ctg gaa ctt tta taa agt cat aac aat gga |
| oGQ977 | forward primer outside *rab-6.2(ok2254)* deletion | caa aat tcc gaa acg tta agt tga cct cta ttc aaa aaa caa |
| oGQ978 | reverse primer outside *rab-6.2(ok2254)* deletion | agc gca agg taa gtt tag ctt gaa cta att ctg ttt aga atg |
| oGQ979 | forward primer inside *rab-6.2(ok2254)* deletion | ctt gat tta att tta gaa aaa tta cag aaa aat gtc gga ctt |
| oGQ980 | reverse primer inside *rab-6.2(ok2254)* deletion | gtt gga gtc tgc aaa aaa gtt ggg gtt aaa tga agc ttt ttt |
| oGQ981 | forward primer for detecting *rsd-3(pk2010)* Tc1 insertion | tct ctg cgc ttt ccg ttc tat ttc ccc gag gca cac |
| oGQ982 | reverse primer for detecting *rsd-3(pk2010)* Tc1 insertion | tca cat tca agc tat gtt gaa aat cgc agc caa |
| oGQ991 | forward primer outside *snx-1(tm847)* deletion | cgc tcc gct gca cac ctc ccc ctt cca cat |
| oGQ992 | reverse primer outside *snx-1(tm847)* deletion | ctt gcg atc ggc atc aaa acg cgc aac ctc ctc acg |
| oGQ993 | forward primer inside *snx-1(tm847)* deletion | ccg gcg gtt atc aat tct att gag gat cac gat cag |
| oGQ994 | reverse primer inside *snx-1(tm847)* deletion | gca gtt tac aag caa tac tgt gta ctt ttt cac ttc tac g |
| oGQ1105 | forward primer outside *rme-1(b1045)* deletion | gtt tac aaa aac gaa tgc ttg ttg gat cga |
| oGQ1106 | reverse primer outside *rme-1(b1045)* deletion | tcg acc ata ttt ttt tgc gaa att aga ggc |
| oGQ1107 | forward primer for matching fragment inside *rme-1(b1045)* deletion | cac gca tac att att gct gag ctt cgt aag |
| oGQ1108 | reverse primer inside *rme-1(b1045)* deletion | tca gca tcc aac tgt cca tcc ttg tca ata |
| oGQ1109 | forward primer outside *apt-9(tm3776)* deletion | gtg aga tca aga aac aat aca act gga caa |
| oGQ1110 | reverse primer outside *apt-9(tm3776)* deletion | cat tgt ttt ctg cta gtt cat tga cat atc cat |
| oGQ1111 | forward primer inside *apt-9(tm3776)* deletion | cag gct ctt gat tat tta gta cgc aat gga |
| oGQ1112 | reverse primer inside *apt-9(tm3776)* deletion | aat aaa gct ttc aaa aga acg gct tgc tct |
| oGQ1542 | reverse primer inside *vps-51(tm4275)* | gaa ctg ttg gaa cgt ctt tat act |

| | deletion | gcg at |
|---|---|---|
| oGQ1543 | forward primer outside *vps-51(tm4275)* deletion | gaa atg aaa tct ctc agc cga agt atg tcg |
| oGQ1544 | reverse primer outside *vps-51(tm4275)* deletion | ctt caa aac cgt aat aag atc ttc tcg ttt |
| oGQ1654 | forward primer inside *vps-53(ok2864)* deletion | cca aga aag tat caa aaa cac tcc aaa tag |
| oGQ1655 | reverse primer inside *vps-53(ok2864)* deletion | gct gat aat gaa gaa ggc gca tgg ttg gat |
| oGQ1656 | forward primer outside *vps-53(ok2864)* deletion | atc aat gca tca ggt tca ctg ctc aac ttg |
| oGQ1657 | reverse primer outside *vps-53(ok2864)* deletion | cgt atc gta gat acc ttc ata ata gag tta |
| oSE270 | forward primer for *vps-52* F08C6.3 that introduces a AgeI and NcoI site in front of the start ATG | c cca ccg gta tcc atg gga atg cct cga aca cgt gtc aac |
| oSE227 | reverse primer for F08C6.3/*vps-52* that matches after the deletion of ok853 | cag ctt ttg agc aca act gac |
| oSE228 | reverse primer for F08C6.3/*vps-52* that matches within the deletion of ok853 | tgg ctc agc tcg act cta act |

Table 2.  List of constructs made and used in this study

| construct | description |
|---|---|
| *Pmyo3::vps-52::mCherry* | For expression of VPS-52::mCherry in the body wall muscle |
| *Pmyo3::vps-52:myfp* | For expression of VPS-52::mYFP in the body wall muscle |
| *Pmyo3::mCherry::vps-53* | For expression of mCherry::VPS-53 in the body wall muscle |
| *Pmyo3::vps-54::myfp* | For expression of VPS-54::mYFP in the body wall muscle |
| *Pmyo3::myfp::vps-51* | For expression of mYFP::VPS-51 in the body wall muscle |
| *Pmyo3::mCherry::vps-51* | For expression of mCherry::VPS-51 in the body wall muscle |
| *Prab3::mCherry::vps-53* | For expression of mCherry::VPS-53 in the neurons |
| *Pvps-52::gfp* | For *vps-52* promoter driven expression of GFP |
| *pHis-parallel2::vps-54 N term* | For recombinant expression of VPS-54 N-terminal (aa1-293) with a 6XHis tag in front |
| *pHis-parallel2::vps-51 N term* | For recombinant expression of VPS-51N-terminal (aa1-374) with a 6XHis tag in front |

| | |
|---|---|
| *Pmyo3::gfp::rab-6.1* | For expression of GFP::RAB-6.1 in the body wall muscle |
| *Pmyo3::gfp::rab-6.2* | For expression of GFP::RAB-6.2 in the body wall muscle |
| *Pmyo3::rab-5 QL* | For expression of RAB-5 dominant active form in the body wall muscle |
| *Pmyo3::rab-5 SN* | For expression of RAB-5 dominant negative form in the body wall muscle |
| *Plag2::unc-50* | For expression of UNC-50 in the distal tip cell |

Table 3. Worm strains used in this study

| Strain name | Genotype |
|---|---|
| | *vps-51(tm4275)* |
| VC625 | *vps-52(ok853)* X |
| VC2202 | *vps-53(ok2864)* III |
| VC985 | *vps-54(ok1463)* V |
| KN555 | *vps-35(hu68)* II |
| CB5600 | *ccIs4251* I; *him-8(e1489)* IV |
| RT258 | *unc-119(ed3)* III; *pwIs50 [lmp-1::GFP + unc-119(+)]* |
| DH1033 | *sqt-1(sc103)* II; *bIs1 [vit-2::GFP + rol-6(su1006)]* X |
| DH1336 | *bIs34 [rme-8::GFP + rol-6(su1006)]* |
| NP745 | unc-*119(ed3)* III*; cdIs40 [pcc1::GFP::CUP-5 + unc-119(+) + myo-2::GFP]* |
| NP822 | *unc-119(ed3)* III*; cdIs54 [pcc1::MANS::GFP + unc-119(+) + myo-2::GFP]* |
| NP705 | *unc-119(ed3)* III; *cdIs29 [pcc1::GFP::TRAM + unc-119(+) + ttx-3::GFP]* |
| NP941 | *unc-119(ed3)* III*; cdIs85 [pcc1::2xFYVE::GFP + unc-119(+) + myo-2::GFP]* |
| VC2117 | *rab-6.2(ok2254)* X |
| NF299 | *cogc-1(k179)* I |
| NF1684 | *cogc-3(k181)* I |
| GS1912 | *arIs37 [pmyo-3::ssGFP]* I; *dpy-20(e1282)* IV |
| | *unc-50(x47)* III |
| | *unc-50(x35)* III |
| | *unc-50(ok1847)* III |
| | *syn-13(tm2037)* I |
| | *syn-16(tm1560)* III |
| PS529 | *unc-101(sy108)* I |
| CB840 | *dpy-23(e840)* X |
| RB662 | *apb-3(ok429)* I |
| VC616 | *dab-1(gk291)* II |
| | *rsd-3(pk2010)* X |

| | | |
|---|---|---|
| | *rsd-3(pk2013)* X | |
| | *snx-1(tm847)* X | |
| | *arl-3(tm1703)* II | |
| DH1201 | *rme-1(b1045)* V | |
| DH1206 | *rme-8(b1023)* I | |
| | *apt-9(tm3776)* X | |
| | *klp-4(tm2114)* X | |
| NF198 | *mig-17(k174)* V | |
| NF773 | *fbl-1(k201)* IV | |
| NF774 | *fbl-1(k206)* IV | |

Table 4.  Transgenic worms generated and used in this study

| Transgene number | Plasmids | | Marker | |
|---|---|---|---|---|
| InLing10 | *Pmyo3::vps-52::mCherry* | 10ng/uL | *ttx3::gfp* | 60ng/uL |
| | *Pmyo3::gfp::GRIP domain* | 10ng/uL | *rol-6* | 60ng/uL |
| InLing11 | *Pmyo3::vps-52::mCherry* | 10ng/uL | *ttx3::gfp* | 60ng/uL |
| | *Pmyo3::gfp::2xFYVE* | 10ng/uL | *rol-6* | 60ng/uL |
| InLing6 | *Pmyo3::vps-52::mCherry* | 5ng/uL | *ttx3::gfp* | 60ng/uL |
| | *Pmyo3::Mans::gfp* | 5ng/uL | *rol-6* | 60ng/uL |
| InLing14 | *Pmyo3::vps-52::mCherry* | 10ng/uL | *ttx3::gfp* | 60ng/uL |
| | *Pmyo3::gfp::rab-6.1* | 10ng/uL | *rol-6* | 60ng/uL |
| InLing15 | *Pmyo3::vps-52::mCherry* | 10ng/uL | *ttx3::gfp* | 60ng/uL |
| | *Pmyo3::gfp::rab-6.2* | 10ng/uL | *rol-6* | 60ng/uL |
| InLing24 | *mig-17::venus* | 100ng/uL | *ttx3::gfp* | 20ng/uL |
| InLing26 | *Plag2::unc50* | 5ng/uL | *ttx3::gfp* | 20ng/uL |
| InLing30 | *Pvps52::gfp* | 20ng/uL | *rol-6* | 40ng/uL |
| InLing38 | *Pmyo3::vps54::myfp* | 10ng/uL | *ttx3::gfp* | 20ng/uL |
| | *Pmyo3::vps52::mCherry* | 10ng/uL | *rol-6* | 30ng/uL |
| InLing46 | *Pmyo3::mCherry::vps53* | 10ng/uL | *myo2::gfp* | 10ng/uL |
| | *Pmyo3::vps52::myfp* | 10ng/uL | *rol-6* | 30ng/uL |
| InLing52 | *Pmyo3::vps54::myfp* | 10ng/uL | *ttx3::gfp* | 20ng/uL |
| | *Pmyo3::mCherry::vps53* | 10ng/uL | *rol-6* | 30ng/uL |
| InLing58 | *Pmyo3::mCherry::rab-2* | 10ng/uL | *ttx-3::gfp* | 20ng/uL |
| | *Pmyo3::vps-52::myfp* | 10ng/uL | *rol-6* | 30ng/uL |
| InLing72 | *Pmyo3::rab-5 SN (inactive)* | 10ng/uL | *ttx3::gfp* | 20ng/uL |
| InLing73 | *Pmyo3::rab-5 QL (active)* | 10ng/uL | *ttx3::gfp* | 20ng/uL |
| InLing78 | *Prab3::mCherry::vps-53* | 10ng/uL | *rol-6* | 30ng/uL |
| | *Prab3::Mans::myfp* | 10ng/uL | | |
| InLing79 | *Prab3::mCherry::vps-53* | 10ng/uL | *rol-6* | 30ng/uL |
| | *Prab3::gfp::GRIP domain* | 10ng/uL | | |
| InLing80 | *Prab3::mCherry::vps-53* | 10ng/uL | *rol-6* | 30ng/uL |
| | *Prab3::gfp::2xFYVE* | 10ng/uL | | |

| InLing92 | *Pmyo3::mCherry::vps-51* | 10ng/uL | *ttx3::gfp* | 30ng/uL |
| | *Pmyo3::vps-52::myfp* | 10ng/uL | *rol-6* | 30ng/uL |
| InLing93 | *Pmyo3::myfp::vps-51* | 10ng/uL | *ttx3::gfp* | 30ng/uL |
| | *Pmyo3::vps-52::mtfp* | 10ng/uL | *rol-6* | 30ng/uL |
| | *Pmyo3::mCherry::vps-53* | 10ng/uL | | |
| InLing96 | *mig-17::venus* | 2ng/uL | *ttx3::gfp* | 30ng/uL |

# IV Results and discussion

## Part I

## UNC-50 is involved in retrograde transport from endosome to Golgi

In *C. elegans*, levamisole sensitive nAChRs mediate fast synaptic transmission at the neuromuscular junctions. A conserved integral membrane protein UNC-50 has been shown to be required for membrane trafficking of levamisole sensitive nAChRs in the body wall muscles (Eimer et al., 2007). However, the molecular pathway UNC-50 is operating in and the precise mechanism how UNC-50 affects levamisole receptor trafficking are not known yet.

## 4.1.1 UNC-50 is localized to the Golgi-endosomal interface

It was reported that UNC-50 is localized to the Golgi system but not to the ER system (Eimer et al., 2007). To determine the exact site of UNC-50 action, we refined the Golgi localization of UNC-50 by using different Golgi and endosomal markers as references. We co-expressed fluorescent protein tagged UNC-50 and several organelle specific markers in body wall muscles (BWMs). As shown in Figure 11, maximum projection confocal images of mRFP::UNC-50 and the trans-Golgi marker GFP::GRIP domain show nearly complete colocalization. The early endosomal marker GFP::2xFYVE domain also shows high degree of colocalization with mRFP::UNC-50 (Figure 11). The colocalization of UNC-50 with late Golgi and endosomal markers suggests that UNC-50 may function at the Golgi endosomal interface. Interestingly, although the COP-I vesicle and ERGIC marker GFP::εCOP weakly overlaps with mRFP::UNC-50, they are mostly adjacent to each other (Figure 11). This is consistent with the fact that UNC-50 localizes to the medial and late Golgi, and it also indicates that UNC-50 is probably not directly associated with the COP-I vesicle mediated trafficking, as

suggested previously by the interaction and colocalization of Gmh1 with Gea1/2p in yeast and human cells (Chantalat et al., 2003; Eimer et al., 2007).
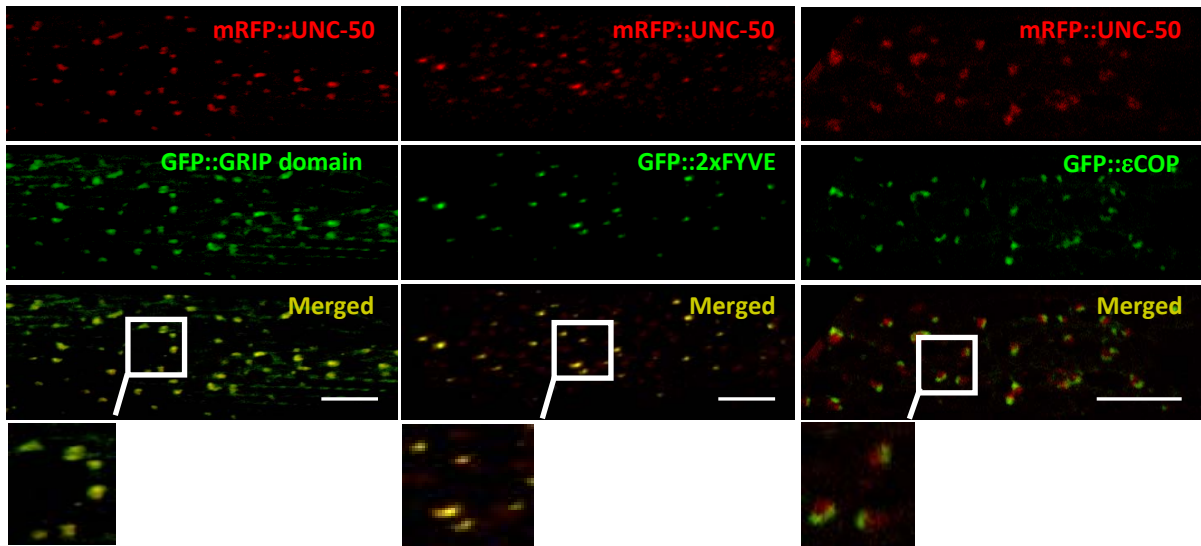


**Figure 11. UNC-50 is localized to the TGN and endosomal systems**

In body wall muscles, mRFP::UNC-50 is overlapping with the TGN marker GFP::GRIP domain and the endosomal marker GFP::2xFYVE. Interestingly, mRFP::UNC-50 and the COPI vesicle marker GFP::εCOP are not colocalized but adjacent to each other. Inserted are magnified parts of the pictures. Scale bar, 5µm.

## 4.1.2 Screen for genetic interactors by synthetic lethality analysis

Although UNC-50 has been implicated to be specifically essential for levamisole receptor sorting in *C. elegans*, more general and evolutionarily conserved function of UNC-50 within the secretory pathway might exist, since UNC-50 shows high conservation between species (Eimer et al., 2007), and some of the organisms like yeast and *Arabidopsis* do not contain nAChRs. In *C. elegans*,

*unc-50* mutants show strong resistance to levamisole, and moderate uncoordinated locomotion (Eimer et al., 2007). Apart from these, *unc-50* mutants appear superficially healthy. The lack of a strong phenotype may be caused by redundancy. As a back-up mechanism, redundancy of protein functions has been reported in many cellular processes (Baugh and Hunter, 2006; Lode et al., 2002; Naor et al., 2005). Since intracellular trafficking is a highly complex system involving many factors, proteins that exert redundant functions with UNC-50 may exist. This could explain why *unc-50* mutants do not have strong phenotypes besides the levamisole receptor trafficking defects. Identification of these functional redundant proteins will help us understand the functions of UNC-50.

An effective way of analyzing redundant protein pathways in *C. elegans* is to look for genetic interactions by performing synthetic lethality analysis. This is based on the assumption that if two proteins have redundant functions, loss of any one will not cause severe phenotypes because the system can bypass it, while simultaneous inactivation of both will lead to lethality (Figure 12). We constructed strains carrying a homozygous *unc-50(x47)* mutation and a heterozygous mutation of genes that are to be tested. 25% of the progenies of these stains will be homozygous double mutants of *unc-50* and the tested gene. If the double mutants show lethality, *unc-50* and the tested gene should have redundant functions (Figure 13).
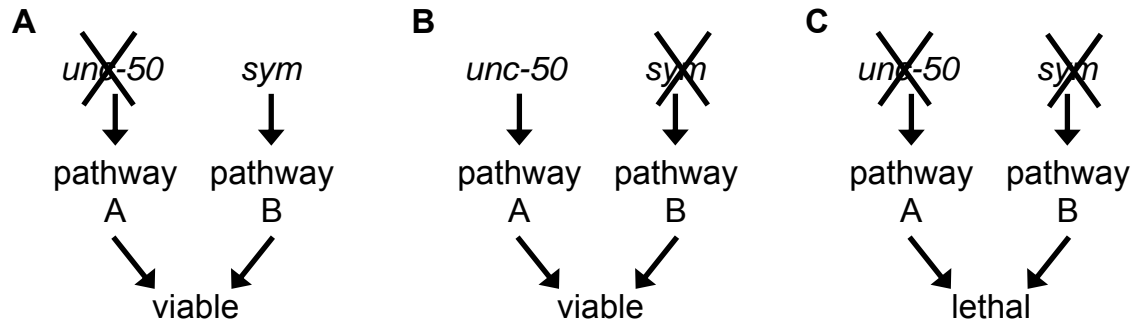
**Figure 12. Schematic diagram of synthetic lethality principle**

(A) Suppose there are two parallel linear molecular pathways: pathway A in which *unc-50* is involved, and pathway B in which *synthetic mutant (sym)* is involved. When *unc-50* is deleted, pathway A is blocked. But the system can still survive by taking pathway B.

(B) When *sym* is deleted, pathway B is blocked. The system can still survive by taking pathway A.
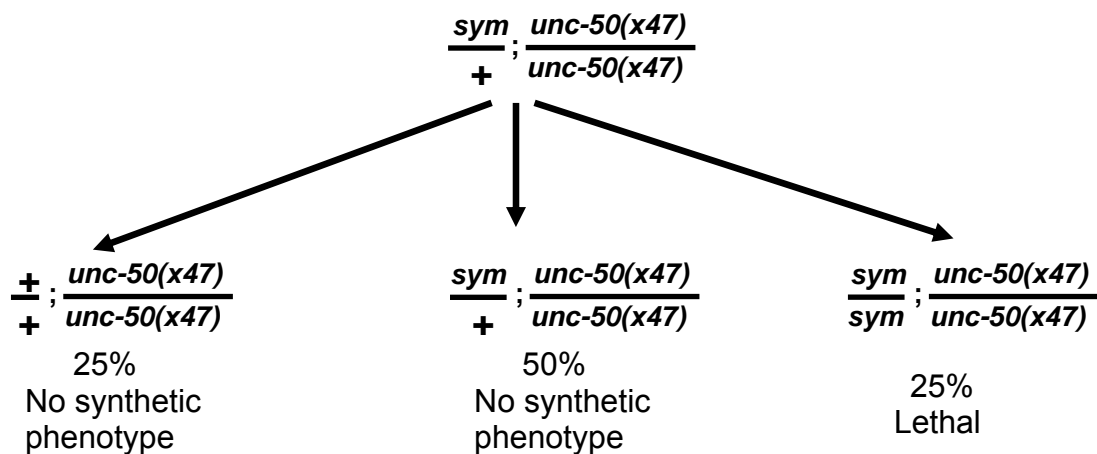
(C) When both pathways are inactivated, the system is not able to survive.



**Figure 13. Synthetic lethality analysis in *C. elegans***

A strain with a homozygous deletion mutation at the endogenous *unc-50(x47)* loci and a heterozygous deletion mutation at *synthetic mutant (sym)* loci was constructed. This strain segregates three types of progenies: mutants with only homozygous *unc-50(x47)* mutation (25% of the progeny), mutants with homozygous *unc-50(x47)* mutation and heterozygous *sym* mutation (50%), mutants with homozygous *unc-50(x47)* and *sym* mutations (25%). The first two types do not show additional phenotype compared to *unc-50(x47)* single mutant, while *unc-50(x47);sym* double mutant show lethality.

### 4.1.3 *unc-50* does not genetically interact with factors involved in anterograde trafficking at the Golgi-endosomal interface

UNC-50 has been localized to the Golgi-endosomal interface. Therefore, we chose candidate genes that encode trafficking factors involved in transport between Golgi and endosomes. Firstly, we tested trafficking factors that have been shown to be mainly involved in anterograde transport and endocytosis. However, none of them showed synthetic lethality with *unc-50* mutation (table 5), suggesting that UNC-50 and these proteins have little functional overlap or the overlapping functions are not essential for survival or embryonic development. Functions of the anterograde transport factors and endocytic factors tested in this study are briefly summarized in the following pages.

The best characterized families of transport vesicles are the clathrin coated vesicles, which are important for both endocytosis and intracellular trafficking. A typical clathrin coated transport vesicle contains three layers: an inner membrane and cargo layer, an outer layer of clathrin scaffold, and an intermediary layer containing adaptor proteins that link the clathrin scaffold to the cargo proteins and inner membrane. Thus, the adaptor proteins are required for maintaining the basic structures of coated vesicles.

**Table 5. Genetic interactions between *unc-50* and factors involved in anterograde trafficking and endocytosis**

| Mutation | Gene identity | synthetic phenotype |
|---|---|---|
| | **Adaptor proteins** | |
| *unc-101(sy108)* | µ1 subunit of adaptor protein complex 1 (AP-1) | normal growth |
| *dpy-23(e840)* | µ2 subunit of adaptor protein complex 2 (AP-2) | normal growth |
| *apb-3(ok429)* | β3 subunit of adaptor protein complex 3 (AP-3) | normal growth |
| *apt-9(tm3776)* | GGA protein | normal growth |
| *dab-1(gk291)* | DISABLED | normal growth |
| | **SNARE protein** | |
| *syn-13(tm2037)* | Syntaxin-13 | normal growth |
| | **Small GTPases** | |
| *arl-3(tm1703)* | ADP-ribosylation factor(ARF)-like protein | normal growth |
| | **Novel domain containing trafficking factors** | |
| *rme-1(b1045)* | EHD  protein required for endocytosis | normal growth |
| *rme-8(b1023)* | J-domain protein required for endocytosis | normal growth |
| | **Motor protein** | |
| *klp-4(tm2114)* | kinesin-like motor protein | normal growth |

UNC-101, DPY-23, and APB-3 are subunits of heterotetrameric adaptor protein complexes (APs). *unc-101* encodes the µ1 subunit of AP-1. In *C. elegans*, UNC-101 has been shown to be critical for transporting odorant receptors to the sensory cilia and for postsynaptic localization of glutamate receptor GLR-1, α7-type nicotinic nAChR ACR-16, and the receptor tyrosine kinase CAM-1/ROR in the interneuron RIA (Dwyer et al., 2001; Margeta et al., 2009). DPY-23 is the µ2 subunit of AP-2. AP-2 is the principal non-clathrin component of purified

endocytic clathrin coated vesicles. AP-2 is the only adaptor complex involved in endocytosis at the plasma membrane. AP-2 binds to different cargo recognizing motifs in cargo proteins, achieving a differential sorting function (Traub, 2009). *dpy-23* mutant displays a mislocalization of clathrin at the synapses, reduced synaptic vesicle numbers and impaired evoked responses (Gu et al., 2008). *apb-3* encodes the β3 subunit of AP-3, which is required for sorting transmembrane cargo to the late endosomal or lysosomal compartments (Owen et al., 2004).

APT-9 is a *C. elegans* ortholog of GGA (Golgi-localized, gamma ear-containing, ADP ribosylation factor-binding proteins) proteins. The GGAs localize at the TGN and facilitate recruitment of clathrin in an ARF-GTP dependent manner (Robinson, 2004). GGAs are required for sorting of mannose 6-phosphate receptors and sortilin from the TGN to the endosomes (Nielsen et al., 2001; Puertollano et al., 2001a; Puertollano et al., 2001b; Takatsu et al., 2001; Zhdankina et al., 2001).

DAB-1 is the only *C. elegans* homologue of Disabled proteins, which belong to a conserved family of monomeric adaptor proteins involved in endocytosis of lipoprotein receptors. DAB-1 localization in oocytes depends on clathrin and AP-2, while *dab-1* mutant is synthetic lethal with mutants in genes of the other two adaptors: *unc-101* and *apb-3* (Holmes et al., 2007).

Syntaxin-13 is an endosome localized SNARE protein, which is involved in homotypic fusion of early endosomes by interacting with calmodulin (Antonin et al., 2002; McBride et al., 1999; Mills et al., 2001). Syntaxin-13 is also required for interaction of endosomes and/or lysosomes with the phagosome (Collins et al., 2002).

arl-3 encodes an ARF (ADP-ribosylation factor)-like small GTPase that has been shown to be expressed in ciliated neurons in *C. elegans* (Blacque et al., 2005; Li et al., 2004). Yeast and human ARL-3 is required for the TGN localization of another ARF-like small GTPase, ARL-1, which recruits several GRIP domain containing long coiled-coil tethering factors like the yeast Imh1p, human Golgin-245 and Golgin-97 (Lu and Hong, 2003; Panic et al., 2003; Setty et al., 2003).

RME-1 is a conserved Eps-15 homology domain (EHD) containing protein. It was shown that RME-1 is involved in endocytic recycling to the plasma membrane (Grant et al., 2001). In *C. elegans*, mutation in *rme-1* impairs recycling of yolk protein receptors, thus causing a severe defect of yolk protein uptake by oocytes (Grant et al., 2001).

rme-8 encodes an endosome localized DnaJ domain protein (Zhang et al., 2001). RME-8 interacts with clathrin uncoating ATPase Hsc70 and the retromer subunit SNX-1 (Chang et al., 2004; Popoff et al., 2009; Shi et al., 2009). RME-8 is suggested to play a role in retrograde transport through endosomes. *rme-8*

mutant displays multiple defects, including strong endocytic defects in oocytes and coelomocytes, missorting of MIG-14/Wntless to the lysosomes and clathrin accumulation on endosomes (Shi et al., 2009; Zhang et al., 2001).

KLP-4 encodes a kinesin-like motor protein that belongs to the kinesin superfamily (KIFs). Its mammalian homologue KIF13A transports mannose-6-phosphate receptor (M6PR) containing vesicles and targets the M6PR from TGN to the plasma membrane via direct interaction with the AP-1 adaptor complex (Nakagawa et al., 2000). Interaction between AP-1 and KIF13A is also essential for delivering melanogenic enzymes from recycling endosomes to nascent melanosomes and for organelle biogenesis (Delevoye et al., 2009).

## 4.1.4 *unc-50* specifically interacts with genes involved in retrograde trafficking at the Golgi-endosomal interface

We reasoned that UNC-50 is probably not involved in anterograde transport or endocytosis, because mutations in genes required for anterograde transport or endocytosis are not lethal in combination with *unc-50* mutation. In contrast, when we tested genes encoding proteins involved in retrograde transport from endosome to Golgi, six candidates showed synthetic lethality with *unc-50* mutation (table 6) (Figure 15).

I constructed a strain containing a homozygous *unc-50(x47)* mutation and a heterozygous *vps-52(ok853)* mutation. Around 26% of its eggs showed embryonic lethality or arrest as young larvae and finally died after a few days. These eggs were identified as the homozygous *unc-50(x47);vps-52(ok853)* double mutants, which was confirmed by PCR. Although individual escapers could be observed, they produce no or few progeny and the whole population die in the end.

**Table 6. Genetic interactions between *unc-50* and retrograde trafficking factors**

| Mutation | Gene identity | synthetic phenotype |
| --- | --- | --- |
| **Tethering complex** | | |
| *vps-52(ok853)* | Subunit of GARP complex | lethal |
| *vps-54(ok1463)* | Subunit of GARP complex | lethal |
| *vps-51(tm4275)* | Subunit of GARP complex | normal growth |
| *cogc-1(k179)* | Subunit of COG complex | lethal |
| *cogc-3(k181)* | Subunit of COG complex | lethal |
| **Vesicle coat protein** | | |
| *vps-35(hu68)* | Subunit of retromer complex | lethal |
| *snx-1(tm847)* | Subunit of retromer complex | slow growth |
| **Small GTPase** | | |
| *rab-6.2(ok2254)* | Rab GTPase | lethal |
| **SNARE protein** | | |
| *syn-16(tm1560)* | Syntaxin-16 | normal growth |
| **Adaptor proteins** | | |
| *rsd-3(pk2010)* | EpsinR | normal growth |
| *rsd-3(pk2013)* | EpsinR | normal growth |

Synthetic lethality is also observed in *unc-50(x47);vps-54(ok1463)* double mutant. This indicates that survival of animals requires the functions of both proteins. Single mutants of *unc-50*, *vps-52* or *vps-54* are superficially wild type, although they produce less progeny than wild type (wild type: 290±7; *unc-50(x47)*: 244±7; *vps-52(ok853)*: 108±7; *vps-54(ok1463)*: 57±5; data represent average ± s.e.m). By co-expressing mRFP fused UNC-50 and mYFP fused VPS-52 in the body wall muscles, we can observe overlapping localization of these two proteins (Figure 14). Based on these facts, we conclude that UNC-50 and VPS-52 or VPS-54 may have redundant cellular functions. VPS-52 and VPS-54 are subunits of the GARP (Golgi associated retrograde protein) complex. In yeast, the GARP complex consists of four subunits, Vps51p, Vps52, Vps53, and Vps54p. The GARP complex belongs to a conserved family of quatrefoil tethering complexes including the exocyst and the conserved oligomeric Golgi (COG) complex, which are composed of multimers of fourfold-symmetric components. Tethering complexes help to make the match by tethering transport vesicles to the acceptor membrane, and also confer specificity for the fusion process by bringing the SNARE proteins in close proximity, thus allowing efficient SNARE pairing. The GARP complex is an effector of the Rab GTPase Ypt6p and the Arf like GTPase Arl1, and thought to function mainly in retrograde transport from endosome to Golgi (Conibear et al., 2003; Liewen et al., 2005; Panic et al., 2003; Siniossoglou and Pelham, 2001; Siniossoglou and Pelham, 2002). A double mutant of *unc-50(x47); vps-51(tm4275)* is viable, suggesting that VPS-51 might be an auxiliary subunit of the *C. elegans* GARP complex. This is consistent with the fact that

yeast *vps51* mutants show weaker growth defects than the other complex components, and the core complex is still correctly assembled and localized in the absence of Vps51p (Conibear et al., 2003; Siniossoglou and Pelham, 2002).
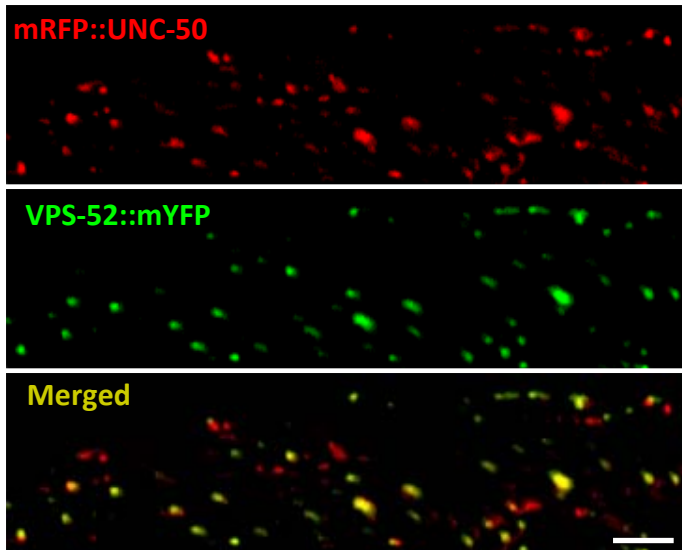


**Figure 14. UNC-50 and VPS-52 show partial colocalization in body wall muscles**

Confocal images showing a partial overlap of mRFP tagged UNC-50 and mYFP tagged VPS-52 in the body wall muscle. Scale bar, 5µm.

Mutations in subunits of COG complex COGC-1 and COGC-3 are also lethal if combined with *unc-50* mutation. COG complex shares structural and functional similarity with the GARP complex. It contains two subcomplexes, with 4 subunits in each (Loh and Hong, 2004; Ungar et al., 2002). Although it also tethers vesicles from the endosomes to the TGN, COG complex is proposed to act at multiple retrograde transport steps within the Golgi as well as from post-Golgi compartments to the Golgi and possibly for ER to Golgi transport (Bruinsma et al., 2004; Oka et al., 2004; Shestakova et al., 2007; Zolov and Lupashin, 2005). In *C. elegans*, *cogc-1(k179)* and *cogc-3(k181)* mutants show gonad migration defects,

which are caused by mislocalization of a Golgi nucleoside diphosphatase (NDPase) MIG-23, leading to underglycosylation of a secreted guiding cue, MIG-17 (Kubota et al., 2006).

Another mutation that is synthetically lethal with *unc-50* is *vps-35*. VPS-35 is the core subunit of the retromer complex, which plays essential roles in recycling cargo protein receptors from endosome back to TGN (Arighi et al., 2004; Coudreuse et al., 2006; Seaman, 2004; Seaman et al., 1997; Seaman et al., 1998; Verges et al., 2004). VPS-35 is required for recruiting cargo proteins into a specialized retrograde transport domain on the endosomal membrane. VPS-35 directly binds to vacuolar hydrolase receptor Vps10p and mannose-6-phosphate receptor to mediate their recycling from endosome to TGN, which is essential for anterograde transport of acidic hydrolase or its precursors to the late endosomes and lysosomes. SNX-1 is an associated subunit of retromer complex. SNX-1 contains a membrane curvature sensing BAR domain and a phox (PX) domain, which is important for the recruitment of retromer complex to the transport vesicles (Carlton et al., 2004). *unc-50(x47); snx-1(tm847)* double mutant is viable but displays mild growth impairment as compared to the single mutants. This is probably due to the redundancy of the SNX family, in which several SNXs seems to be inter-exchangeable (Rojas et al., 2007; Schwarz et al., 2002).

The last gene that shows synthetic lethality with *unc-50* is *rab-6.2*, encoding a TGN-localized small GTPase. Small GTPases are molecular switches that

shuttle between a GTP bound active form and a GDP bound inactive form. RAB-6.1 and RAB-6.2 are two isoforms of RAB-6 in *C. elegans*. Only the *rab-6.2* mutant was used here because the *rab-6.1* mutant is lethal. RAB-6 has essential roles in multiple Golgi trafficking pathways, particularly intra-Golgi and endosome to Golgi retrograde transport. In yeast, the RAB-6 homologue Ypt6p recruits the GARP complex to the TGN and regulates the COG complex function (Siniossoglou and Pelham, 2001; Sun et al., 2007). RAB-6 also shows strong interactions with long coiled-coil tethering factors like Imh1p in yeast and GCC185 in mammals (Barr, 1999; Li and Warner, 1996; Tsukada and Gallwitz, 1996).
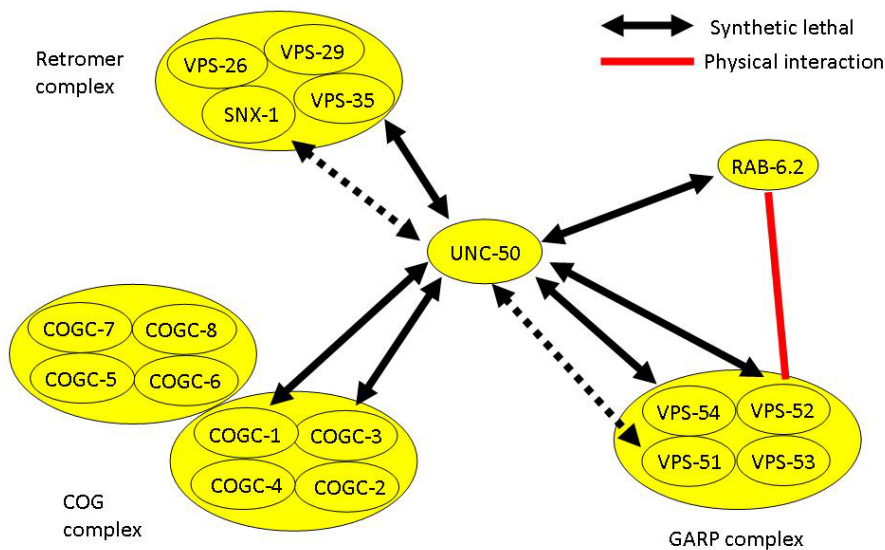


**Figure 15.** ***unc-50*** **mutation is synthetic lethal with mutations in trafficking factors involved in retrograde transport from endosome to Golgi**

Syntaxin-16 is a TGN localized SNARE. It is required for efficient retrograde transport of MPRs from endosome to TGN (Amessou et al., 2007; Ganley et al., 2008; Medigeshi and Schu, 2003). *unc-50(x47);syn-16(tm1506)* show normal

growth like the single mutants. Even a triple mutant *unc-50(x47);syn-13(tm2037);syn-16(tm1506)* is also viable. This may result from the large redundancy of SNAREs in the TGN-endosome interface.

*rsd-3* encodes the epsin-related protein (epsinR). epsinR is a monomeric adaptor protein that directly associates with clathrin and AP-1 at the TGN (Kalthoff et al., 2002). Although hosting anterograde transport at the TGN, epsinR also mediates recycling of mannose 6-phosphate receptor and SNARE Vti1b from late endosomes and lysosomes to TGN or early endosomes (Chidambaram et al., 2004; Hirst et al., 2004; Miller et al., 2007). However, *unc-50(x47);rsd-3(pk2010)* and *unc-50(x47);rsd-3(pk2010)* double mutants are viable like the single mutants.

In summary, we found that *unc-50* mutation shows specific synthetic lethality with mutations in genes encoding trafficking factors involved in retrograde transport from endosome to Golgi (Figure 15). Simultaneously interrupting the functions of UNC-50 and factors involved in anterograde transport or endocytosis did not result in a lethality phenotype. This suggests that UNC-50 might also be specifically required for retrograde transport from endosome to the Golgi.

## 4.1.5 Discussion

Based on the data from yeast, *C. elegans* and humans, we propose our model for UNC-50 function (Figure 16). There are two parallel or functionally redundant pathways at the TGN. One pathway is obligated for tethering vesicles from the

endosomes to the TGN. ARL3 binds to the integral membrane protein SYS1 on the surface of the TGN (Behnia et al., 2004; Setty et al., 2004). ARL3 recruits ARL1 to the TGN. Binding of the IMH1 GRIP domain to ARL1 brings this long coiled-coil tethering protein to the TGN (Panic et al., 2003). ARL1 also binds to the multiple subunit tethering complex GARP (Panic et al., 2003), which interacts with the TLG1 SNARE (Siniossoglou and Pelham, 2001). GARP localization to the TGN is primarily dependent on active GTP bound RAB-6 (Siniossoglou and Pelham, 2001). In the other pathway, UNC-50 is interacting with ARF-GEFs Gea1p and Gea2p (Chantalat et al., 2003), thus regulating membrane trafficking mediated by COPI vesicles and clathrin coated vesicles. UNC-50 might be involved in multiple transport events including protein sorting at the TGN and retrograde transport from endosome to the Golgi. It has been shown that UNC-50 is critical for levamisole receptor sorting after the receptor assembly (Eimer et al., 2007). Thus, the missorting of levamisole receptors in *unc-50* mutants occurs most likely at the TGN.
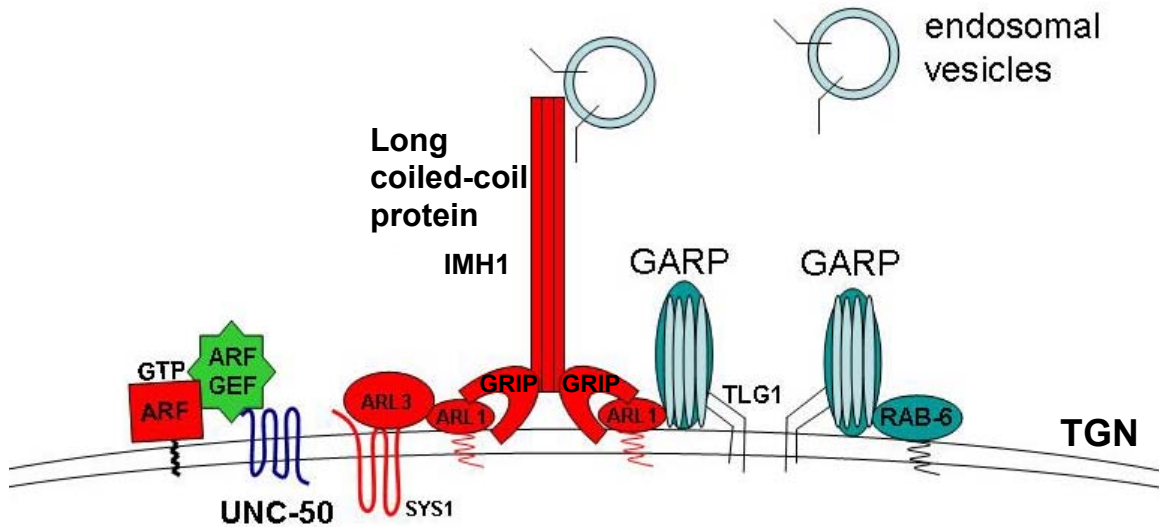
**Figure 16. Model of UNC-50 action**

Two parallel or functional redundant pathways exist at the TGN. UNC-50 is interacting with ARF-GEFs Gea1p and Gea2p, and regulating membrane trafficking mediated by COPI vesicles and clathrin coated vesicles. The other pathway is responsible for tethering endosomal vesicles to the TGN. ARL3 binds to the integral membrane protein SYS1 on the surface of the TGN. ARL3 recruits ARL1 to the TGN. Binding of the IMH1 GRIP domain to ARL1 brings this long coiled-coil tethering protein to the TGN. ARL1 also binds to a second vesicle tethering complex GARP, which interacts with the TLG1 SNARE. GARP primarily requires RAB-6(GTP) for localization to the TGN.

So far it is unclear how UNC-50 contributes to the correct sorting of levamisole receptors. It is possible that UNC-50 may stabilize levamisole receptor subunits by direct physical association with them. However, it appears that this is not likely to be true. A recent tandem affinity purification of the levamisole-sensitive nAChR from *C. elegans* was performed and a large-scale mass spectrometry of co-purified components revealed several novel regulators of levamisole receptors.

65

These include the calcineurin A subunit TAX-6, the copine NRA-1 and SOC-1, which acts in receptor tyrosine kinase (RTK) signaling (Gottschalk et al., 2005). However, UNC-50 was not found in this assay, indicating that UNC-50 may not interact with levamisole receptor subunits or if so then through a third player.

Recently, it has been shown that UNC-50 is also required for cell surface transport of ACR-2 containing nAChR, which is expressed in *C. elegans* cholinergic motor neurons. A gain of function mutant of *acr-2* displays hyperactivity of ACR-2 nAChR, thus causing muscle convulsions. This defect is suppressed by *unc-50* mutations as well as mutations in other subunits comprising ACR-2 receptor, like UNC-38 and UNC-63 (Jospin et al., 2009). Interestingly, UNC-38 and UNC-63 are also subunits of levamisole receptors (Culetto et al., 2004). Thus, levamisole receptor and ACR-2 receptor share subunits and both require UNC-50 for cell surface trafficking. It is possible that UNC-50 mediates levamisole receptor and ACR-2 receptor trafficking by interacting with the two common subunits UNC-38 and UNC-63.

Assembly and oligomerization of nAChRs occur within the ER in a sequential and ordered manner (Green and Millar, 1995; Smith et al., 1987). Several ER-resident chaperones are facilitating this process: non-specific chaperones like BIP and calnexin, as well as the nAChR specific chaperone RIC-3 (Forsayeth et al., 1992; Gelman et al., 1995; Halevi et al., 2002). The *C. elegans* Bip/Hsp70 homologues HSP-1, HSP-3, and HSP-4 were also found associated with

unassembled UNC-29 or LEV-1 subunits in a tandem affinity purification of these tagged subunits. The ER chaperones mostly dissociate from the subunits once the receptors are assembled (Gottschalk et al., 2005).

After pentameric assembly in the ER, the levamisole receptors are normally transported to the Golgi for modification and sorting, although it is possible that the receptors are directly delivered to the plasma membrane. In the Golgi, levamisole receptors may undergo posttranslational modification, like glycosylation and phosphorylation (Baker and Peng, 1993; Dellisanti et al., 2007; Hopfield et al., 1988; Huganir et al., 1986; Huganir et al., 1984; Kreienkamp et al., 1994; Peng et al., 1993; Poulter et al., 1989; Ramanathan and Hall, 1999; Wallace, 1994), which needs the action of different enzymes. If UNC-50 is required for maintaining the localization of these enzymes in the Golgi, then depletion of UNC-50 will cause defective modification and mislocalization of levamisole receptors.

Afterwards, levamisole receptors are transported to the TGN, where they are recruited by certain cargo carriers and concentrated in specialized vesicles that target the plasma membrane. In yeast, the UNC-50 homologue Gmh1p interacts with two ARF GEFs Gea1p and Gea2p. Gmh1p is localized to the early Golgi and functions at the ER-Golgi interface (Chantalat et al., 2003). However, in *C. elegans*, UNC-50 localizes to the Golgi, TGN and endosomes (Figure 11), thus it is more likely to act at the medial Golgi and Golgi-endosomal interface. It is

possible that UNC-50 is required for recruiting ARF-GEFs to a specialized microdomain of the Golgi or TGN, which separates some factors away. Otherwise, the levamisole receptors would be transported to the lysosomal pathways, as default setting. If UNC-50 is indispensable for sorting these degradative factors away, then the loss of UNC-50 will lead to missorting of levamisole receptors to the lysosomal systems.

In our study, we found that UNC-50 plays redundant roles with GARP complex, retromer complex and COG complex in retrograde transport from endosome to Golgi. Based on studies about how these trafficking factors recycle cargo protein receptors from endosome back to Golgi, a similar mechanism for UNC-50 can be proposed. The default degradative factors may not be inhibited directly by UNC-50. Signaling molecules from the synapses may also be involved. If more levamisole receptors are required at the postsynaptic membrane, the signaling molecules are released from the synapses by endocytosis, enter the early endosomes and are transported back to the TGN or Golgi with the assistance of UNC-50. Once they reach TGN or Golgi, they inhibit the degradative factors of levamisole receptors. Thus more levamisole receptors can be incorporated into the synapses. One reasonable way to find out UNC-50 downstream effectors that regulate levamisole receptor sorting is to perform a genetic screen for mutations that suppress the levamisole resistance phenotype in *unc-50* mutants.

# Part II

# UNC-50 controls distal tip cell migration by

# regulating secretion of MIG-17

The synthetic lethality analysis suggests that UNC-50 is involved in an evolutionarily conserved membrane transport pathway regulating Golgi retrieval at the Golgi-endosomal interface. We reasoned that if UNC-50 would be involved in a general transport pathway, there should be additional substrates that might be affected by loss of UNC-50 activity. Therefore, we re-examined *unc-50* mutant animals to detect additional phenotypes.

## 4.2.1 *unc-50* mutants display gonad morphology defects

By careful examination under a dissecting microscope and differential interference contrast (DIC) microscope, we found that *unc-50* mutants show an abnormal morphology of the posterior gonad (Figure 18). *C. elegans* adult hermaphrodites have two symmetrical U-shaped gonad arms, whose morphology is determined by the migration path of the leading cells located at the distal end of the elongating gonad. These cells are referred as distal tip cells (DTCs) (Figure 17) (Hedgecock et al., 1987; Kimble, 1981). The elongation of the gonads initiate at the vulva region on the ventral side of the body. Three phases can be defined over the whole gonad elongation process: phase 1, initial migration along the ventral body wall muscle; phase 2, migration from ventral to dorsal side of the body by crossing the midline; phase 3, migration along the dorsal body wall muscle in an opposite direction to phase 1 (Hedgecock et al., 1987; Su et al., 2000). We observed that in a population of *unc-50(x47)* mutant worms, 63.9% of animals do not show a U-like shape posterior gonad. Instead, the gonad arm which is supposed to be positioned on the dorsal side shows large overlap with

the gonad arm on the ventral side (Figure 18). Thus, in *unc-50* mutants the DTCs do not cross the midline to the dorsal side but instead migrate back on the ventral side.
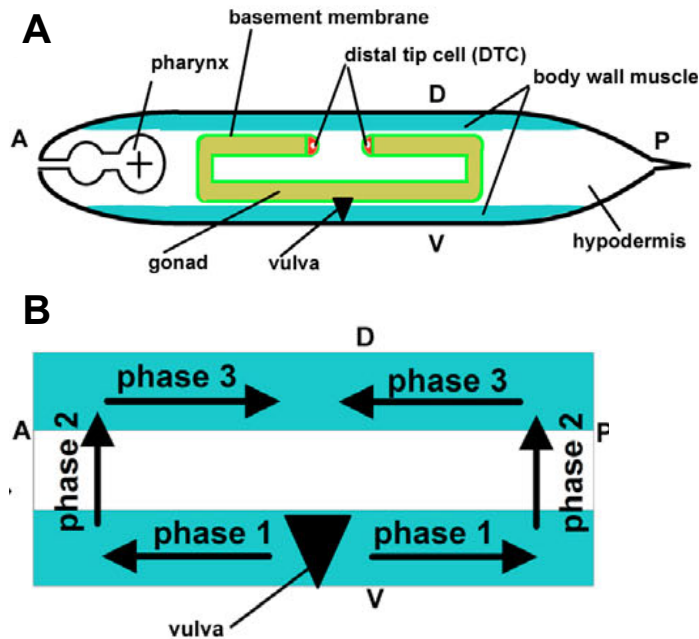


**Figure 17. Schematic diagrams of gonad morphology in the wild type hermaphrodite and phases of DTC migration (adapted from Kubota et al., 2006)**

(A) Ventral and dorsal body wall muscles are shown in blue. Gonad arms (yellow) are surrounded by basement membranes (green). The uncolored part corresponds to the lateral hypodermis. Two DTCs (red) are generated at the anterior and posterior ends of the gonad arms, located at the ventral mid-body, and migrate in a U-shaped pattern during gonad development. A: anterior, P: posterior, D: dorsal, V: ventral.

(B) DTC migration comprises three phases: the initial migration on the ventral body wall muscle (phase 1), the ventral-to-dorsal migration along the lateral hypodermis (phase 2) and the migration along the dorsal body wall muscle (phase 3) (Hedgecock et al., 1987; Su et al., 2000).

Interestingly, we found that the DTC migration defect in *unc-50* mutants highly resembles the phenotype in *mig-17(k174)* mutant, in which 39.8% of the worms

show this defect (Figure 18, 19). *mig-17* encodes an ADAM (<u>A</u> <u>D</u>isintegrin <u>A</u>nd <u>M</u>etalloprotease) family protein. MIG-17 is secreted from the body wall muscles and controls the DTC migration by localizing to the gonadal basement membrane.
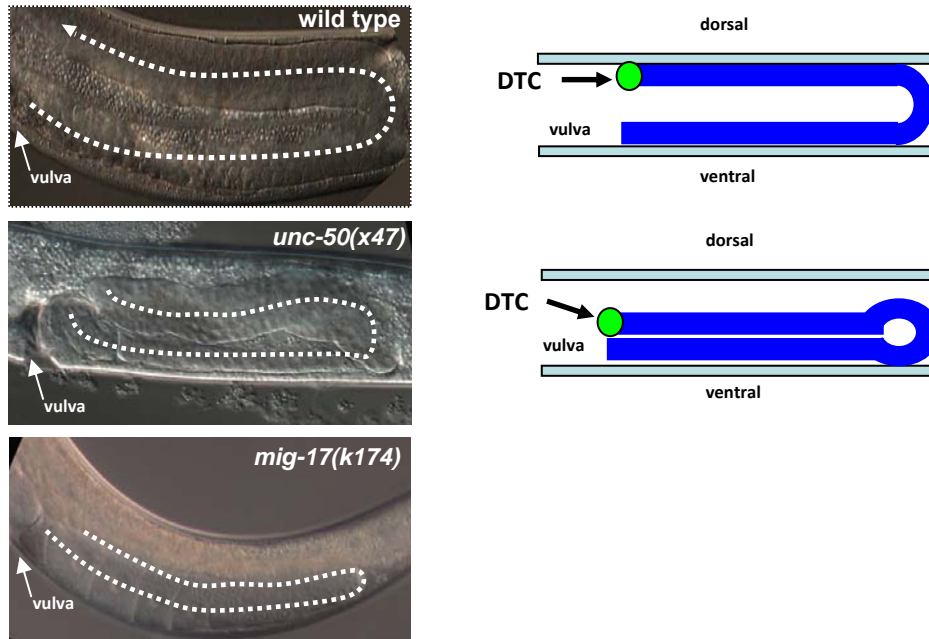


**Figure 18. *unc-50(x47)* mutant phenocopies *mig-17(k174)* mutant in DTC migration defect**

Normal gonad in wild type animals shows a U-like shape, with two arms attached to ventral and dorsal side of the body wall muscles. In *unc-50(x47)* mutant, one gonad arm is attached to the ventral body wall muscle and the other arm places at the middle line of the body or also attaches to the ventral body wall muscle. This phenotype is similar in *mig-17(k174)* mutant and caused by a mis-migration of the DTCs. Pictures were taken under a DIC microscope.

**4.2.2 UNC-50 is required in body wall muscle for normal DTC migration**

Since UNC-50 has been shown to be ubiquitously expressed (Eimer et al., 2007), we wanted to determine the tissue in which UNC-50 activity is required for proper DTC migration. It is possible that losing UNC-50 in the DTC will cause an abnormal migration path. In order to verify this idea, we tried to rescue the DTC migration defects in *unc-50(x47)* mutant by expressing UNC-50 under a DTC specific promoter *Plag2*. However, we did not see a significant reduction in the percentage of defects (60.5%, Figure 19). Considering the fact that UNC-50 has an important function in body wall muscles to regulate levamisole receptor trafficking (Eimer et al., 2007), we expressed UNC-50 under the control of a body wall muscle specific promoter *Pmyo3* in *unc-50(x47)* mutant. As shown in Figure 19, expression of UNC-50 exclusively in body wall muscles is sufficient to rescue DTC migration defects in *unc-50(x47)* mutant. These results suggest that UNC-50 dependent signals from the body wall muscles have important roles in regulating DTC migration. Since UNC-50 is involved in Golgi transport, this might be a membrane protein or secreted factor from body wall muscles.

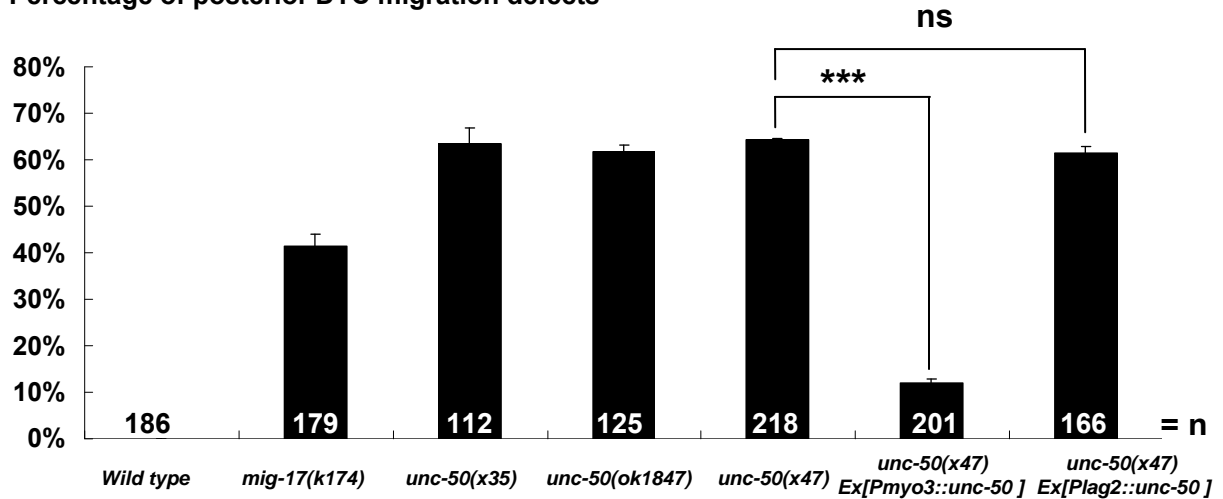**Percentage of posterior DTC migration defects**



**Figure 19. Muscle expression of UNC-50 rescues DTC migration defect in *unc-50(x47)* mutant**

41.3% of the *mig-17(k174)* mutant worms show DTC migration defect. 63.4% of *unc-50(x35)*, 61.6% of *unc-50 (ok1847)*, and 64.2% of the *unc-50(x47)* mutant worms show DTC migration defect. Expression of UNC-50 in the body wall muscles reduces the DTC defect in *unc-50(x47)* mutant to 11.9%. However, expression of UNC-50 in DTCs of *unc-50(x47)* mutant does not rescue this phenotype, since they show DTC defect in 61.4% of the transgenic worms. (Three independent experiments were performed on each strain. Total number of animals analyzed is indicated in the graph bars. Error bars represent standard deviation. ***=p<0.005, ns=not significant, by student's T-test.)

## 4.2.3 UNC-50 and MIG-17 act in the same pathway to control DTC migration

It was shown that expression of MIG-17 in the body wall muscles or ectopically in DTCs rescues the DTC migration phenotype in *mig-17(k174)* mutant (Nishiwaki et al., 2000). In *unc-50* mutants and *mig-17(k174)* mutant, phenotypes are similar,

and both result from an impaired signaling from the body wall muscle. Since MIG-17 is a secreted factor, we reasoned that UNC-50 may regulate the secretion of MIG-17 from body wall muscles.

To analyze this further, we looked at genes that have been shown to interact with *mig-17*. It was shown that dominant mutations in the *fbl-1* gene bypass the requirement for MIG-17 activity in directing DTC migration. *fbl-1* encodes a protein which is highly homologous to the human fibulin-1 spliced isoforms (Kubota et al., 2004). Fibulins belong to a family of extracellular matrix proteins. Fibulins are able to bind to calcium and associate with basement membranes, blood plasma and elastic extracellular matrix fibers (Timpl et al., 2003). In *C. elegans*, FBL-1 is synthesized in the gut cells and localized to the gonadal basement membrane in a MIG-17 dependent way. Two single amino acid substitution mutants *k201* (glycine-249-glutamate), and *k206* (histidine-251-tyrosine) were isolated and mapped to the third calcium binding EGF-like motif region of the FBL-1C isoform. Both *fbl-1(k201);mig-17(k174)* and *fbl-1(k206); mig-17(k174)* show normal gonad morphology (Kubota et al., 2004).

If UNC-50 is required for MIG-17 secretion, then the *fbl-1* suppressor mutations should suppress the DTC migration defects in *unc-50* mutants. So we constructed double mutants *unc-50(x47); fbl-1(k201)* and *unc-50(x47); fbl-1(k206)*. Strikingly, the two *fbl-1* point mutations show significant rescue of DTC migration defects in *unc-50(x47)* mutant. Other alleles of *unc-50* mutant are also

suppressed by the *fbl-1* point mutants (Figure 20). Further more, we made a double mutant of *unc-50(x47); mig-17(k174)* and found that the percentage of worms showing DTC migration defect in the double mutant is not different from that in the *unc-50(x47)* single mutant (Figure 21). These data suggest that UNC-50 and MIG-17 are acting in the same genetic pathway to regulate DTC migration. Thus, it is likely that UNC-50 directly regulate MIG-17 secretion or processing.
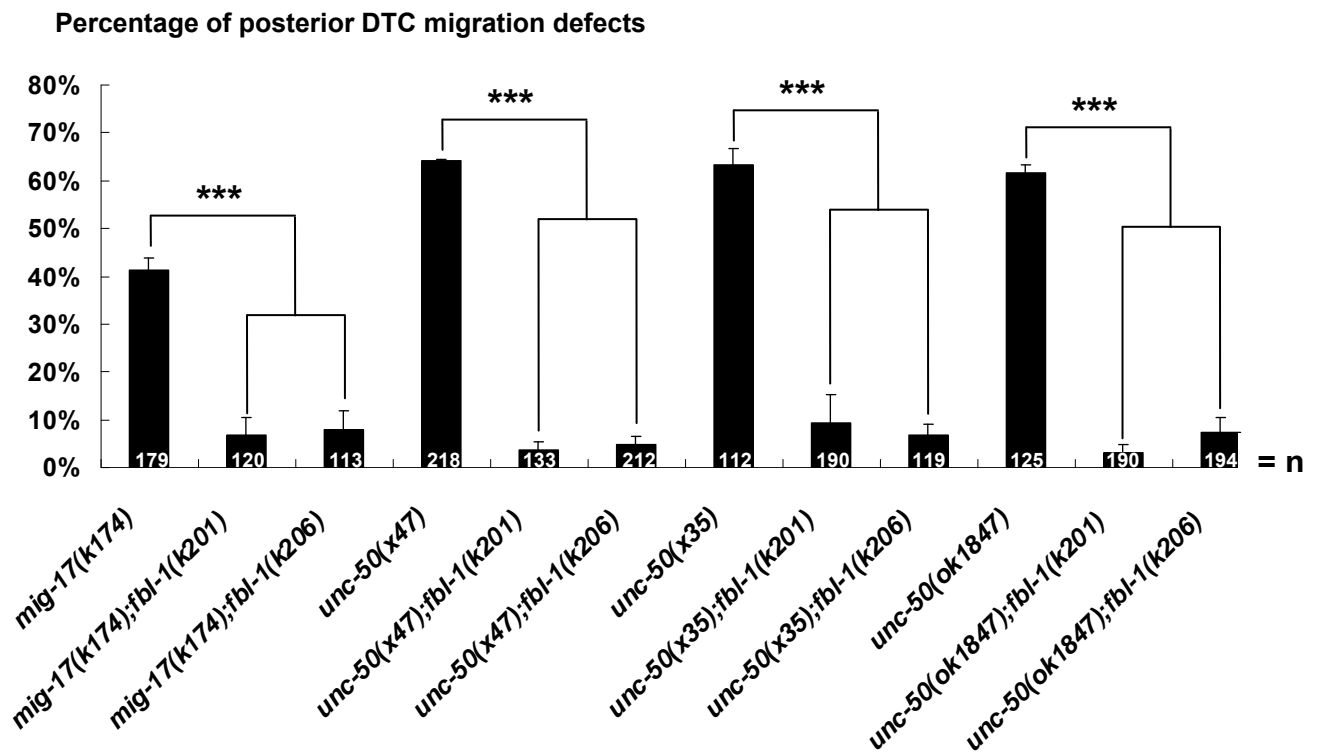
**Percentage of posterior DTC migration defects**



**Figure 20. Point mutations in *fbl-1* suppress DTC migration defect in *mig-17* and *unc-50* mutants**

When combined with point mutation *fbl-1(k201)* or *fbl-1(k206)*, *mig-17(k174)* and *unc-50* mutants show much less DTC migration defect than the single mutants. (Three independent experiments were performed on each strain. Total number of animals analyzed is indicated in the graph bars. Error bars represent standard deviation. \*\*\*=p<0.005 , by student's T-test.)

**Percentage of posterior DTC migration defects**

ns

70%

60%

50%

40%

30%

20%

10%

0%

179   218   220   = n

*mig-17(k174)*   *unc-50(x47)*   *unc-50(x47); mig-17(k174)*
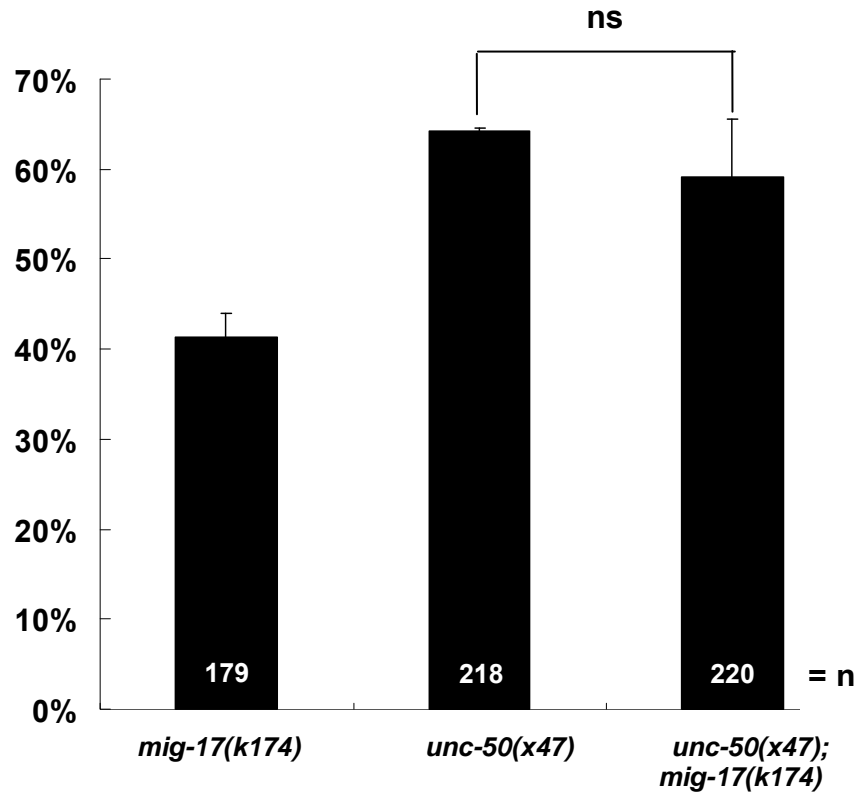
**Figure 21.** *mig-17* **and** *unc-50* **act in the same genetic pathway to control DTC migration**

Double mutant of *unc-50(x47);mig-17(k174)* shows similar percentage of DTC defect (59.1%±6.4%) as *unc-50(x47)* single mutant (64.2%±0.3%). (Three independent experiments were performed on each strain. Total number of animals analyzed is indicated in the graph bars. Error bars represent standard deviation. ns=not significant, by student's T-test.)

## 4.2.4 Overexpressed and secreted MIG-17::Venus can be localized and processed normally in *unc-50* mutants

Recently, it was shown that MIG-17 contains several functional domains. MIG-17 is secreted from the muscle cells as a proform with a glycosylated N-terminal prodomain. The prodomain plays an essential role in localizing MIG-17 to the gonadal basement membrane. Then upon some unknown signals, MIG-17

77

autocatalytically cleaves off its prodomain to form the mature and active matrix metalloprotease. The mature form is anchored to gonadal basement membranes and contains a metalloprotease (MP) domain, a disintegrin (DI) domain, and a protease and lacunin (PLAC) domain (Figure 22) (Ihara and Nishiwaki, 2007).
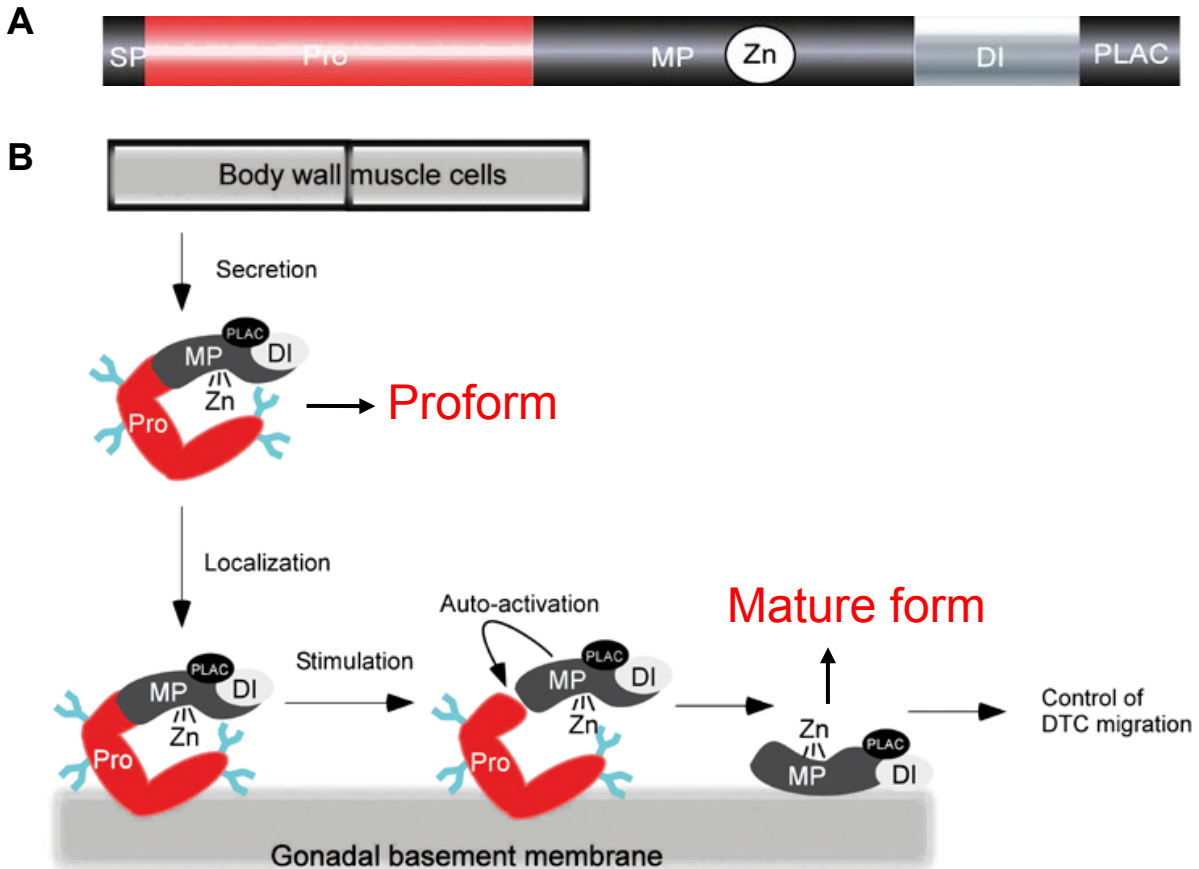


**Figure 22. Model of MIG-17 action in gonad development (Adapted from Ihara and Nishiwaki, 2007)**

(A) Full length MIG-17 contains a prodomain at the N-terminal, followed by a metalloprotease (MP) domain, a disintegrin (DI) domain, and a protease and lacunin (PLAC) domain at the C-terminal.

(B) MIG-17 is secreted from the body wall muscle as a proform, which contains a glycosylated prodomain. MIG-17 localizes at the gonadal basement membrane by its prodomain. Then the prodomain is cleaved by auto-catalyzed activation. The rest part of MIG-17 becomes the mature form and controls the DTC migration.

In order to determine the localization and processing of MIG-17 in *unc-50* mutants, we overexpressed MIG-17::Venus under its own promoter in wild type and *unc-50(x47)* mutant worms. As shown in Figure 24A, MIG-17::Venus concentrates on the basement membrane of the U-shaper gonad in wild type. This localization appears unchanged in *unc-50(x47)* mutant (Figure 24A). We further examined the MIG-17::Venus localization by immunostaining worm cross sections with an anti-GFP antibody which also detects Venus-YFP. In both wild type and *unc-50(x47)* mutant, clustered MIG-17::Venus can be detected on the gonadal surface (Figure 24B). Then we made crude extracts from these transgenic worms, and performed western blotting with anti-GFP antibody. Two bands can be observed on the membrane: a 100kD band representing the proform of MIG-17::Venus and a 70kD band representing the mature form. The two bands were seen for both wild type and *unc-50(x47)* mutants. This indicates that overexpressed MIG-17 can be secreted and processed to its mature form in *unc-50* mutants. Thus, UNC-50 is not required for MIG-17 processing nor for the correct localization of the active metalloprotease to the basement membrane. Since MIG-17::Venus is overexpressed, this may mask the possible MIG-17 sorting defects by oversaturating the secretory system, thus forcing the secretion of MIG-17 in *unc-50* mutants.
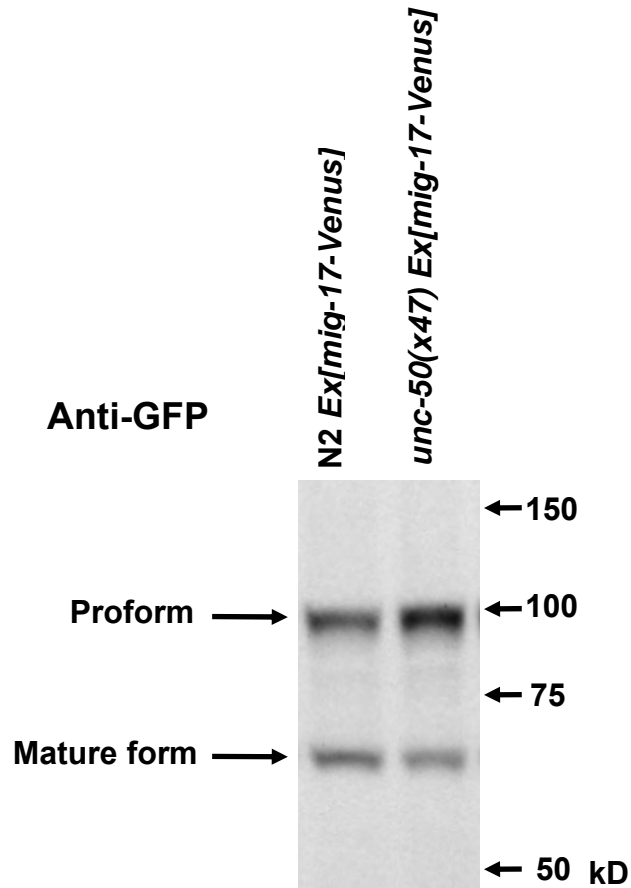
**Anti-GFP**

N2 Ex[mig-17-Venus]

unc-50(x47) Ex[mig-17-Venus]

Proform →

← 150

← 100

← 75

Mature form →

← 50 kD

**Figure 23. MIG-17-Venus expression is normal in *unc-50(x47)* mutants**

Transgenic worms that express MIG-17-Venus were constructed on the background of wild type and *unc-50(x47)* mutant. Western blot was performed on crude extracts of these two strains, with detection by anti-GFP antibody. For both strains, we can detect a band of about 100kD, which represents the proform, and a band of around 70kD, representing the mature form of MIG-17-Venus.

**A**



**B**
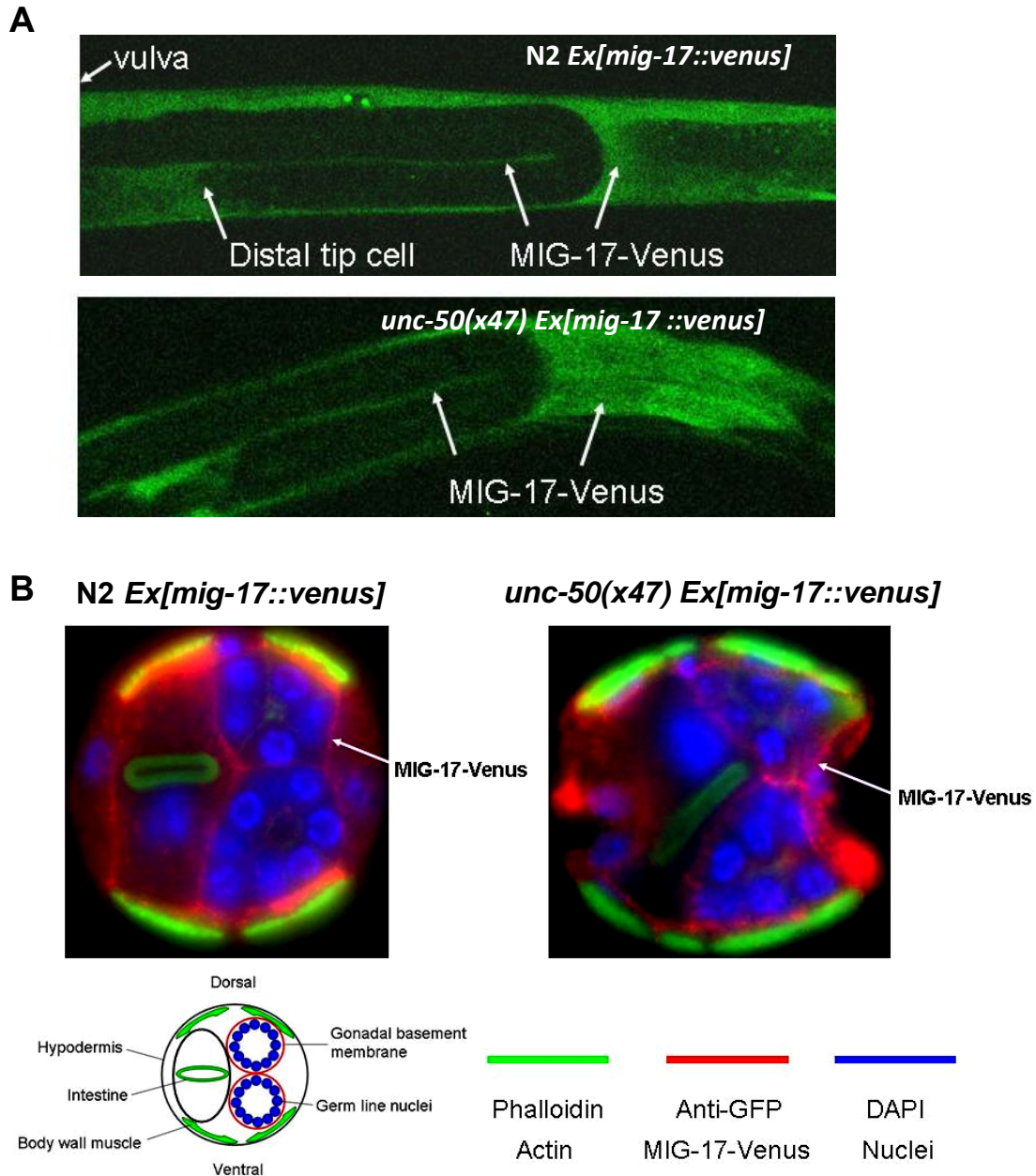


**Figure 24. MIG-17::Venus localization is not impaired in *unc-50(x47)* mutants**

(A) Confocal images of wild type and *unc-50(x47)* worms expressing MIG-17::Venus. MIG-17::Venus can be detected on gonadal basement membrane in both wild type and *unc-50(x47)*.

(B) Immunostaining of cross sections of wild type and *unc-50(x47)* worms expressing MIG-17::Venus. Nuclei in the gonad are labeled with DAPI. Body wall muscles are marked with phalloidin bound actin. MIG-17::Venus is detected with anti-GFP antibody. MIG-17::Venus punctuate structures are concentrated on the surface of gonad in both wild type and *unc-50(x47)*.

## 4.2.5 Overexpression of MIG-17::Venus rescues DTC migration defect in *unc-50* mutants in a dose dependent manner

An interesting phenomenon we found was that in *unc-50(x47)* mutant worms that overexpress MIG-17::Venus, the DTC migration defect was largely rescued (Figure 25). To test whether just the overexpression of a secreted protein within the secretory system of *unc-50* mutant may unspecifically allow MIG-17 secretion, we overexpressed an unrelated protein, secreted GFP, in body wall muscles of *unc-50* mutants. However, we did not observe significant reduction in DTC migration defects as compared to *unc-50* mutants (Figure 25). It was shown that very low level expression of MIG-17::GFP is sufficient to rescue the DTC migration defect in *mig-17(k174)* mutant (Ihara and Nishiwaki, 2007). We were therefore wondering whether expression of MIG-17::Venus at lower levels would be still able to rescue the DTC defects in unc-50 mutants. We generated transgenic lines expressing low amount of MIG-17::Venus in *mig-17(k174)* and *unc-50(x47);mig-17(k174)* mutants. As shown in Figure 26, these low-copy arrays rescued the DTC migration defect in *mig-17(k174)* mutant very well. However, in *unc-50(x47);mig-17(k174)* mutant, no significant rescue could be detected. This suggests that in *unc-50* mutants, MIG-17 is not efficiently secreted, leading to the DTC migration defects. However, UNC-50 is not strictly required for MIG-17 secretion, since oversaturating the secretory system with MIG-17 allows MIG-17 to be secreted. Thus, UNC-50 activity might be necessary for efficient secretion of MIG-17.
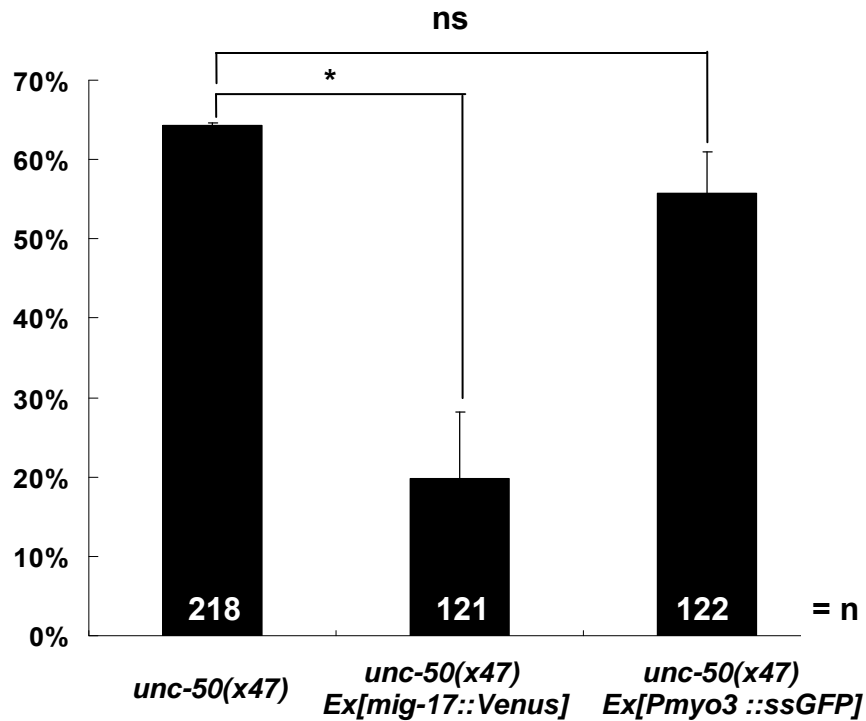
**Percentage of posterior DTC migration defects**



**Figure 25. High expression of MIG-17-Venus in the body wall muscles of *unc-50(x47)* mutant rescues the DTC migration defect in *unc-50(x47)* mutant**

In *unc-50(x47)* mutant, 64.2%±0.3% of the worms show DTC migration defect. When MIG-17-Venus is expressed in a high level in *unc-50(x47)*, only 19.8%±8.4% of the worms show DTC defect. This rescuing effect is MIG-17::Venus specific, since overexpression of ssGFP in the body wall muscles did not rescue the DTC defect in *unc-50(x47)* mutant (55.7%±5.2%). (Three independent experiments were performed on each strain. Total number of animals analyzed is indicated in the graph bars. Error bars represent standard deviation. *=p<0.05, ns=not significant, by student's T-test.)

**Percentage of posterior DTC migration defects**
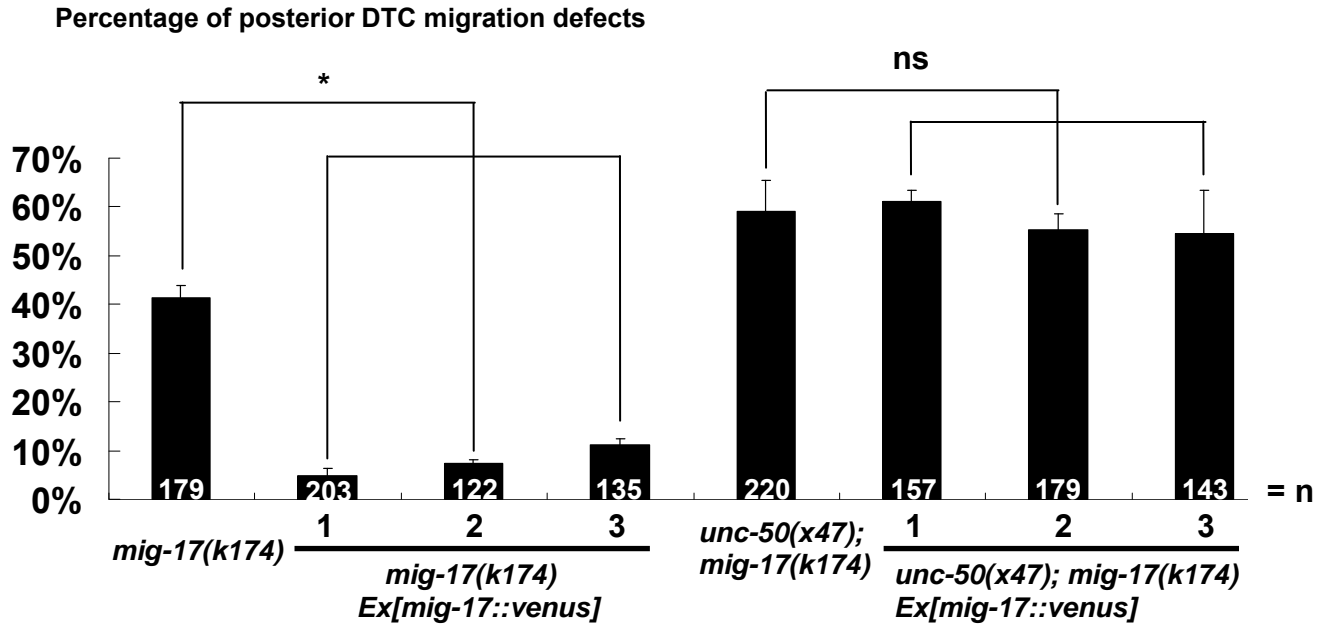


**Figure 26. Rescue of DTC migration defect in *unc-50(x47)* mutant by expressing MIG-17-Venus is a dose-dependent effect**

Plasmids mixture containing low concentration of MIG-17-venus was injected into the gonads of *mig-17(k174)* and *unc-50(x47);mig-17(k174)* mutant worms to make transgenic lines. Three transgenic lines were created for both *mig-17(k174)* and *unc-50(x47);mig-17(k174)*. This low level expression of MIG-17-Venus is sufficient for rescuing the DTC defect in *mig-17(k174)* mutant: from to 41.3%±2.6% to 4.9%±1.4%, 7.4%±0.6%, or 11.1%±1.4%, concerning the rates of defect. However, this is not able to rescue the DTC defect in *unc-50(x47);mig-17(k174)* mutant, since the three transgenic lines show defect in 61.1%±2.2%, 55.3%±3.2%, 54.5%±9% of the worms, which is not significantly different from 59.1%±6.4% for *unc-50(x47);mig-17(k174)* itself. (Three independent experiments were performed on each strain. Total number of animals analyzed is indicated in the graph bars. Error bars represent standard deviation. *=$p<0.05$, ns= not significant, by student's T-test.)

## 4.2.6 RAB-5 dominant negative form rescues the DTC migration defect in *unc-50* mutants

From the synthetic lethality analysis, we got evidence that UNC-50 might be a general trafficking factor involved in retrograde transport from endosome to Golgi. MIG-17 is a soluble protein that needs to be secreted from the body wall muscles. So it is possible that UNC-50 is required to regulate MIG-17 secretion. In *unc-50(x47)* mutants, the levamisole receptor subunit UNC-29 is missorted to lysosomes and degraded. Genetic blocking of lysosomal pathway makes UNC-29 reappear in total crude extracts of *unc-50(x47)* mutant worms, shown by western blot (Eimer et al., 2007). In order to test the fate of endogenous MIG-17 in the secretory pathway of *unc-50(x47)* mutants, we introduced a dominant negative (DN) form of RAB-5 into *unc-50* mutant background. This dominant negative RAB-5 contains a single amino acid substitution (S34N), rendering it in a GDP bound inactive state. Conversion of early endosomes to late endosomes involves recruitment of Rab7 GEF VPS39 mediated by active Rab5 (Rink et al., 2005). Thus, expression of RAB-5 (DN) would interrupt the normal endosomal functions and result in a re-routing of MIG-17::Venus in the secretory pathway. As shown in Figure 27, transgenic *unc-50*(x47) mutant worms expressing RAB-5 (DN) have a much lower percentage of DTC migration defect than the non-transgenic *unc-50(x47)* mutant. Dominant active RAB-5, which is predominantly GTP bound, failed to rescue the DTC phenotype in *unc-50(x47)* mutant. These data indicate that MIG-17 is probably mis-routed to lysosomes and degraded in

*unc-50(x47)* mutant and by interfering with lysosomal pathway, part of MIG-17 is re-routed to be secreted, thus rescuing the DTC migration defect in unc-50 mutant.

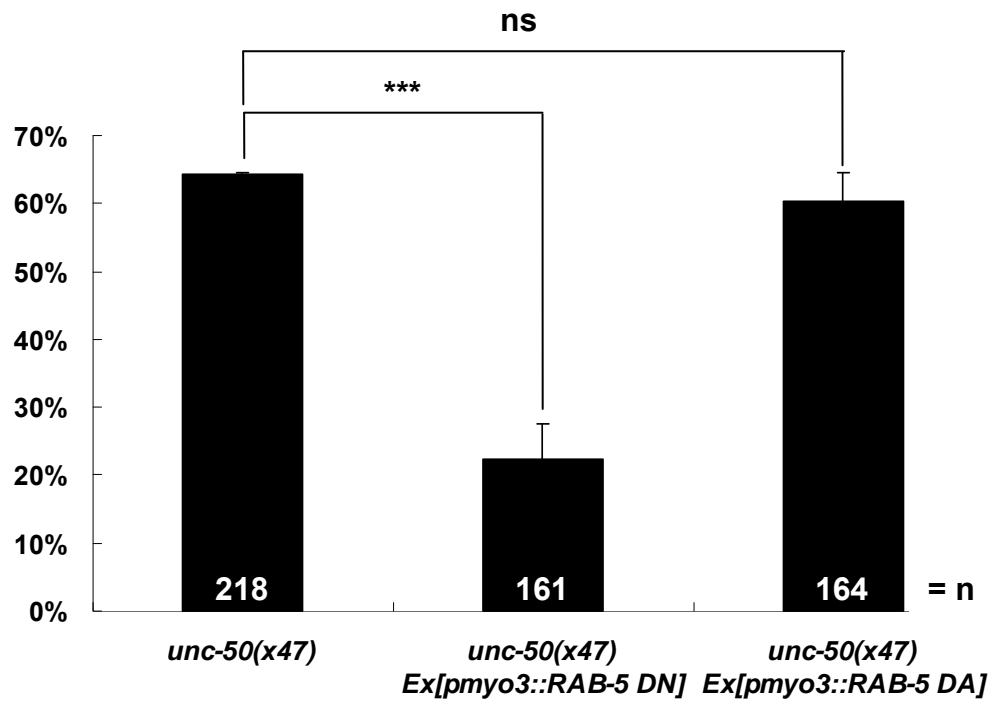**Percentage of posterior DTC migration defects**



**Figure 27. Expression of dominant negative form of RAB-5 in body wall muscles rescuing the DTC migration defect in *unc-50* mutants**

When dominant negative form of RAB-5 is expressed in the body wall muscles of *unc-50(x47)* mutants, percentage of DTC defect decreases from 64.2%±0.3% to 22.4%±5.2%. Expression of dominant active form of RAB-5 failed to rescue the DTC phenotype, as the defect rate remains at 60.4%±4.3%. (Three independent experiments were performed on each strain. Total number of animals analyzed is indicated in the graph bars. Error bars represent standard deviation. ***=p<0.005, ns= not significant, by student's T-test.)

## 4.2.7 Discussion

We observed DTC migration defects in *unc-50* mutants, which is similar to that seen in *mig-17* mutants. Defects in both mutants result from impaired signaling from the body wall muscles. *unc-50* and *mig-17* share the same genetic pathway to control DTC migration. Overexpression of MIG-17::Venus rescues the DTC migration defects in *unc-50* mutants. Once overexpressed in *unc-50* mutants, part of MIG-17::Venus can be secreted from the muscle cells and properly localized to the gonadal basement membrane to direct DTC migration like they do in wild type worms. However, when expressed at very low level, MIG-17::Venus failed to rescue the defects in *unc-50* mutants although they are enough to rescue the phenotype in *mig-17(k174)* mutant. Since this low level expression of MIG-17::Venus is not detectable by microscope, we were not able to determine whether they are secreted  and whether they are localized correctly.

MIG-17::Venus is secreted as a proform containing the prodomain, which is critical for MIG-17::Venus localization on the membrane. After targeted on the gonadal membrane, MIG-17:::Venus became a mature form by autocatalytic cleavage of the prodomain (Ihara and Nishiwaki, 2007). Thus on western blotting membrane, anti-GFP antibodies can recognize two bands: proform at 100kD and mature form at 70kD (Figure 23). We noticed that in wild type worms overexpressing MIG-17::Venus, the proform to mature form ratio is much lower than that in *unc-50* mutant expressing similar level of MIG-17::Venus (1:3 as measured in Figure 23). This suggests that higher fraction of MIG-17::Venus stay

as proform in *unc-50* mutants than in wild type. It is possible that this higher ratio of proform represents that more MIG-17::Venus are trapped in the body wall muscles in *unc-50* mutant.

We also found that interfering with the endosomal pathway by expressing a dominant negative form of RAB-5 rescues the DTC phenotype in *unc-50* mutants. RAB-5 is the key regulator of early endocytic events. Overexpression of RAB-5 dominant negative form inhibits receptor-mediated and fluid-phase endocytosis (Barbieri et al., 2000; Galperin and Sorkin, 2003; Mukhopadhyay et al., 1997; Schmidlin et al., 2001; Seachrist et al., 2000; Volpicelli et al., 2001), and delocalizes a RAB-5 effector EEA1 (Early Endosome Antigen1) from the early endosomes (Christoforidis et al., 1999; Haas et al., 2005; Simonsen et al., 1998). There are two possibilities for the rescuing effect of RAB-5 (DN): 1) Secreted MIG-17::Venus is constantly endocytosed and recycled by the body wall muscle cells, which might be mediated by RAB-5. Suppressing this process by expressing RAB-5 DN reduces the amount of recycled MIG-17::Venus. More MIG-17::Venus remains outside the muscle cells and bound to the gonadal membrane, thus decreasing the rate of DTC migration defect. 2) EEA1 is an important regulator of endosomal functions like endosome docking and fusion (Christoforidis et al., 1999; McBride et al., 1999) and it is recruited to the early endosomes by GTP bound RAB-5 (Simonsen et al., 1998). Keeping RAB-5 at the GDP bound form makes it detach from the early endosomes (Haas et al., 2005) and might cause impaired endosomal functions including cargo sorting. Thus

MIG-17::Venus that would have been sorted to the lysosomes might be re-routed from the degradative pathway under such conditions and get partial recovery.

Through the synthetic lethality analysis, we show that mutants in the COG complex subunits *cogc-1(k179)* and *cogc-3(k181)* are lethal in combination with *unc-50(x47)*. This indicates that UNC-50 and the COG complex have redundant or parallel cell functions, which are critical for animal viability. Interestingly, in COG complex subunit mutants *cogc-1(k179)* and *cogc-3(k181)*, the similar DTC migration defects observed in *mig-17* mutants are also reported. Knockdown of any of the other six COG subunits also produces similar defects, suggesting that an integrate COG complex is required. However, COG complex seems not directly required for secretion of MIG-17 from the body wall muscles, but is necessary for the glycosylation and gonadal localization of MIG-17. A membrane bound Golgi nucleoside diphosphatase (NDPase) required for proper glycosylation and localization of MIG-17, MIG-23, is mislocalized and destabilized in *cogc-1(k179)* and *cogc-3(k181)* mutants (Kubota et al., 2006; Nishiwaki et al., 2004). This raises the possibility that the COG complex is required for maintaining the proper localizations of a subset of glycosylation enzymes in the Golgi.

COG activity is required for correct MIG-17 glycosylation and thus for its activity. However, it appears that UNC-50 regulates MIG-17 function in a different way. In *cogc-1(k179)* and *cogc-3(k181)* mutants overexpressing MIG-17::Venus, DTC

migration defect is not rescued. And secreted MIG-17::Venus can not be localized to the gonadal basement membrane properly in the COG mutants. In contrast, expression of MIG-17::Venus rescues the DTC migration defect in *unc-50* mutants in a dose dependent manner. Once secreted, MIG-17::Venus is correctly localized to the surface of gonadal membrane, independent of UNC-50. Thus, the glycosylation of MIG-17::Venus in *unc-50* mutant seems to be normal. UNC-50 might specifically regulate the secretion of MIG-17. Although UNC-50 and the COG complex have overlapping functions, they may regulate MIG-17 dependent DTC migration in different manners.

In summary, our data support the model that UNC-50 is required for the proper secretion of MIG-17. It is possible that MIG-17 needs a cargo carrier, which recruits MIG-17 into secretory vesicles at the TGN and dissociates from MIG-17 after the vesicles fuse with the plasma membrane. UNC-50 might be required for retrograde transport of MIG-17 secretion carriers from endosomes to TGN. In *unc-50* mutants, MIG-17 carrier might be missorted to the lysosomes degraded, thus causing secretion defect of MIG-17 (Figure 28).
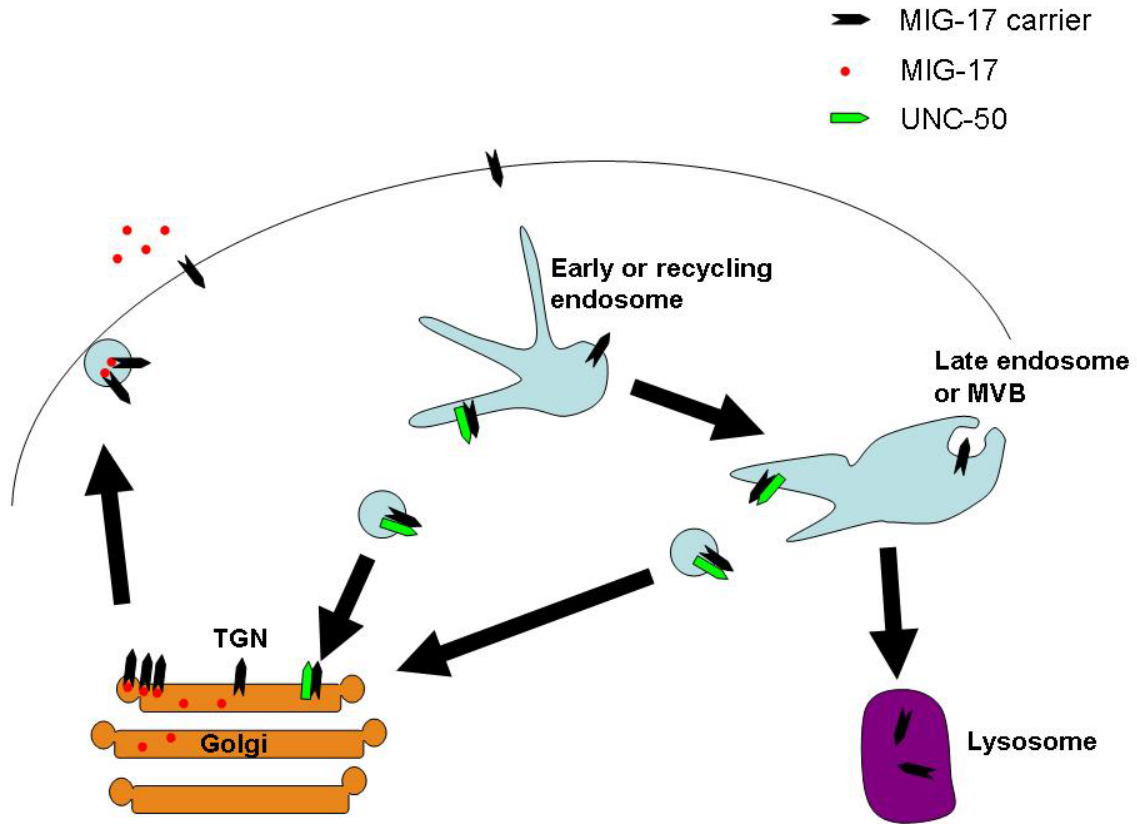
**Figure 28. Model of UNC-50 regulated MIG-17 secretion**

MIG-17 is transported through Golgi and TGN. At TGN, MIG-17 is recruited into secretory vesicles by MIG-17 carriers. Secretory vesicles fuse with the plasma membrane and MIG-17 carriers release MIG-17 to the extracellular space. Afterwards, MIG-17 carriers are endocytosed to early endosomes. They are either sorted to the lysosomes via the late endosome or recycled back to the TGN with the assistance of UNC-50. Without UNC-50, most MIG-17 carriers are sorted to the lysosomal pathway and degraded.

**Part III**

**Characterization of the GARP complex in *C. elegans***

We discovered that UNC-50 and the GARP complex have redundant functions, based on the fact that a combination of mutations in *unc-50* and one of the GARP complex subunit is lethal. GARP complex belongs to a conserved family of quatrefoil tethering complexes including the exocyst and the conserved oligomeric Golgi (COG) complex, which are composed of multimers of fourfold-symmetric components. Tethering complexes help to make the match by tethering transport vesicles to the acceptor membrane, and also confer specificity for the fusion process by bringing the SNARE proteins in close proximity to allow efficient SNARE pairing. The GARP complex is an effector of the Rab GTPase Ypt6p and the Arf like GTPase Arl1, and thought to function mainly in retrograde transport from endosome to Golgi (Conibear et al., 2003; Liewen et al., 2005; Panic et al., 2003; Siniossoglou and Pelham, 2001; Siniossoglou and Pelham, 2002). However, the GARP complex has not been described in *C. elegans* yet. In order to characterize retrograde membrane transport from endosome to Golgi, we made the first functional analysis of the GARP complex in *C. elegans*.

## 4.3.1 Identification of the GARP complex in *C. elegans* and cloning of the VPS-51 subunit

GARP complex function has been previously described in yeast and mammalian cell culture. To study the function of the GARP complex in a multicellular organism, we identified orthologs of the different subunits in the nematode *C. elegans* (Figure 29). Previously it has been suggested that the mammalian GARP complex contains just three subunits (Koumandou et al., 2007; Liewen et

al., 2005; Perez-Victoria et al., 2008), unlike yeast. By using the minimal conserved protein domain described for the yeast Vps51p we searched the *C. elegans* protein databases by iterated BLAST searches. This search revealed a match for the uncharacterized ORF B0414.8, in addition to the *C. elegans* COG and exocyst complexes. This domain had independently been identified as Dor1 like domain and shown to be closely related to the COG and exocyst subunits Cog8 and Sec5, respectively (Whyte and Munro, 2001). However, this newly identified class of proteins was not linked to the GARP complex. Since the COG and exocyst subunits have been identified, we reasoned that ORF B0414.8 might encode the missing VPS-51 subunit of the GARP complex (Figure 29). To see whether B0414.8 colocalizes with the rest of the GARP complex we expressed a translational mCherry-B0414.8 fusion protein and determined its localization relative to the other GARP subunits. As shown in Figure 30, the localization of mCherry-B0414.8 completely overlapped with that of VPS-52-YFP as well as with the other subunits (data not shown). All GARP subunits showed perfect colocalization with each other (Figure 30). To further demonstrate that B0414.8 is indeed an integral part of the *C. elegans* GARP complex we co-immunoprecipitated the other subunits with B0414.8 and vice versa (Figure 31). This strongly suggests that the metazoan GARP complex has four subunits like yeast, and that B0414.8 is the missing VPS-51 subunit.
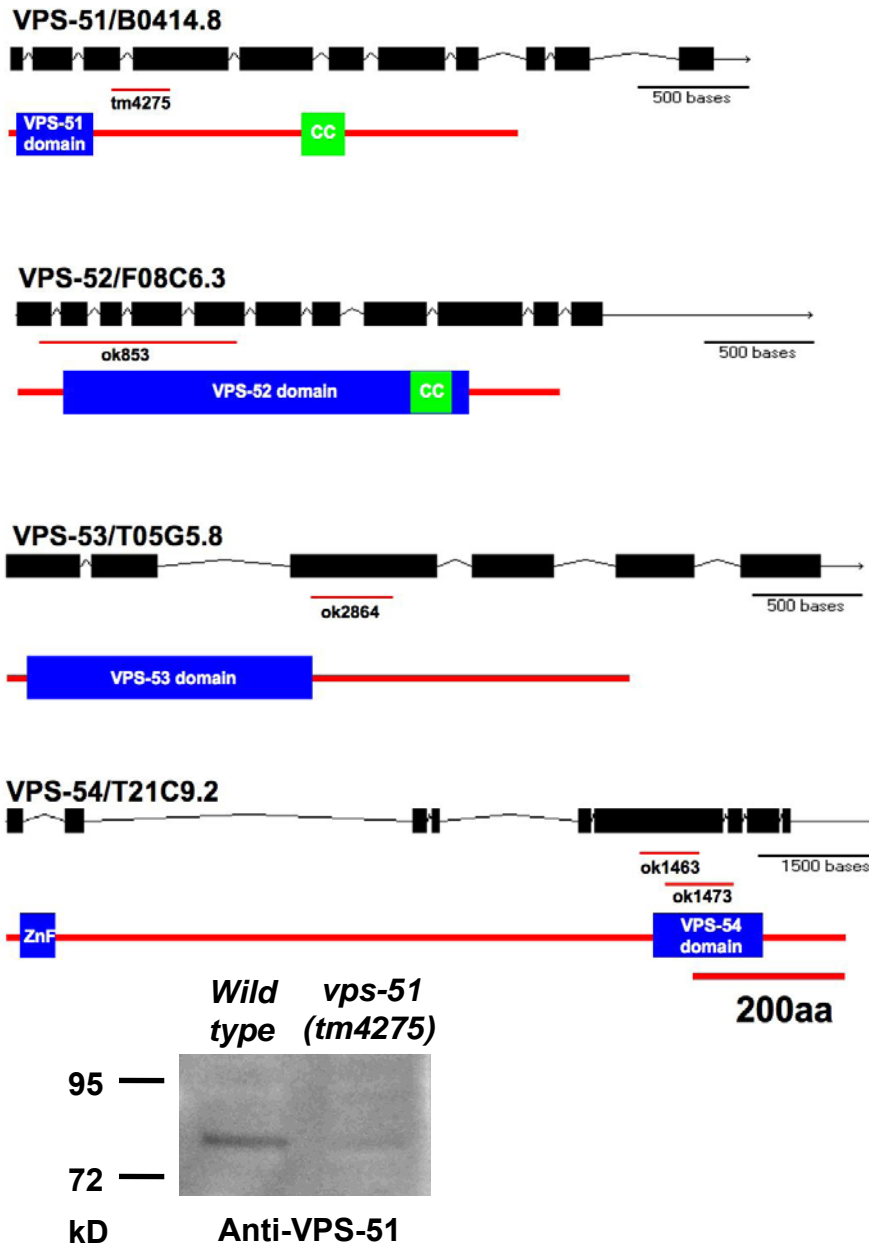
**Figure 29. Gene structures and domain organizations of *C. elegans* GARP complex subunits**

*C. elegans* GARP complex contains four subunits: *vps-52*, *vps-53*, *vps-54* and a novel subunit *vps-51*. The names of ORF are annotated after corresponding genes. Available deletions inside genes are also annotated. CC represents coiled-coil domain. ZnF represents zinc finger domain. Antibody raised against N-terminal fragment of VPS-51 recognizes a band of 80kD, which is absent in *vps-51(tm4275)* mutant.
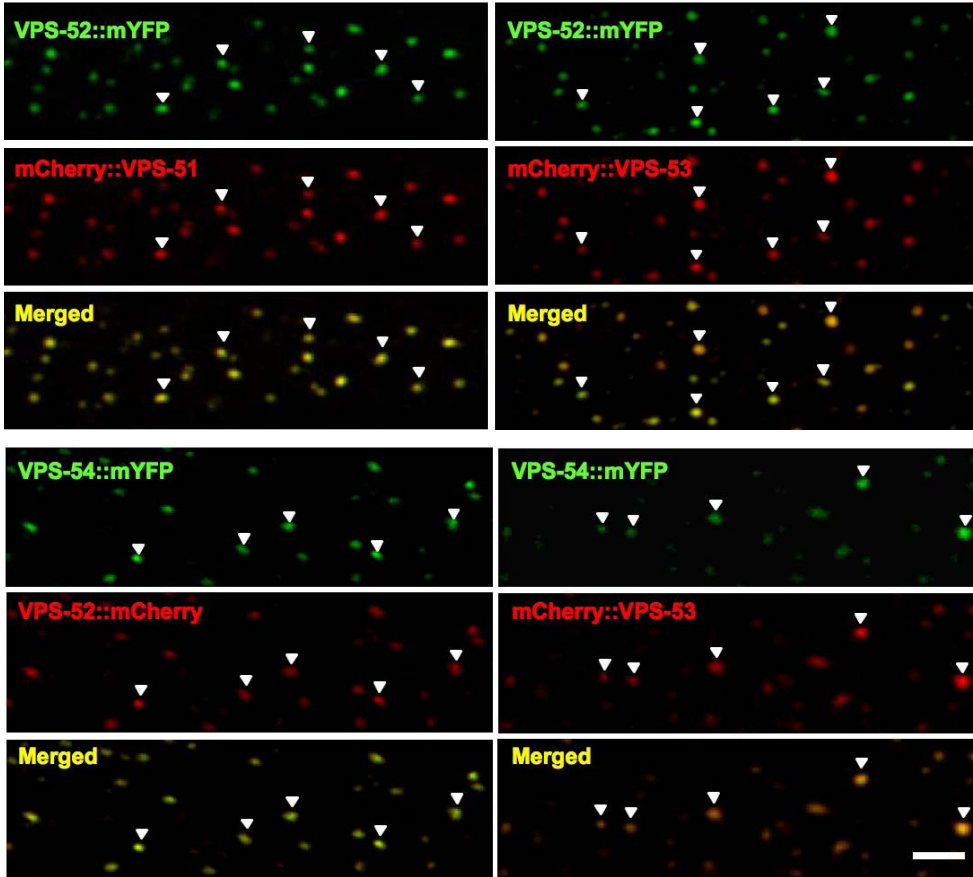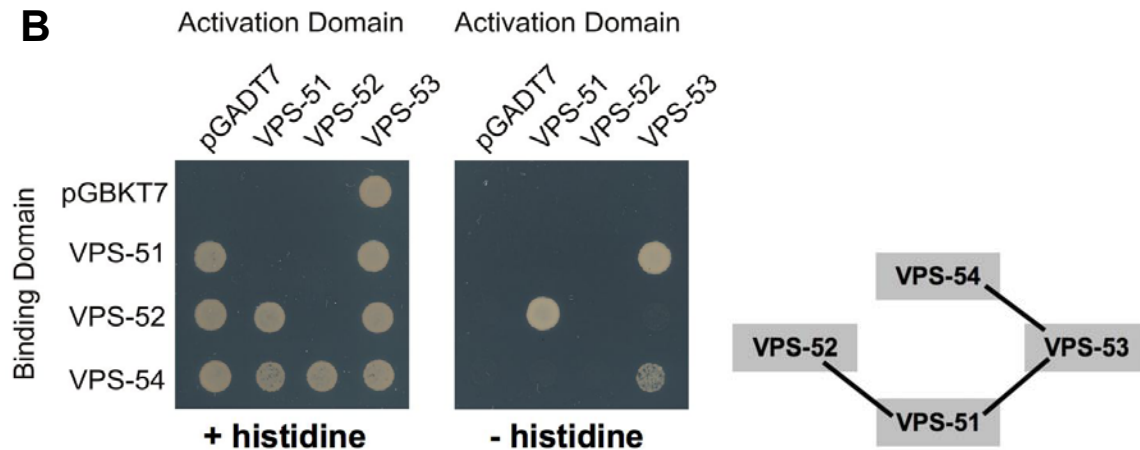
**Figure 30. GARP complex subunits colocalize with each other in body wall muscles**

Confocal microscopy images were taken from body wall muscles of wild type background transgenic worms expressing different combinations of fluorescent protein tagged GARP complex subunits as indicated. Scale bar, 5µm
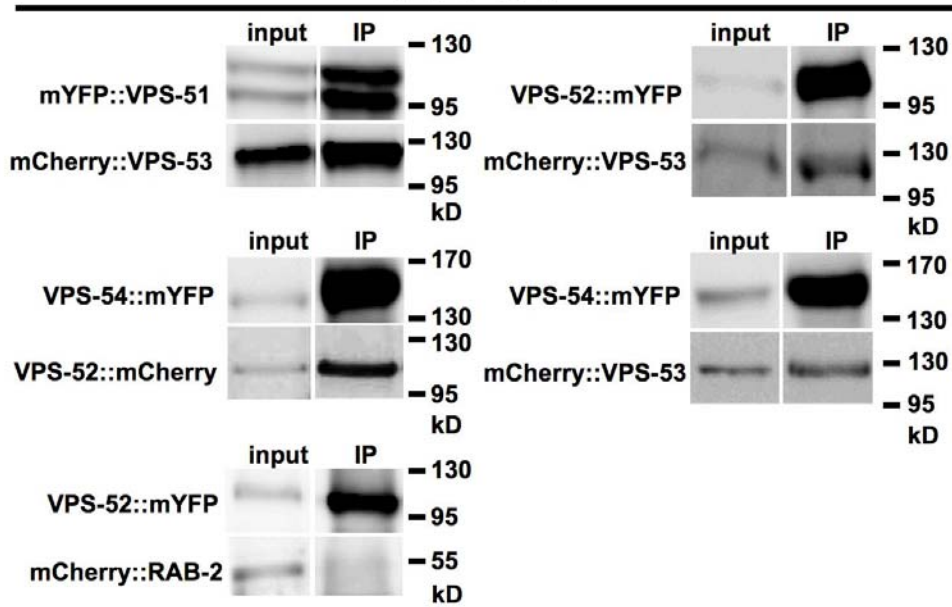
**Figure 31. Subunits of GARP complex physically interact with each other**

(A) Co-immunoprecipitations were performed from mixed stage extracts of wild type background transgenic worms expressing combinations of fluorescent protein tagged GARP complex subunits as indicated. mCherry::RAB-2 was used as a negative control.

(B) Interaction between GARP subunits as determined by yeast two hybrid assays (by Mandy Hannemann). The growth medium without histidine selects for interactions. pGADT7 and pGBKT7 are the empty vectors.

## 4.3.2 Vps51 is evolutionarily conserved and present in all eukaryotic organisms

In contrast to the 164 amino acids (aa) yeast Vps51p, *C. elegans* VPS-51 consists of 700 amino acids. Except for the Vps51 homology domain (Figure 32) and a coiled coil motif, there are no clearly recognizable domains present in VPS-51 (Figure 29). By using the newly identified Vps51 domain (see supplementary materials) we were able to identify clear VPS-51 orthologs in all eukaryotic organisms. The Vps51 ortholog group is phylogenetically separated from the COG and exocyst subunits (supplementary materials). In contrast to the yeast family, plant and animal Vps51 proteins are around 700-900 amino acids, and 700-1700 amino acids for the different protists lineages of heterologous single-celled eukaryotes ranging from *Monosiga* and *Dictyostelium* to *Plasmodium* and *Trypanosoma*. Almost all Vps51 proteins comprise the same domain architecture with the Vps51 domain at the N-terminus and no recognizable domains except some coiled coil regions C-terminally. Among metazoan Vps51 proteins motif detection revealed several conserved regions beside the Vps51 domain that are present in almost all Vps51 proteins (supplementary materials). This suggests that a common ancestor possessed a GARP complex containing a large Vps51 subunit, and that all subsequent alterations, e.g. the truncation of Vps51 in the yeast family, were caused by secondary sequence loss during evolution. The low similarity between the yeast and metazoan Vps51 proteins (Figure 32) might explain why Vps51 had not been identified outside yeast before (Koumandou et al., 2007).

**Figure 32. VPS-51 domain is conserved through species**

Alignment of VPS-51 domains from different species. Conserved amino acids are boxed in black and similar in grey.

## 4.3.3 The *C. elegans* GARP complex stably associates with Golgi and endosomal domains

Transcriptional fusions of the *vps-51*, *-52*, and *-53* promoters to GFP revealed that the GARP complex subunits are ubiquitously expressed, with particularly strong expression in neuronal cells (Figure 33). This suggests that GARP complex activity is required in many cell types as in mammals (Liewen et al., 2005). Localization studies using fluorescently tagged GARP subunits showed that the *C. elegans* GARP complex extensively co-localizes with the GFP-tagged GRIP domain from the trans-Golgi golgin T05G5.9 (Figure 34A) in body wall muscle cells. It showed a more partial overlap with endosomal domains labeled by the phospho-inositol-3-phosphate (PI3P) binding GFP-2xFYVE domain fusion (Figure 34A). This is consistent with the findings in yeast and mammals that the GARP complex localizes to the late Golgi (Conboy and Cyert, 2000; Conibear and Stevens, 2000; Perez-Victoria et al., 2008) and endosomal compartments, as well as vesicular structures distributed throughout the cell body (Liewen et al.,

2005). However, we found that the GARP complex in *C. elegans* also shows extensive co-localization with more early-medial Golgi markers like α–mannosidaseII (Figure 34A) in body wall muscles. In *C. elegans* body wall muscles the Golgi mini stacks are quite small (only about 200 nm diameter). Since they form an integral unit with an ER exit site and endosomal compartment (Figure 34B) colocalization might reflect the diffraction-limited localization of two fluorescence signals to the same secretion unit. Therefore, we reanalyzed the localization of the GARP complex in macrophage-like coelomocytes in *C. elegans*, which contain mostly a series of parallel Golgi stacks of about 500-800 nm in size (Figure 34D). In coelomocytes the fluorescently tagged GARP subunit VPS-52::mCherry showed perfect overlap with the medial Golgi marker Mans-GFP while there was no co-localization detectable between VPS-52::mCherry and the endosomal marker GFP::2xFYVE (Figure 34C). This suggests that the GARP complex localizes quite broadly to Golgi complex. The good overlap between the GARP complex and the medial Golgi markers may suggest that the GARP complex also contribute to vesicle tethering to earlier Golgi compartments than the TGN.

In all cases, the *C. elegans* GARP complex subunits largely overlapped with the staining seen for the two Rab6 orthologs, RAB-6.1 and RAB-6.2. Consistent with previous reports, we were able to co-immunoprecipitate the GARP complex with either Rab6 GTPase (Figure 35). This demonstrates that the *C. elegans* GARP complex also binds Rab6, like in yeast and mammals (Liewen et al., 2005;

Siniossoglou and Pelham, 2001).

*Pvps-51*::GFP
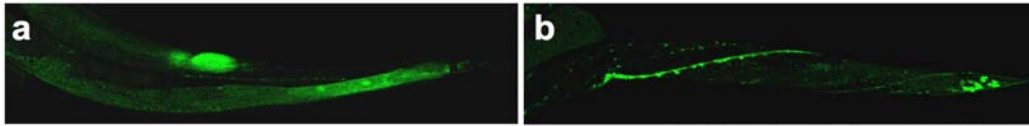


*Pvps-52*::GFP
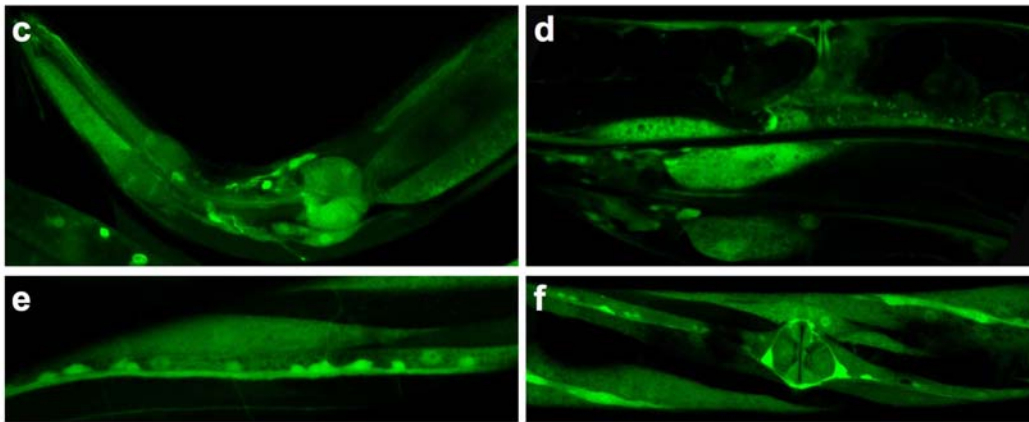


*Pvps-53*::GFP



**Figure 33. GARP complex is ubiquitously expressed**
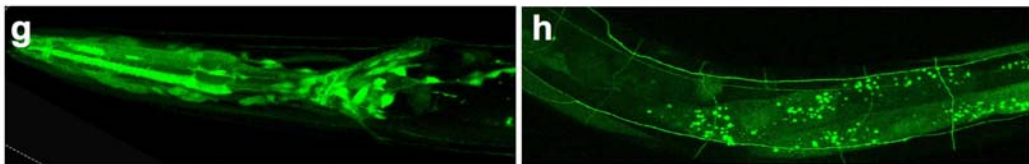
(a-b) Expression of GFP driven by *vps-51* promoter is mostly seen in neurons and intestine cells.

(c-f) GFP expression driven by *vps-52* promoter is visible in all cell types: pharyngeal,

intestine, distal tip cells, coelomocytes, body wall muscles, and neurons.

(g-h) Expression of GFP driven by *vps-53* promoter is mainly present in neurons, pharyngeal and

intestine cells.
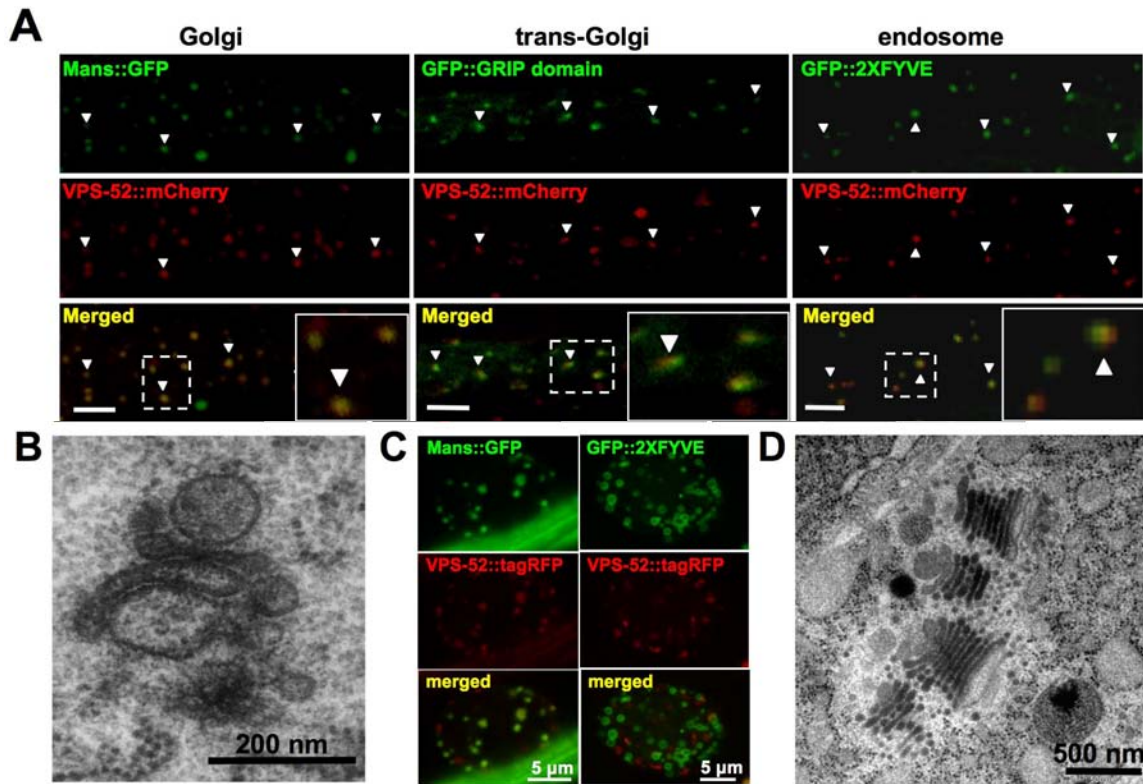
**Figure 34. GARP complex localizes to the Golgi endosomal interface**

(A) GARP complex localization overlaps with the medial Golgi (Mans::GFP), late Golgi (GFP::GRIP domain) and partially with endosomal domains (GFP::2xFYVE) in body wall muscles; scale bar represents 5 µm.

(B) Thin plastic section EM pictures of a Golgi mini stack present in *C. elegans* body wall muscles; scale bar represents 200 nm. (Picture by Jan Hegermann)

(C) GARP complex localization overlaps with the medial Golgi (Mans::GFP) but not with endosomal domains (GFP::2xFYVE) in coelomocytes; scale bar represents 5 µm.

(D) Thin plastic section EM pictures of Golgi stacks present in *C. elegans* coelomocytes; scale bar represents 500 nm. (Picture by Jan Hegermann)

The yeast GARP complex is recruited to Golgi membranes by the Rab6 GTPase Ypt6p. This localization is lost in *ypt-6* null mutants, rendering the GARP complex diffusely distributed throughout the cytoplasm (Conibear and Stevens, 2000). To

test whether the localization of the *C. elegans* GARP complex is also affected by loss of Rab6 activity, we analyzed *rab-6.2* mutant animals and found that the GARP complex is localized normal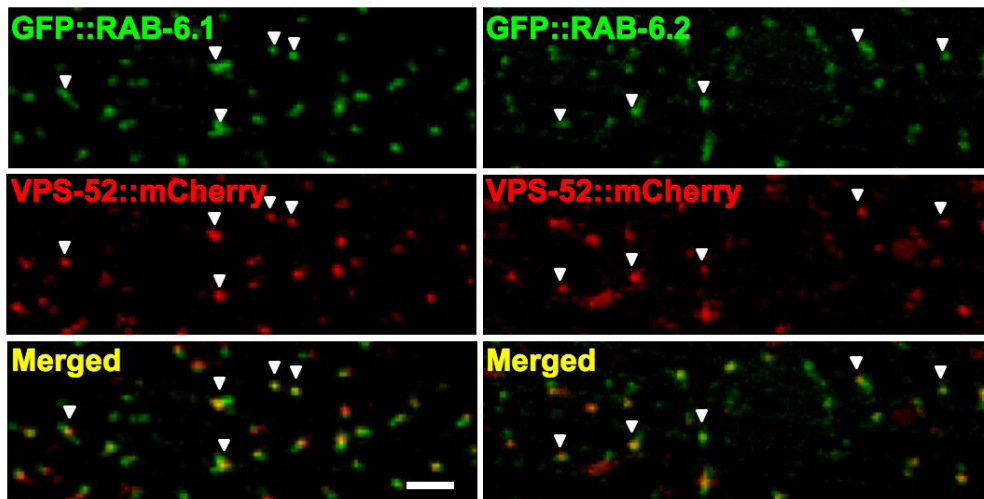ly (Figure 36). The lethality of *rab-6.1* as well as *rab-6.1; rab-6.2* double mutants prevented us from testing GARP complex localization in these strains. Therefore, it is likely that despite the loss of RAB-6.2 the GARP complex is still localized through its interaction with RAB-6.1.
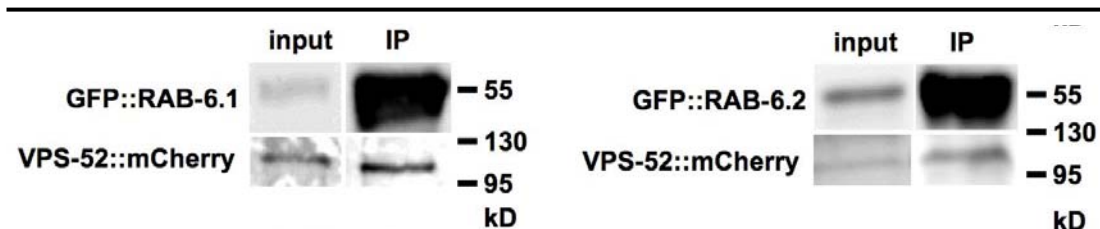


**Figure 35. GARP complex interacts with RAB-6 in *C. elegans***

Confocal images show that VPS-52::mCherry co-localizes with GFP::RAB-6.1 and GFP::RAB-6.2. Scale bar, 5µm. Co-immnoprecipitation was performed on mixed stage extracts of wild type background transgenic worms expressing VPS-52::mCherry together with either GFP::RAB-6.1 or GFP::RAB-6.2.

In yeast it has been demonstrated that if one of the core subunits Vps52p, 53p, or 54p is missing, the remaining subunits are rendered unstable and are degraded (Conibear and Stevens, 2000). To test whether the *C. elegans* complex behaves similarly, we determined the stability and localization of the remaining core GARP subunits when one is deleted. As shown in Figure 29, there are deletion mutants available for all GARP subunits in *C. elegans*. All deletions lead to frame shifts truncating the proteins before the coiled coil regions that are required for complex incorporation (Perez-Victoria et al., 2008; Siniossoglou and Pelham, 2002). Therefore, these deletions should be molecular null alleles. To our surprise, deletion of any of the four GARP complex subunits in *C. elegans* did not lead to a mislocalization of the remaining subunits nor to their instability (Figure 36). So far it has only been reported that the yeast Vps51p subunit is dispensable for core complex localization and stability (Conibear et al., 2003; Siniossoglou and Pelham, 2002).

To understand the reason for this difference we analyzed possible interactions between the different GARP subunits in *C. elegans* by yeast two-hybrid assays. Based on our finding, it might be expected that each subunit would display multiple interactions within the complex as has been suggested previously for the mammalian GARP complex (Liewen et al., 2005; Perez-Victoria et al., 2008). However, in our hands only VPS-51 interacts with VPS-52 and VPS-53 in the yeast two-hybrid system (Figure 31).
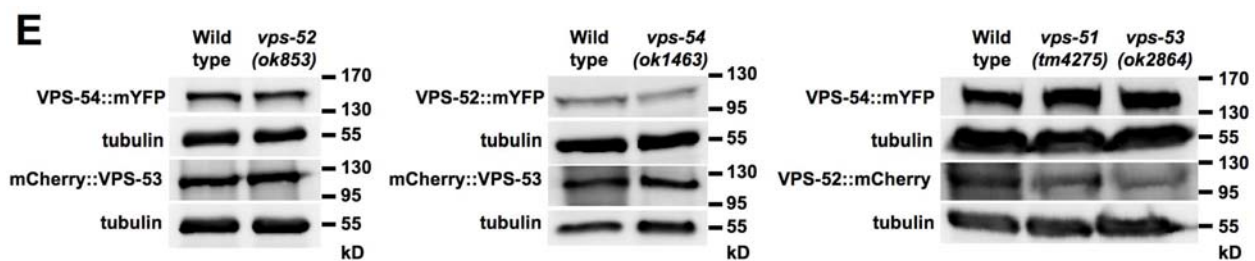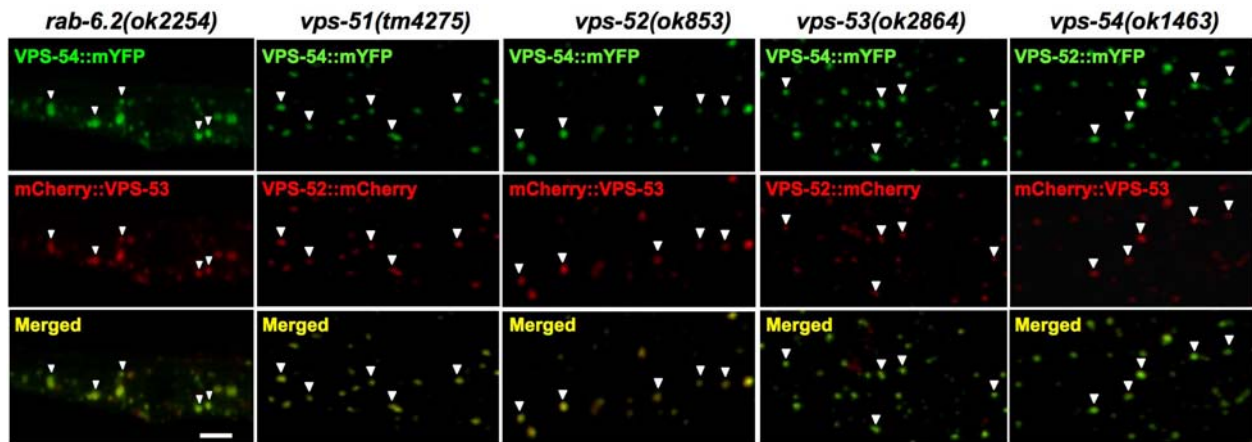
**Figure 36. GARP complex keeps stable when individual subunit or RAB-6 is missing**

Confocal images show that combination of fluorescent protein tagged residual GARP complex subunits still show colocalization in body wall muscles of mutant worms, in which one GARP subunit or RAB-6 is deleted. Scale bar, 5μm. Western blot was performed on mixed stage extracts of single GARP subunit deletion mutant worms expressing combination of fluorescent protein tagged residual GARP complex subunits as indicated.

Additionally, we could detect an interaction between VPS-53 and VPS-54. This creates a linear 52-51-53-54 interaction network within the *C. elegans* GARP complex. The reported interactions reconfirm that VPS-51 is indeed a subunit of the *C. elegans* GARP complex. Since only binary interactions were tested in the two-hybrid system we may have missed interactions that depend on the presence of more than two partners. In addition, it is also possible that isolated subunits or subcomplexes have independent means to localize to the Golgi-

endosomal interface. Therefore, it is important to test the functional activity of the remaining GARP subunits when one subunit is missing.

## 4.3.4 Loss of GARP activity leads to alterations in lysosomal morphology

To functionally characterize the GARP complex in a multicellular organism we analyzed deletion mutant strains of each subunit in *C. elegans* (Figure 29). Surprisingly, homozygous deletion mutants of each single GARP subunit were viable. However, mutants in the core subunits *vps-52, vps-53* and *vps-54* had reduced brood sizes (*vps-52(ok853)* 108±7, N=39; *vps-53(ok2864)* 102±12, N=24; *vps-54(ok1463)* 57±5, N=32) as compared to wild type (290±7, N=25). Since the brood size defects could be rescued by mating homozygous *vps-52* or *vps-54* mutant hermaphrodites with wild type males, it is likely that mutations in the *C. elegans* GARP complex lead to sperm defects as reported for mouse Vps54 mutants (Schmitt-John et al., 2005). The brood size defects (198±7, N=25) are less severe in *vps-51(tm4275)* animals, suggesting that VPS-51 might be an auxiliary subunit of the GARP core complex as has been proposed in yeast (Conibear et al., 2003; Siniossoglou and Pelham, 2002). In addition to their brood size defects, GARP mutant animals appeared slightly pale, grew more slowly than wild type and displayed reduced locomotion (data not shown), although their morphological appearance was largely normal. This suggests that in *C. elegans* GARP complex function is not strictly required for viability. Thus it is likely that a redundant pathway is able to compensate for the loss of GARP complex function.
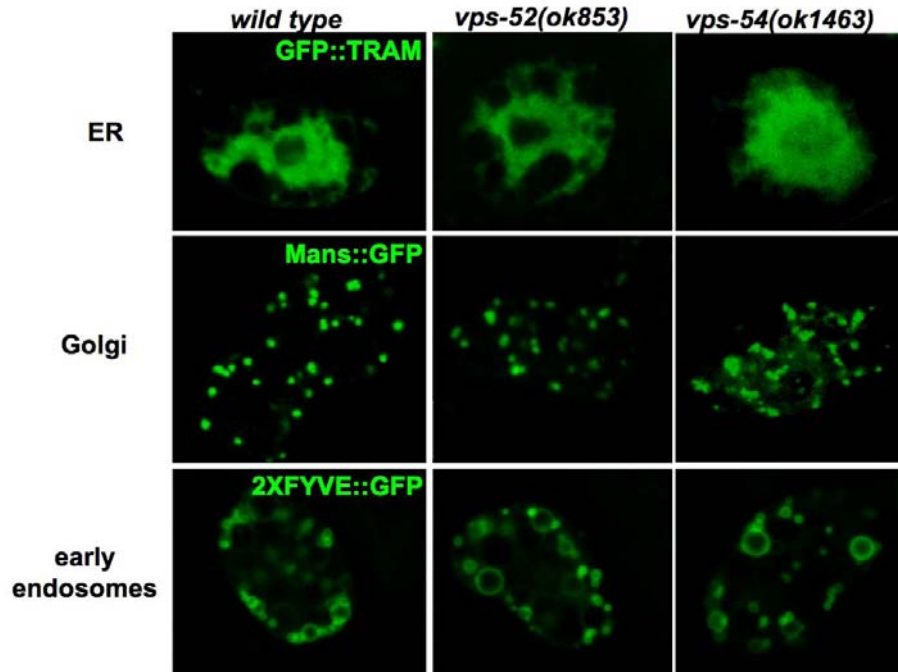
**Figure 37. GARP complex mutants show normal ER, Golgi and early endosomes in coelomocytes**

Distribution and morphology of ER marker GFP::TRAM, Golgi marker Mans::GFP, and early endosome marker 2xFYVE::GFP are not changed in *vps-52(ok853)* and *vps-54(ok1463)* mutants, compared with wild type. Scale bar, 5µm.

To study how the loss of GARP complex function affects intracellular transport, we analyzed the effects of GARP mutations on the morphology of intracellular compartments. We analyzed coelomocytes in *C. elegans*, which are macrophage like scavenger cells which reside in the body cavity and constantly filter the pseudocoelomic body fluid by bulk endocytosis. They are highly active in membrane transport and are therefore widely used to study endocytic membrane transport (Fares and Greenwald, 2001). Using transgenic marker strains we did not observe any differences in structures of the secretory pathway such as the endoplasmatic reticulum (ER) and Golgi complex, nor did we detect alterations in

the early endocytic pathway (early and late endosomes) (Figure 37). In contrast, we observed strongly enlarged lysosomal structures labeled by the transmembrane proteins CUP-5/mucolipin and LMP-1 (Treusch et al., 2004). In mutants of the GARP core complex, large vesicular structures with a diameter of more than 4 µm were detected (Figure 38) which were already detectable by DIC microscopy (Figure 38).

An electron microscopic analysis revealed that these large structures are protein-rich as they are stained by osmium like lysosomes (Figure 39). These large lysosomal structures were never detected in wild type coelomocytes (Figure 39). Mutations in the GARP core complex *vps52/vps53/vps54* also led to alterations in lysosomal morphology in yeast (Conboy and Cyert, 2000; Conibear and Stevens, 2000; Siniossoglou and Pelham, 2001; Siniossoglou and Pelham, 2002).

**Figure 38. GARP complex mutants show enlarged lysosomes in coelomocytes**

(A) Confocal images taken from coelomocytes show that late endosomes marked by RME-8::GFP appear to be normal in *vps-52(ok853)* and *vps-54(ok1463)* mutants. However, lysosomes marked by LMP-1::GFP and late ensosome-lysosome intermediates marked by CUP-5::GFP are significantly enlarged in *vps-52, vps-53 and vps-54* mutants, while these structures are slightly enlarged in *vps-51(tm4275)* mutant.

(B) RME-8::GFP, CUP-5::GFP, and LMP-1::GFP positive vesicles are grouped into three categories by sizes: smaller than 2μm , between 2μm and 4μm, bigger than 4μm. Percentages of each category are shown. Error bars represent s.e.m.
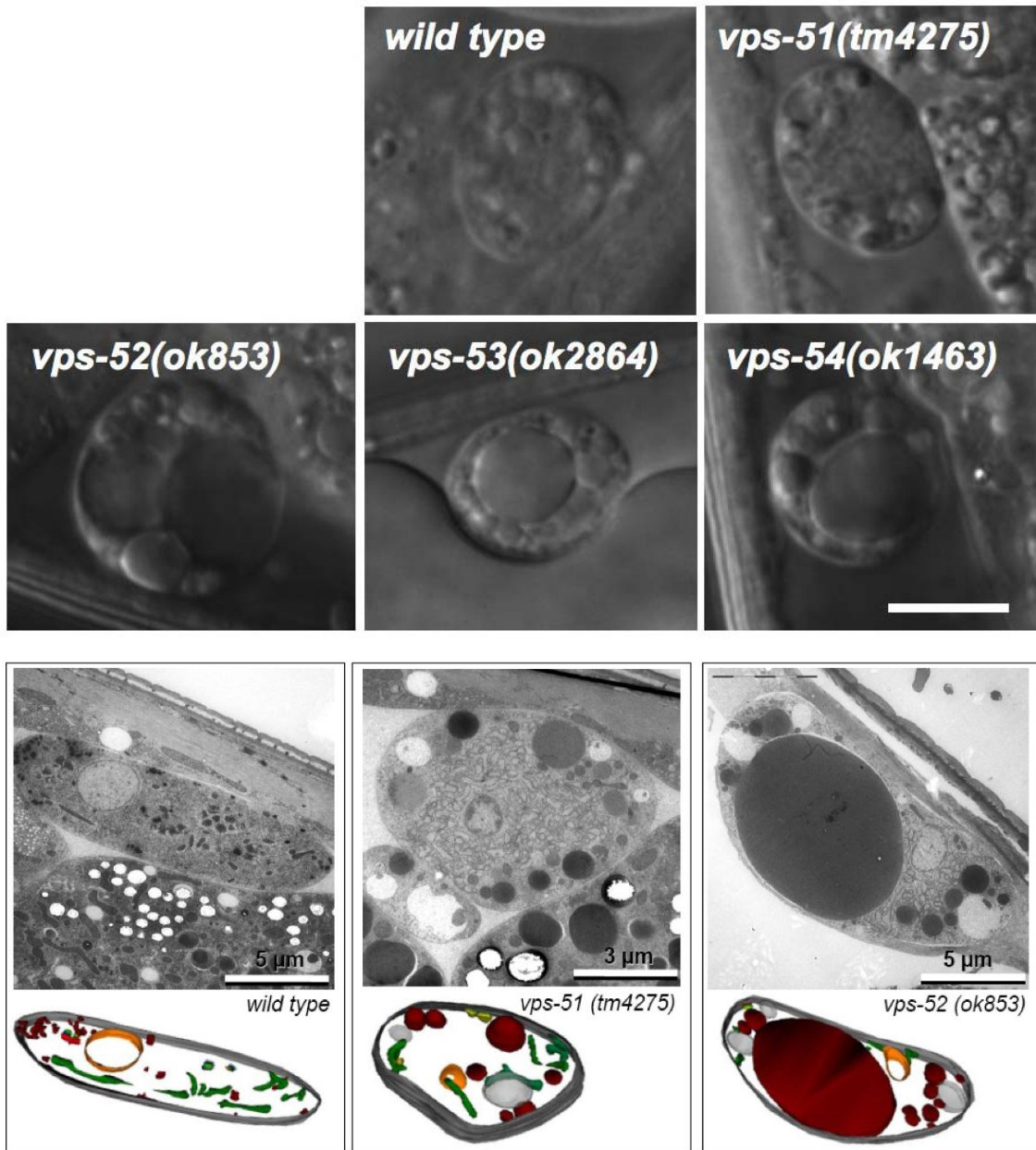
**Figure 39. GARP complex mutants show enlarged lysosomes in coelomocytes**

DIC microscopy (upper panels) and electron microscopy (lower panels) pictures (by Jan Hegermann) of coelomocytes in wild type and GARP mutants are shown. Scale bar, 5µm in upper panels.

However, the uptake and transport kinetics of endocytosed material, such as Texas Red labeled BSA injected into the body cavity and uptake of yolk protein by oocytes, were not affected in GARP mutant coelomocytes (Figure 40, 42). Furthermore, the fluorescence level of GFP that has been secreted into the body cavity and taken up by coelomocytes (Fares and Greenwald, 2001) was similar between GARP mutants and wild type (Figure 41). This indicates that lysosomal turnover of GFP is similar to wild type. Therefore, lysosomes are likely functional in GARP mutants despite the morphological alterations.

Taken together, we showed that in *vps-52(ok853)*, *vps-53(ok2864)*, and *vps-54(ok1463)* mutants, significantly enlarged lysosomal structures can be frequently observed in macrophage like cells-coelomocytes. *vps-51(tm4275)* mutant also showed this defect, although in a much milder degree.
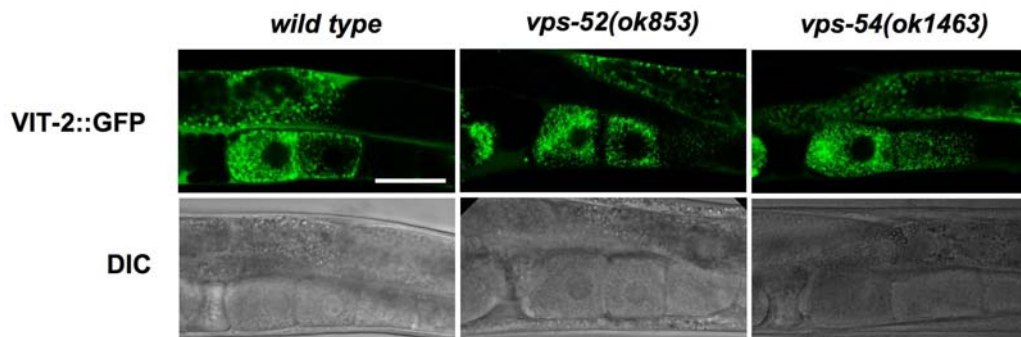


**Figure 40. GARP complex mutants show normal receptor mediated endocytosis**

Yolk protein VIT-2::GFP is expressed and secreted from intestine cells, and taken up by oocytes in a receptor mediated manner. No significant change in VIT-2:GFP endocytosis can be observed in *vps-52(ok853)* and *vps-54(ok1463)* mutants. Scale bar, 50μm.
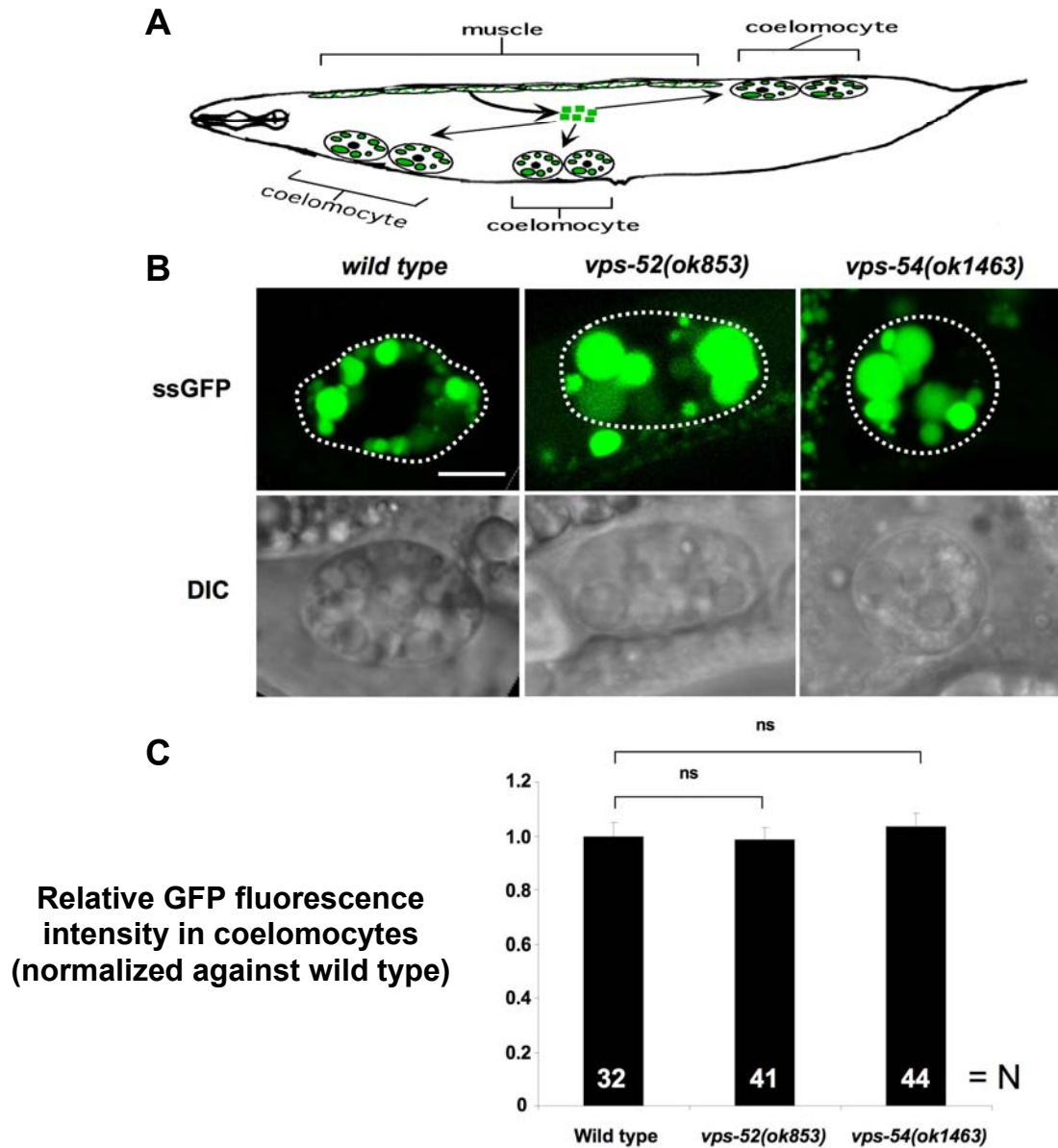
**Figure 41. GARP complex mutants show normal fluid phase endocytosis**

(A) An integrated transgenic worm strain expresses secreted GFP from the body wall muscles. GFP secreted into the body cavity is subsequently endocytosed by the six macrophage like cells-coelomocytes (Adapted from Fares and Greenwald, 2001).

(B) Confocal pictures show that ssGFP endocytosis by coelomocytes appears normal in *vps-52(ok853)* and *vps-54(ok1463)* mutants. Scale bar, 5μm.

(C) Quantification of ssGFP fluorescence intensity in coelomocytes shows no significant difference between wild type and *vps-52(ok853)* and *vps-54(ok1463)* mutants.
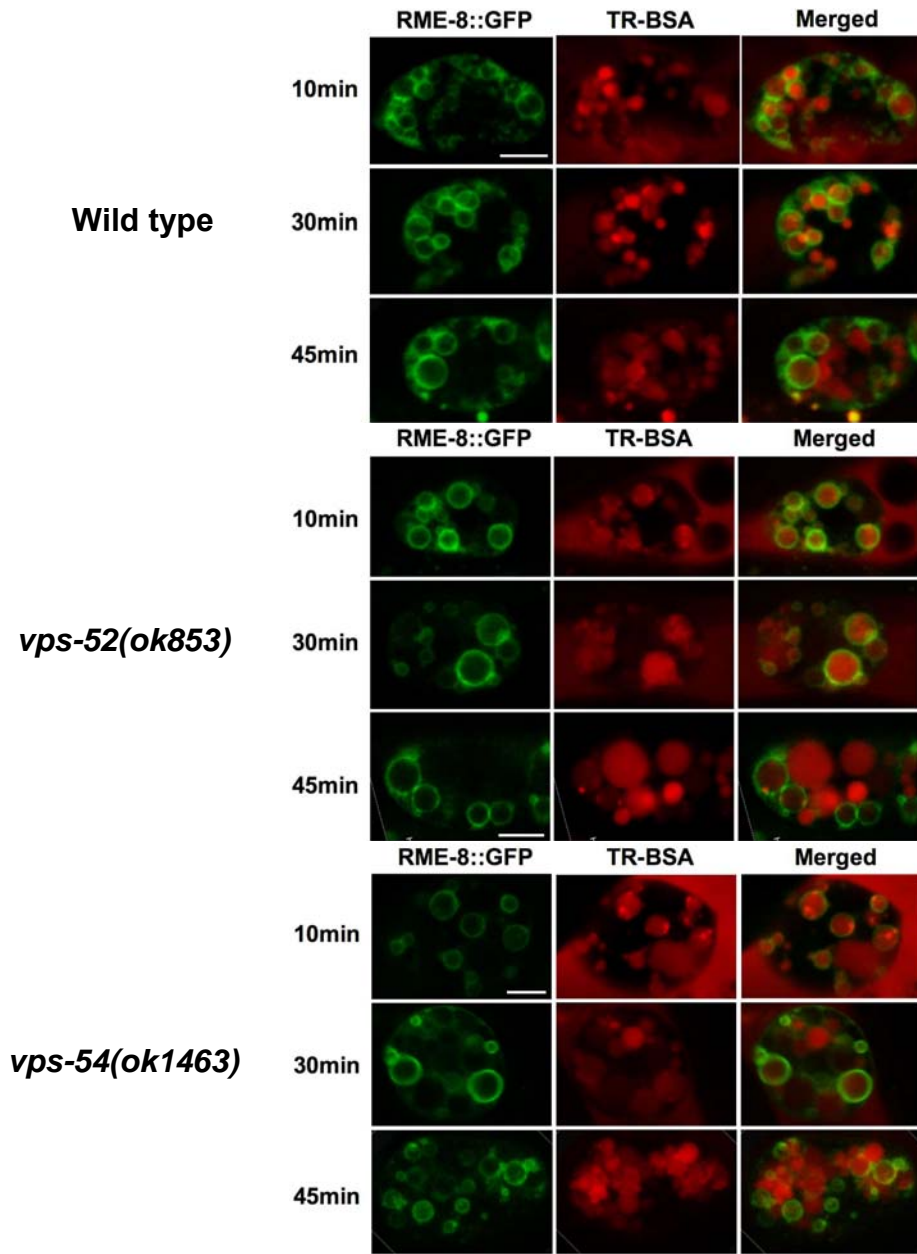
**Figure 42. GARP complex mutants show normal dynamics of endocytosis**

Texas-Red BSA was injected into the body cavities of worms expressing late endosomal marker RME-8::GFP in coelomocytes. Confocal images were taken at the indicated time spot after injection. 10 minutes after injection, TR-BSA already entered the RME-8::GFP positive structures. After 30 minutes, part of TR-BSA exited from RME-8::GFP vesicles and entered later structures. At 45 minutes, most TR-BSA entered later structures. This dynamic process seems not changed in *vps-52(ok853)* and *vps-54(ok1463)* mutants. Scale bar, 5µm.

### 4.3.5 VPS-51 is required for GARP complex function

Despite being an integral part of the GARP complex, *vps51* mutants in yeast display weaker growth defects than the other complex components. This is consistent with the fact that the core complex is still correctly assembled and localized in the absence of Vps51p (Conibear et al., 2003; Siniossoglou and Pelham, 2002). This led to the idea that Vps51 might be an auxiliary GARP subunit. However, *vps51* mutants do show phenotypes similar to the rest of the GARP subunits. In yeast, Vps51p has been shown to affect the sorting of soluble vacuolar proteins and the recycling of the plasma membrane SNARE Snc1p. In addition, inactivation of Vps51p leads to fragmented vacuoles and defects in autophagosome formation similar to mutants in the other subunits (Conibear et al., 2003; Reggiori et al., 2003; Siniossoglou and Pelham, 2002). In *C. elegans*, *vps-51* mutants also show enlarged lysosomal structures although these structures never reached the size seen in the core complex mutants (Figure 38, 39). Thus, the VPS-51 subunit in *C. elegans* also contributes to basic GARP complex function. Vps51 subunits may be essential for more specialized functions of the GARP complex in particular cellular pathways in multicellular organisms. This would explain its evolutionary conservation (supplementary materials).

### 4.3.6 The GARP complex supports multiple retrograde routes to the early and late Golgi through differential SNARE interactions

Yeast Vps51p was shown to bind to the late Golgi t-SNARE Tlg1p (Conibear et

al., 2003; Siniossoglou and Pelham, 2002). This led to the attractive model that the Vps51 subunit might be responsible for SNARE recruitment at the target membrane. The Tlg1 interaction motif was mapped to the very N-terminus of Vps51p (aa 18-30) and shown to form a short helix that interacts with a three-helix bundle formed by Tlg1p (Fridmann-Sirkis et al., 2006; Siniossoglou and Pelham, 2002). Surprisingly, a deletion of the N-terminal domain of Vps51p or mutations that eliminate Tlg1p binding do not affect the ability of Vps51p to recycle proteins back to the Golgi. This led to the idea that the Vps51p/Tlg1p interaction may just increase the efficiency of the fusion reaction with the target membrane by ensuring the presence of all components required.

Recently, similar SNARE interactions have been demonstrated for the other GARP complex subunits. The mammalian GARP complex has been shown to directly bind late Golgi SNAREs Syntaxin-6, -10 and -16 as well as VAMP4 (Liewen et al., 2005; Perez-Victoria and Bonifacino, 2009). Our identification of metazoan Vps51 made it possible that these reported SNARE interactions could have been mediated by endogenous Vps51 co-purified with the other tagged GARP subunits.

We therefore systematically tested the interactions of each complex subunit with all *C. elegans* SNARE proteins by yeast two-hybrid analysis (Figure 43). VPS-54 interacted with the Syntaxin-5 ortholog, SYX-5, and Membrin/GS27 ortholog, MEMB-2. VPS-52 showed an additional binding to Synatxin-16 (SYX-16) and

weak binding to the second worm membrin ortholog, MEMB-1. VPS-51 interacted specifically with Syntaxin-5 as well as with both MEMB-1 and MEMB-2. Furthermore, VPS-51 also binds the late Golgi SNAREs Syntaxin-16 and the Vti1 ortholog, VTI-1 (Figure 43). The SNARE interactions with VPS-53 could not be tested since it is auto-activating when fused to the DNA binding domain within the yeast two-hybrid system. These results demonstrate that there are direct interactions of each GARP subunit with a specific set of Golgi SNAREs.

## Binding Domain

| | VPS-51 | | VPS-52 | | VPS-54 | | SNARE Type |
|---|---|---|---|---|---|---|---|
| | His - | His + | His - | His + | His - | His + | |
| empty | | ○ | | ○ | | ○ | |
| SYX-5 | ○ | ○ | ○ | ○ | ○ | ○ | ◀ Qa |
| SYX-6 | | ○ | | ○ | | ○ | |
| SYX-13 | | ○ | | ○ | | ○ | |
| SYX-16 | ○ | ○ | ○ | ○ | | ○ | ◀ Qa |
| SYX-17 | | ○ | | | | ○ | |
| VAMP-7 | | ○ | | ○ | | ○ | |
| VAMP-8 | | ○ | | ○ | | ○ | |
| YKT-6 | | ○ | | ○ | | ○ | |
| VTI-1 | ○ | ○ | | ○ | | ○ | ◀ Qb |
| NBET-1 | | ○ | | ○ | | ○ | |
| GOS-28 | | ○ | | ○ | | ○ | |
| MEMB-1 | ○ | ○ | ○ | ○ | | ○ | ◀ Qb |
| MEMB-2 | ○ | ○ | ○ | ○ | ○ | ○ | ◀ Qb |
| p53/T-Antigen | ○ | ○ | ○ | ○ | ○ | ○ | |
| p53/pGADT-7 | | ○ | | ○ | | ○ | |

*Activation Domain*
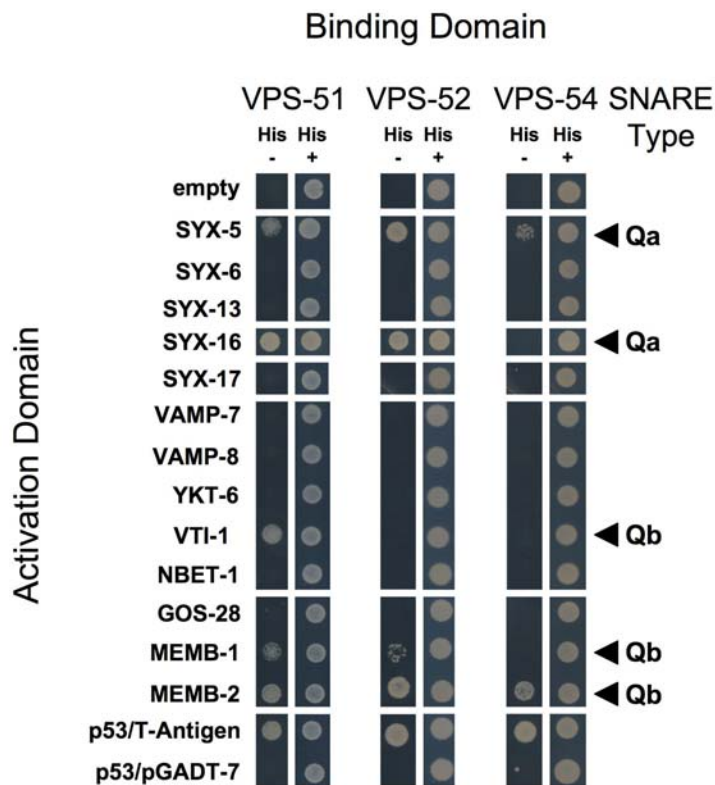
**Figure 43. GARP complex subunits interact with early and late Golgi SNAREs (by Mandy Hannemann)**

Direct protein interactions of GARP subunits with Golgi and endosomal SNAREs were assayed by yeast two-hybrid analysis. The growth medium without histidine was used to select for interactions. pGADT7 and pGBKT7 are the empty vectors. Among the SNAREs showing interactions with GARP complex, SYX-16 and VTI-1 are late Golgi SNAREs, while SYX-5, MEMB-1 and MEMB-2 are early Golgi SNAREs.

The COG tethering complex has also been shown to bind to the early Golgi SNARE Sed5/Syntaxin-5 (Bruinsma et al., 2004; Shestakova et al., 2007). Therefore, the COG and GARP complexes may be redundantly required for retrograde Golgi transport. *C. elegans* mutants in the COG subunits COGC-1 and -3 are viable (Kubota et al., 2006), but display synthetic lethality when combined with mutations in the GARP complex (Figure 44). This suggests that COG and GARP complexes share overlapping functions for Golgi retrieval. Furthermore, GARP complex mutant is also synthetic lethal with mutant in retromer complex (Figure 44). This supports the conclusion that the GARP complex is required for retrograde transport from endosomes to Golgi in *C. elegans*.

In summary, these results support a model in which the GARP tethering complex orchestrates retrograde transport to the Golgi through several trafficking routes by differentially binding to specific early and late Golgi SNARE pairs.
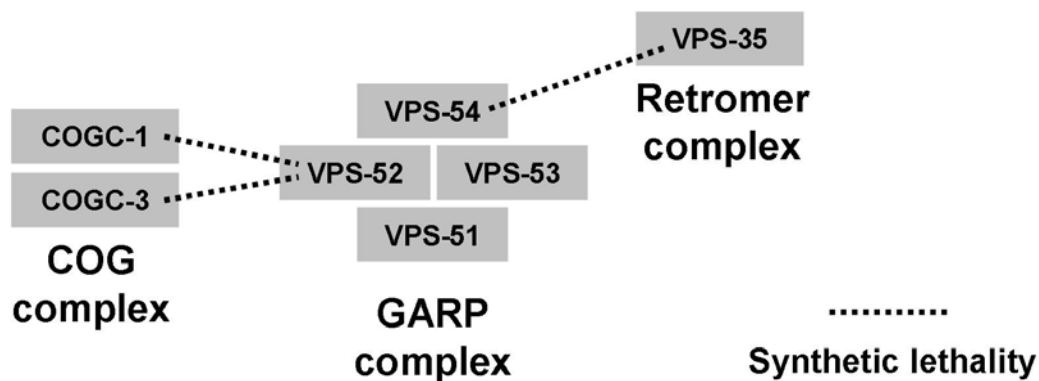


**Figure 44. GARP complex genetically interacts with the COG complex and the retromer complex**

*vps-52(ok853)* mutation is lethal if combined with *cogc-1(k179)* or *cogc-3((k181)* mutation. *vps-54(ok1463); vps-35(hu68)* double mutant also shows lethality.

## 4.3.7 Discussion

We show that in GARP mutants, significantly enlarged lysosomal structures can be frequently observed in coelomocytes. A similar lysosomal phenotype has been reported in mutants of the *C. elegans* Pikfyve/Fab1p phosphoinositide kinase PPK-3, which phosphorylates phosphatidylinositol-3-monophosphate [PtdIns(3)P] into phosphatidylinositol-3,5-bisphosphate [PtdIns(3,5)P2] (Nicot et al., 2006). PtdIns(3)P binds to the FYVE domains of early endosomal antigen EEA1, which are implicated respectively in early endosome fusion and in receptor sorting in multivesicular bodies (MVBs) (Gruenberg and Stenmark, 2004). Fab1p mediated production of PtdIns(3,5)P2 is essential for sorting membrane proteins into the lumen of vacuole in yeast or MVBs (Odorizzi et al., 1998). PtdIns(3)P is mostly found on early endosomes and internal membranes of MVBs, whereas PtdIns(3,5)P2 is distributed on the external membrane of MVBs. We have preliminary data showing that in *vps-52(ok853)*, *vps-53(ok2864)*, and *vps-54(ok1463)* mutants, PtdIns(3,5)P2 levels are decreased as much as in *ppk-3* mutants. Thus, the localization or function of PI3-5 kinase PPK-3 may depend on GARP complex mediated retrograde trafficking.

We show that VPS-51 is evolutionarily conserved in metazoans. VPS-51 is required for maintaining normal lysosomal morphology, although to a lesser extent than other GARP subunits. This suggests that VPS-51 may contribute to more specific functions of the GARP complex. In agreement with this, the zebrafish Vps51 ortholog *fat free* (*ffr*) has been shown to regulate fat metabolism

(Farber et al., 2001; Ho et al., 2006), although no link to the GARP complex has been made. *fat-free* mutant fish embryos display lipid processing defects in the pancreas and vesicular recycling defects in the intestine, as well as degeneration of biliary epithelial cells and dilated Golgi structures within the digestive tract. However, the growth and morphology of *ffr* mutant fish were normal (Ho et al., 2006). These results indeed suggest that Vps51 may serve as an adaptor for the GARP complex that has adopted specific functions in multicellular systems. These functions were dispensable in yeast and thus yeast Vps51 was shortened to a minimal unit.

We report that GARP complex subunits interact with a specific set of Golgi SNAREs, as shown by yeast two-hybrid assays. Interestingly, Syntaxin-5 and Membrin as well as Syntaxin-16 and Vti1 are each Qa and Qb SNARE combinations of two Golgi SNARE complexes, respectively. SNARE complex assembly requires four parallel α-helixes to form an extended coiled coil. Each SNARE donates an α–helix and based on its positions within the SNARE complex are called $Q_a$, $Q_b$, $Q_c$ and R SNARE (Jahn and Scheller, 2006). Whereas the $Q_{abc}$ SNARE triplex Syntaxin-16/Vti1/Syntaxin-6 is localized to the late Golgi /TGN and forms a SNARE complex with the R SNARE VAMP4, the Syntaxin-5/Membrin/BET1 triplex localizes to the early and medial Golgi and has been reported to associate with the R SNARE SEC22 (Jahn and Scheller, 2006). The corresponding yeast SNARE complexes are Sed5/Bos1/Bet1/Sec22 and Tlg2/Vti1/Tlg1/Snc1/2, respectively (Burri and Lithgow, 2004). In addition, a separate SNARE complex consisting of Sed5/Vti1/Sft1/Ykt6 has also been

reported to mediate vesicular transport from the prevacuolar compartment (PVC) to the early Golgi (Fischer von Mollard and Stevens, 1999), which was reported to be Ypt6/Rab6 dependent (Bensen et al., 2001). The fact that the *C. elegans* GARP complex interacts with specific SNARE pairs at the cis and trans sides of the Golgi suggests that the GARP complex supports tethering of transport vesicles to the early and late Golgi. Furthermore, the concomitant binding to a Qa and Qb SNARE of the same complex may mechanistically explain how the GARP complex supports SNARE assembly by holding two of the four partners in place. This strongly supports the previous finding that the mammalian GARP complex, in addition to its tethering function, also promotes SNARE assembly (Perez-Victoria and Bonifacino, 2009). Based on the fact that yeast Vps51p binds to the Qc SNARE Tlg1 and the mammalian GARP complex to the Qc SNARE Syntaxin-6 as well as to the R SNARE VAMP4, it is likely that these interactions have been changed during evolution.

# Curriculum Vitae

## *Personal information*

Name:                          Ling Luo

Citizenship:                   China

Date and place of birth:       Nov 2nd .1983, Xin Yu, Jiang Xi, China

Current address:               Mittelstr.1A, 37077, Göttingen, Germany

Email:                         lluo1@gwdg.de

## *Education*

10.2006-            PhD candidate in Neuroscience Early Stage Research

                    Training (NEUREST) Program, Max-Planck Institute for

                    Biophysical Chemistry, Göttingen, Germany

10.2005-10.2006     Master study in MSc/PhD/MD Neuroscience Program,

                    International Max Planck Research School / University of

                    Göttingen, Germany

09.2001-07.2005     Bachelor of Science, majored in biological sciences,

                    Peking University, Beijing, China

## *Scholarships*

10.2006-08.2009   Marie Curie Host Fellowships for Early Stage Researchers

                  Training, EU Research Program

09.2005-08.2006   Stipend International Max Planck Research School, Germany

# List of publications

Sumakovic M, Hegermann J, **Luo L**, HussonSJ, Schwarze K, Olendrowitz C, Schoofs L, Richmond J and Eimer S. UNC-108/RAB-2 and its effector RIC-19 are involved in dense core vesicle maturation in *C. elegans*, *J Cell Biol.* 2009

**Luo L**, Hannemann M, Koenig S, Hegermann J, Ailion M, Cho M.-K, Zweckstetter M, Rensing S.A and Eimer S. The *C. elegans* GARP complex contains the conserved Vps51 subunit and interacts with early and late Golgi SNAREs. (*Submitted*)

# VI References

Albuquerque, E.X., M. Alkondon, E.F. Pereira, N.G. Castro, A. Schrattenholz, C.T. Barbosa, R. Bonfante-Cabarcas, Y. Aracava, H.M. Eisenberg, and A. Maelicke. 1997. Properties of neuronal nicotinic acetylcholine receptors: pharmacological characterization and modulation of synaptic function. *J Pharmacol Exp Ther*. 280:1117-36.

Albuquerque, E.X., E.F. Pereira, M. Alkondon, and S.W. Rogers. 2009. Mammalian nicotinic acetylcholine receptors: from structure to function. *Physiol Rev*. 89:73-120.

Amessou, M., A. Fradagrada, T. Falguieres, J.M. Lord, D.C. Smith, L.M. Roberts, C. Lamaze, and L. Johannes. 2007. Syntaxin 16 and syntaxin 5 are required for efficient retrograde transport of several exogenous and endogenous cargo proteins. *J Cell Sci*. 120:1457-68.

Antonin, W., D. Fasshauer, S. Becker, R. Jahn, and T.R. Schneider. 2002. Crystal structure of the endosomal SNARE complex reveals common structural principles of all SNAREs. *Nat Struct Biol*. 9:107-11.

Appenzeller-Herzog, C., and H.P. Hauri. 2006. The ER-Golgi intermediate compartment (ERGIC): in search of its identity and function. *J Cell Sci*. 119:2173-83.

Arighi, C.N., L.M. Hartnell, R.C. Aguilar, C.R. Haft, and J.S. Bonifacino. 2004. Role of the mammalian retromer in sorting of the cation-independent mannose 6-phosphate receptor. *J Cell Biol*. 165:123-33.

Auld, D.S., T.J. Kornecook, S. Bastianetto, and R. Quirion. 2002. Alzheimer's disease and the basal forebrain cholinergic system: relations to beta-amyloid peptides, cognition, and treatment strategies. *Prog Neurobiol*. 68:209-45.

Baker, L.P., and H.B. Peng. 1993. Tyrosine phosphorylation and acetylcholine receptor cluster formation in cultured Xenopus muscle cells. *J Cell Biol*. 120:185-95.

Bany, I.A., M.Q. Dong, and M.R. Koelle. 2003. Genetic and cellular basis for acetylcholine inhibition of Caenorhabditis elegans egg-laying behavior. *J Neurosci*. 23:8060-9.

Barbieri, M.A., R.L. Roberts, A. Gumusboga, H. Highfield, C. Alvarez-Dominguez, A. Wells, and P.D. Stahl. 2000. Epidermal growth factor and membrane trafficking. EGF receptor activation of endocytosis requires Rab5a. *J Cell Biol*. 151:539-50.

Barlowe, C., L. Orci, T. Yeung, M. Hosobuchi, S. Hamamoto, N. Salama, M.F. Rexach, M. Ravazzola, M. Amherdt, and R. Schekman. 1994. COPII: a membrane coat formed by Sec proteins that drive vesicle budding from the endoplasmic reticulum. *Cell*. 77:895-907.

Barr, F.A. 1999. A novel Rab6-interacting domain defines a family of Golgi-targeted coiled-coil proteins. *Curr Biol*. 9:381-4.

Baugh, L.R., and C.P. Hunter. 2006. MyoD, modularity, and myogenesis: conservation of regulators and redundancy in C. elegans. *Genes Dev*. 20:3342-6.

Behnia, R., B. Panic, J.R. Whyte, and S. Munro. 2004. Targeting of the Arf-like GTPase Arl3p to the Golgi requires N-terminal acetylation and the membrane protein Sys1p. *Nat Cell Biol.* 6:405-13.

Belenkaya, T.Y., Y. Wu, X. Tang, B. Zhou, L. Cheng, Y.V. Sharma, D. Yan, E.M. Selva, and X. Lin. 2008. The retromer complex influences Wnt secretion by recycling wntless from endosomes to the trans-Golgi network. *Dev Cell.* 14:120-31.

Ben-Tekaya, H., K. Miura, R. Pepperkok, and H.P. Hauri. 2005. Live imaging of bidirectional traffic from the ERGIC. *J Cell Sci.* 118:357-67.

Bensen, E.S., B.G. Yeung, and G.S. Payne. 2001. Ric1p and the Ypt6p GTPase function in a common pathway required for localization of trans-Golgi network membrane proteins. *Mol Biol Cell.* 12:13-26.

Blacque, O.E., E.A. Perens, K.A. Boroevich, P.N. Inglis, C. Li, A. Warner, J. Khattra, R.A. Holt, G. Ou, A.K. Mah, S.J. McKay, P. Huang, P. Swoboda, S.J. Jones, M.A. Marra, D.L. Baillie, D.G. Moerman, S. Shaham, and M.R. Leroux. 2005. Functional genomics of the cilium, a sensory organelle. *Curr Biol.* 15:935-41.

Bonifacino, J.S., and R. Rojas. 2006. Retrograde transport from endosomes to the trans-Golgi network. *Nat Rev Mol Cell Biol.* 7:568-79.

Boulin, T., M. Gielen, J.E. Richmond, D.C. Williams, P. Paoletti, and J.L. Bessereau. 2008. Eight genes are required for functional reconstitution of the Caenorhabditis elegans levamisole-sensitive acetylcholine receptor. *Proc Natl Acad Sci U S A.* 105:18590-5.

Brenner, S. 1974. The genetics of Caenorhabditis elegans. *Genetics.* 77:71-94.

Bruinsma, P., R.G. Spelbrink, and S.F. Nothwehr. 2004. Retrograde transport of the mannosyltransferase Och1p to the early Golgi requires a component of the COG transport complex. *J Biol Chem.* 279:39814-23.

Burri, L., and T. Lithgow. 2004. A complete set of SNAREs in yeast. *Traffic.* 5:45-52.

Carlton, J., M. Bujny, B.J. Peter, V.M. Oorschot, A. Rutherford, H. Mellor, J. Klumperman, H.T. McMahon, and P.J. Cullen. 2004. Sorting nexin-1 mediates tubular endosome-to-TGN transport through coincidence sensing of high- curvature membranes and 3-phosphoinositides. *Curr Biol.* 14:1791-800.

Chang, H.C., M. Hull, and I. Mellman. 2004. The J-domain protein Rme-8 interacts with Hsc70 to control clathrin-dependent endocytosis in Drosophila. *J Cell Biol.* 164:1055-64.

Chantalat, S., R. Courbeyrette, F. Senic-Matuglia, C.L. Jackson, B. Goud, and A. Peyroche. 2003. A novel Golgi membrane protein is a partner of the ARF exchange factors Gea1p and Gea2p. *Mol Biol Cell.* 14:2357-71.

Chidambaram, S., N. Mullers, K. Wiederhold, V. Haucke, and G.F. von Mollard. 2004. Specific interaction between SNAREs and epsin N-terminal homology (ENTH) domains of epsin-related proteins in trans-Golgi network to endosome transport. *J Biol Chem.* 279:4175-9.

Christianson, J.C., and W.N. Green. 2004. Regulation of nicotinic receptor expression by the ubiquitin-proteasome system. *EMBO J.* 23:4156-65.

Christoforidis, S., H.M. McBride, R.D. Burgoyne, and M. Zerial. 1999. The Rab5 effector EEA1 is a core component of endosome docking. *Nature*. 397:621-5.

Collins, R.F., A.D. Schreiber, S. Grinstein, and W.S. Trimble. 2002. Syntaxins 13 and 7 function at distinct steps during phagocytosis. *J Immunol*. 169:3250-6.

Conboy, M.J., and M.S. Cyert. 2000. Luv1p/Rki1p/Tcs3p/Vps54p, a yeast protein that localizes to the late Golgi and early endosome, is required for normal vacuolar morphology. *Mol Biol Cell*. 11:2429-43.

Conibear, E., J.N. Cleck, and T.H. Stevens. 2003. Vps51p mediates the association of the GARP (Vps52/53/54) complex with the late Golgi t-SNARE Tlg1p. *Mol Biol Cell*. 14:1610-23.

Conibear, E., and T.H. Stevens. 2000. Vps52p, Vps53p, and Vps54p form a novel multisubunit complex required for protein sorting at the yeast late Golgi. *Mol Biol Cell*. 11:305-23.

Conti-Fine, B.M., M. Milani, and H.J. Kaminski. 2006. Myasthenia gravis: past, present, and future. *J Clin Invest*. 116:2843-54.

Corringer, P.J., N. Le Novere, and J.P. Changeux. 2000. Nicotinic receptors at the amino acid level. *Annu Rev Pharmacol Toxicol*. 40:431-58.

Coudreuse, D.Y., G. Roel, M.C. Betist, O. Destree, and H.C. Korswagen. 2006. Wnt gradient formation requires retromer function in Wnt-producing cells. *Science*. 312:921-4.

Culetto, E., H.A. Baylis, J.E. Richmond, A.K. Jones, J.T. Fleming, M.D. Squire, J.A. Lewis, and D.B. Sattelle. 2004. The Caenorhabditis elegans unc-63 gene encodes a levamisole-sensitive nicotinic acetylcholine receptor alpha subunit. *J Biol Chem*. 279:42476-83.

Culotti, J.G., and W.L. Klein. 1983. Occurrence of muscarinic acetylcholine receptors in wild type and cholinergic mutants of Caenorhabditis elegans. *J Neurosci*. 3:359-68.

DeChiara, T.M., D.C. Bowen, D.M. Valenzuela, M.V. Simmons, W.T. Poueymirou, S. Thomas, E. Kinetz, D.L. Compton, E. Rojas, J.S. Park, C. Smith, P.S. DiStefano, D.J. Glass, S.J. Burden, and G.D. Yancopoulos. 1996. The receptor tyrosine kinase MuSK is required for neuromuscular junction formation in vivo. *Cell*. 85:501-12.

Delevoye, C., I. Hurbain, D. Tenza, J.B. Sibarita, S. Uzan-Gafsou, H. Ohno, W.J. Geerts, A.J. Verkleij, J. Salamero, M.S. Marks, and G. Raposo. 2009. AP-1 and KIF13A coordinate endosomal sorting and positioning during melanosome biogenesis. *J Cell Biol*. 187:247-64.

Dellisanti, C.D., Y. Yao, J.C. Stroud, Z.Z. Wang, and L. Chen. 2007. Crystal structure of the extracellular domain of nAChR alpha1 bound to alpha-bungarotoxin at 1.94 A resolution. *Nat Neurosci*. 10:953-62.

Dwyer, N.D., C.E. Adler, J.G. Crump, N.D. L'Etoile, and C.I. Bargmann. 2001. Polarized dendritic transport and the AP-1 mu1 clathrin adaptor UNC-101 localize odorant receptors to olfactory cilia. *Neuron*. 31:277-87.

Dziewczapolski, G., C.M. Glogowski, E. Masliah, and S.F. Heinemann. 2009. Deletion of the alpha 7 nicotinic acetylcholine receptor gene improves

cognitive deficits and synaptic pathology in a mouse model of Alzheimer's disease. *J Neurosci.* 29:8805-15.

Eimer, S., A. Gottschalk, M. Hengartner, H.R. Horvitz, J. Richmond, W.R. Schafer, and J.L. Bessereau. 2007. Regulation of nicotinic receptor trafficking by the transmembrane Golgi protein UNC-50. *EMBO J.* 26:4313-23.

Farber, S.A., M. Pack, S.Y. Ho, I.D. Johnson, D.S. Wagner, R. Dosch, M.C. Mullins, H.S. Hendrickson, E.K. Hendrickson, and M.E. Halpern. 2001. Genetic analysis of digestive physiology using fluorescent phospholipid reporters. *Science.* 292:1385-8.

Fares, H., and I. Greenwald. 2001. Regulation of endocytosis by CUP-5, the Caenorhabditis elegans mucolipin-1 homolog. *Nat Genet.* 28:64-8.

Fertuck, H.C., and M.M. Salpeter. 1976. Quantitation of junctional and extrajunctional acetylcholine receptors by electron microscope autoradiography after 125I-alpha-bungarotoxin binding at mouse neuromuscular junctions. *J Cell Biol.* 69:144-58.

Fiala, J.C. 2005. Reconstruct: a free editor for serial section microscopy. *J Microsc.* 218:52-61.

Fischer von Mollard, G., and T.H. Stevens. 1999. The Saccharomyces cerevisiae v-SNARE Vti1p is required for multiple membrane transport pathways to the vacuole. *Mol Biol Cell.* 10:1719-32.

Fleming, J.T., M.D. Squire, T.M. Barnes, C. Tornoe, K. Matsuda, J. Ahnn, A. Fire, J.E. Sulston, E.A. Barnard, D.B. Sattelle, and J.A. Lewis. 1997. Caenorhabditis elegans levamisole resistance genes lev-1, unc-29, and unc-38 encode functional nicotinic acetylcholine receptor subunits. *J Neurosci.* 17:5843-57.

Forsayeth, J.R., Y. Gu, and Z.W. Hall. 1992. BiP forms stable complexes with unassembled subunits of the acetylcholine receptor in transfected COS cells and in C2 muscle cells. *J Cell Biol.* 117:841-7.

Franch-Marro, X., F. Wendler, S. Guidato, J. Griffith, A. Baena-Lopez, N. Itasaki, M.M. Maurice, and J.P. Vincent. 2008. Wingless secretion requires endosome-to-Golgi retrieval of Wntless/Evi/Sprinter by the retromer complex. *Nat Cell Biol.* 10:170-7.

Francis, M.M., S.P. Evans, M. Jensen, D.M. Madsen, J. Mancuso, K.R. Norman, and A.V. Maricq. 2005. The Ror receptor tyrosine kinase CAM-1 is required for ACR-16-mediated synaptic transmission at the C. elegans neuromuscular junction. *Neuron.* 46:581-94.

Fridmann-Sirkis, Y., H.M. Kent, M.J. Lewis, P.R. Evans, and H.R. Pelham. 2006. Structural analysis of the interaction between the SNARE Tlg1 and Vps51. *Traffic.* 7:182-90.

Friedlander, R., E. Jarosch, J. Urban, C. Volkwein, and T. Sommer. 2000. A regulatory link between ER-associated protein degradation and the unfolded-protein response. *Nat Cell Biol.* 2:379-84.

Gally, C., S. Eimer, J.E. Richmond, and J.L. Bessereau. 2004. A transmembrane protein required for acetylcholine receptor clustering in Caenorhabditis elegans. *Nature.* 431:578-82.

Galperin, E., and A. Sorkin. 2003. Visualization of Rab5 activity in living cells by FRET microscopy and influence of plasma-membrane-targeted Rab5 on clathrin-dependent endocytosis. *J Cell Sci*. 116:4799-810.

Ganley, I.G., E. Espinosa, and S.R. Pfeffer. 2008. A syntaxin 10-SNARE complex distinguishes two distinct transport routes from endosomes to the trans-Golgi in human cells. *J Cell Biol*. 180:159-72.

Garcia, L.R., P. Mehta, and P.W. Sternberg. 2001. Regulation of distinct muscle behaviors controls the C. elegans male's copulatory spicules during mating. *Cell*. 107:777-88.

Gautam, M., P.G. Noakes, J. Mudd, M. Nichol, G.C. Chu, J.R. Sanes, and J.P. Merlie. 1995. Failure of postsynaptic specialization to develop at neuromuscular junctions of rapsyn-deficient mice. *Nature*. 377:232-6.

Gelman, M.S., W. Chang, D.Y. Thomas, J.J. Bergeron, and J.M. Prives. 1995. Role of the endoplasmic reticulum chaperone calnexin in subunit folding and assembly of nicotinic acetylcholine receptors. *J Biol Chem*. 270:15085-92.

Gendrel, M., G. Rapti, J.E. Richmond, and J.L. Bessereau. 2009. A secreted complement-control-related protein ensures acetylcholine receptor clustering. *Nature*. 461:992-6.

Geula, C., and M.M. Mesulam. 1995. Cholinesterases and the pathology of Alzheimer disease. *Alzheimer Dis Assoc Disord*. 9 Suppl 2:23-8.

Glass, D.J., D.C. Bowen, T.N. Stitt, C. Radziejewski, J. Bruno, T.E. Ryan, D.R. Gies, S. Shah, K. Mattsson, S.J. Burden, P.S. DiStefano, D.M. Valenzuela, T.M. DeChiara, and G.D. Yancopoulos. 1996. Agrin acts via a MuSK receptor complex. *Cell*. 85:513-23.

Glick, B.S., and V. Malhotra. 1998. The curious status of the Golgi apparatus. *Cell*. 95:883-9.

Gotti, C., and F. Clementi. 2004. Neuronal nicotinic receptors: from structure to pathology. *Prog Neurobiol*. 74:363-96.

Gottschalk, A., R.B. Almedom, T. Schedletzky, S.D. Anderson, J.R. Yates, 3rd, and W.R. Schafer. 2005. Identification and characterization of novel nicotinic receptor-associated proteins in Caenorhabditis elegans. *EMBO J*. 24:2566-78.

Grant, B., Y. Zhang, M.C. Paupard, S.X. Lin, D.H. Hall, and D. Hirsh. 2001. Evidence that RME-1, a conserved C. elegans EH-domain protein, functions in endocytic recycling. *Nat Cell Biol*. 3:573-9.

Gray, R., A.S. Rajan, K.A. Radcliffe, M. Yakehiro, and J.A. Dani. 1996. Hippocampal synaptic transmission enhanced by low concentrations of nicotine. *Nature*. 383:713-6.

Green, W.N., and N.S. Millar. 1995. Ion-channel assembly. *Trends Neurosci*. 18:280-7.

Gruenberg, J., and H. Stenmark. 2004. The biogenesis of multivesicular endosomes. *Nat Rev Mol Cell Biol*. 5:317-23.

Gu, M., K. Schuske, S. Watanabe, Q. Liu, P. Baum, G. Garriga, and E.M. Jorgensen. 2008. Mu2 adaptin facilitates but is not essential for synaptic vesicle recycling in Caenorhabditis elegans. *J Cell Biol*. 183:881-92.

Haas, A.K., E. Fuchs, R. Kopajtich, and F.A. Barr. 2005. A GTPase-activating protein controls Rab5 function in endocytic trafficking. *Nat Cell Biol*. 7:887-93.

Halevi, S., J. McKay, M. Palfreyman, L. Yassin, M. Eshel, E. Jorgensen, and M. Treinin. 2002. The C. elegans ric-3 gene is required for maturation of nicotinic acetylcholine receptors. *EMBO J*. 21:1012-20.

Hedgecock, E.M., J.G. Culotti, D.H. Hall, and B.D. Stern. 1987. Genetics of cell and axon migrations in Caenorhabditis elegans. *Development*. 100:365-82.

Hirst, J., S.E. Miller, M.J. Taylor, G.F. von Mollard, and M.S. Robinson. 2004. EpsinR is an adaptor for the SNARE protein Vti1b. *Mol Biol Cell*. 15:5593-602.

Ho, S.Y., K. Lorent, M. Pack, and S.A. Farber. 2006. Zebrafish fat-free is required for intestinal lipid absorption and Golgi apparatus structure. *Cell Metab*. 3:289-300.

Holmes, A., A. Flett, D. Coudreuse, H.C. Korswagen, and J. Pettitt. 2007. C. elegans Disabled is required for cell-type specific endocytosis and is essential in animals lacking the AP-3 adaptor complex. *J Cell Sci*. 120:2741-51.

Hopfield, J.F., D.W. Tank, P. Greengard, and R.L. Huganir. 1988. Functional modulation of the nicotinic acetylcholine receptor by tyrosine phosphorylation. *Nature*. 336:677-80.

Hsu, S.C., D. TerBush, M. Abraham, and W. Guo. 2004. The exocyst complex in polarized exocytosis. *Int Rev Cytol*. 233:243-65.

Huganir, R.L., A.H. Delcour, P. Greengard, and G.P. Hess. 1986. Phosphorylation of the nicotinic acetylcholine receptor regulates its rate of desensitization. *Nature*. 321:774-6.

Huganir, R.L., K. Miles, and P. Greengard. 1984. Phosphorylation of the nicotinic acetylcholine receptor by an endogenous tyrosine-specific protein kinase. *Proc Natl Acad Sci U S A*. 81:6968-72.

Ihara, S., and K. Nishiwaki. 2007. Prodomain-dependent tissue targeting of an ADAMTS protease controls cell migration in Caenorhabditis elegans. *EMBO J*. 26:2607-20.

Jahn, R., and R.H. Scheller. 2006. SNAREs--engines for membrane fusion. *Nat Rev Mol Cell Biol*. 7:631-43.

Jarosch, E., U. Lenk, and T. Sommer. 2003. Endoplasmic reticulum-associated protein degradation. *Int Rev Cytol*. 223:39-81.

Ji, D., R. Lape, and J.A. Dani. 2001. Timing and location of nicotinic activity enhances or depresses hippocampal synaptic plasticity. *Neuron*. 31:131-41.

Johannes, L., and V. Popoff. 2008. Tracing the retrograde route in protein trafficking. *Cell*. 135:1175-87.

Jospin, M., Y.B. Qi, T.M. Stawicki, T. Boulin, K.R. Schuske, H.R. Horvitz, J.L. Bessereau, E.M. Jorgensen, and Y. Jin. 2009. A neuronal acetylcholine receptor regulates the balance of muscle excitation and inhibition in Caenorhabditis elegans. *PLoS Biol*. 7:e1000265.

Kalthoff, C., S. Groos, R. Kohl, S. Mahrhold, and E.J. Ungewickell. 2002. Clint: a novel clathrin-binding ENTH-domain protein at the Golgi. *Mol Biol Cell.* 13:4060-73.

Keller, S.H., J. Lindstrom, M. Ellisman, and P. Taylor. 2001. Adjacent basic amino acid residues recognized by the COP I complex and ubiquitination govern endoplasmic reticulum to cell surface trafficking of the nicotinic acetylcholine receptor alpha-Subunit. *J Biol Chem.* 276:18384-91.

Kim, J., D.S. Poole, L.E. Waggoner, A. Kempf, D.S. Ramirez, P.A. Treschow, and W.R. Schafer. 2001. Genes affecting the activity of nicotinic receptors involved in Caenorhabditis elegans egg-laying behavior. *Genetics.* 157:1599-610.

Kimble, J.E. 1981. Strategies for control of pattern formation in Caenorhabditis elegans. *Philos Trans R Soc Lond B Biol Sci.* 295:539-51.

Kloepper, T.H., C.N. Kienle, and D. Fasshauer. 2008. SNAREing the basis of multicellularity: consequences of protein family expansion during evolution. *Mol Biol Evol.* 25:2055-68.

Koumandou, V.L., J.B. Dacks, R.M. Coulson, and M.C. Field. 2007. Control systems for membrane fusion in the ancestral eukaryote; evolution of tethering complexes and SM proteins. *BMC Evol Biol.* 7:29.

Kreienkamp, H.J., S.M. Sine, R.K. Maeda, and P. Taylor. 1994. Glycosylation sites selectively interfere with alpha-toxin binding to the nicotinic acetylcholine receptor. *J Biol Chem.* 269:8108-14.

Kubota, Y., R. Kuroki, and K. Nishiwaki. 2004. A fibulin-1 homolog interacts with an ADAM protease that controls cell migration in C. elegans. *Curr Biol.* 14:2011-8.

Kubota, Y., M. Sano, S. Goda, N. Suzuki, and K. Nishiwaki. 2006. The conserved oligomeric Golgi complex acts in organ morphogenesis via glycosylation of an ADAM protease in C. elegans. *Development.* 133:263-73.

Ladinsky, M.S., D.N. Mastronarde, J.R. McIntosh, K.E. Howell, and L.A. Staehelin. 1999. Golgi structure in three dimensions: functional insights from the normal rat kidney cell. *J Cell Biol.* 144:1135-49.

Lang, T., and R. Jahn. 2008. Core proteins of the secretory machinery. *Handb Exp Pharmacol*:107-27.

Leuzinger, W., and A.L. Baker. 1967. Acetylcholinesterase, I. Large-Scale Purification, Homogeneity, and Amino Acid Analysis. *Proc Natl Acad Sci U S A.* 57:446-451.

Lewis, J.A., C.H. Wu, H. Berg, and J.H. Levine. 1980a. The genetics of levamisole resistance in the nematode Caenorhabditis elegans. *Genetics.* 95:905-28.

Lewis, J.A., C.H. Wu, J.H. Levine, and H. Berg. 1980b. Levamisole-resistant mutants of the nematode Caenorhabditis elegans appear to lack pharmacological acetylcholine receptors. *Neuroscience.* 5:967-89.

Li, B., and J.R. Warner. 1996. Mutation of the Rab6 homologue of Saccharomyces cerevisiae, YPT6, inhibits both early Golgi function and ribosome biosynthesis. *J Biol Chem.* 271:16813-9.

Li, Y., W.G. Kelly, J.M. Logsdon, Jr., A.M. Schurko, B.D. Harfe, K.L. Hill-Harfe, and R.A. Kahn. 2004. Functional genomic analysis of the ADP-ribosylation factor family of GTPases: phylogeny among diverse eukaryotes and function in C. elegans. *FASEB J.* 18:1834-50.

Liewen, H., I. Meinhold-Heerlein, V. Oliveira, R. Schwarzenbacher, G. Luo, A. Wadle, M. Jung, M. Pfreundschuh, and F. Stenner-Liewen. 2005. Characterization of the human GARP (Golgi associated retrograde protein) complex. *Exp Cell Res.* 306:24-34.

Liu, K.S., and P.W. Sternberg. 1995. Sensory regulation of male mating behavior in Caenorhabditis elegans. *Neuron.* 14:79-89.

Lode, A., C. Paret, and G. Rodel. 2002. Molecular characterization of Saccharomyces cerevisiae Sco2p reveals a high degree of redundancy with Sco1p. *Yeast.* 19:909-22.

Loh, E., and W. Hong. 2004. The binary interacting network of the conserved oligomeric Golgi tethering complex. *J Biol Chem.* 279:24640-8.

Lowe, M., and T.E. Kreis. 1998. Regulation of membrane traffic in animal cells by COPI. *Biochim Biophys Acta.* 1404:53-66.

Lu, L., and W. Hong. 2003. Interaction of Arl1-GTP with GRIP domains recruits autoantigens Golgin-97 and Golgin-245/p230 onto the Golgi. *Mol Biol Cell.* 14:3767-81.

Margeta, M.A., G.J. Wang, and K. Shen. 2009. Clathrin adaptor AP-1 complex excludes multiple postsynaptic receptors from axons in C. elegans. *Proc Natl Acad Sci U S A.* 106:1632-7.

Martinez-Menarguez, J.A., H.J. Geuze, J.W. Slot, and J. Klumperman. 1999. Vesicular tubular clusters between the ER and Golgi mediate concentration of soluble secretory proteins by exclusion from COPI-coated vesicles. *Cell.* 98:81-90.

McBride, H.M., V. Rybin, C. Murphy, A. Giner, R. Teasdale, and M. Zerial. 1999. Oligomeric complexes link Rab5 effectors with NSF and drive membrane fusion via interactions between EEA1 and syntaxin 13. *Cell.* 98:377-86.

McKay, J.P., D.M. Raizen, A. Gottschalk, W.R. Schafer, and L. Avery. 2004. eat-2 and eat-18 are required for nicotinic neurotransmission in the Caenorhabditis elegans pharynx. *Genetics.* 166:161-9.

McMahan, U.J. 1990. The agrin hypothesis. *Cold Spring Harb Symp Quant Biol.* 55:407-18.

Medigeshi, G.R., and P. Schu. 2003. Characterization of the in vitro retrograde transport of MPR46. *Traffic.* 4:802-11.

Mello, C.C., J.M. Kramer, D. Stinchcomb, and V. Ambros. 1991. Efficient gene transfer in C.elegans: extrachromosomal maintenance and integration of transforming sequences. *EMBO J.* 10:3959-70.

Millar, N.S., and C. Gotti. 2009. Diversity of vertebrate nicotinic acetylcholine receptors. *Neuropharmacology.* 56:237-46.

Miller, S.E., B.M. Collins, A.J. McCoy, M.S. Robinson, and D.J. Owen. 2007. A SNARE-adaptor interaction is a new mode of cargo recognition in clathrin-coated vesicles. *Nature.* 450:570-4.

Mills, I.G., S. Urbe, and M.J. Clague. 2001. Relationships between EEA1 binding partners and their role in endosome fusion. *J Cell Sci.* 114:1959-65.

Mukhopadhyay, A., A.M. Barbieri, K. Funato, R. Roberts, and P.D. Stahl. 1997. Sequential actions of Rab5 and Rab7 regulate endocytosis in the Xenopus oocyte. *J Cell Biol.* 136:1227-37.

Munier-Lehmann, H., F. Mauxion, U. Bauer, P. Lobel, and B. Hoflack. 1996. Re-expression of the mannose 6-phosphate receptors in receptor-deficient fibroblasts. Complementary function of the two mannose 6-phosphate receptors in lysosomal enzyme targeting. *J Biol Chem.* 271:15166-74.

Nakagawa, T., M. Setou, D. Seog, K. Ogasawara, N. Dohmae, K. Takio, and N. Hirokawa. 2000. A novel motor, KIF13A, transports mannose-6-phosphate receptor to plasma membrane through direct interaction with AP-1 complex. *Cell.* 103:569-81.

Naor, D., S. Nedvetzki, N. Assayag, R.L. Thurmond, J.F. Huang, and E.A. Turley. 2005. The mechanism of molecular redundancy in autoimmune inflammation in the context of CD44 deficiency. *Ann N Y Acad Sci.* 1050:52-63.

Nicot, A.S., H. Fares, B. Payrastre, A.D. Chisholm, M. Labouesse, and J. Laporte. 2006. The phosphoinositide kinase PIKfyve/Fab1p regulates terminal lysosome maturation in Caenorhabditis elegans. *Mol Biol Cell.* 17:3062-74.

Nicoziani, P., F. Vilhardt, A. Llorente, L. Hilout, P.J. Courtoy, K. Sandvig, and B. van Deurs. 2000. Role for dynamin in late endosome dynamics and trafficking of the cation-independent mannose 6-phosphate receptor. *Mol Biol Cell.* 11:481-95.

Nielsen, M.S., P. Madsen, E.I. Christensen, A. Nykjaer, J. Gliemann, D. Kasper, R. Pohlmann, and C.M. Petersen. 2001. The sortilin cytoplasmic tail conveys Golgi-endosome transport and binds the VHS domain of the GGA2 sorting protein. *EMBO J.* 20:2180-90.

Nishiwaki, K., N. Hisamoto, and K. Matsumoto. 2000. A metalloprotease disintegrin that controls cell migration in Caenorhabditis elegans. *Science.* 288:2205-8.

Nishiwaki, K., Y. Kubota, Y. Chigira, S.K. Roy, M. Suzuki, M. Schvarzstein, Y. Jigami, N. Hisamoto, and K. Matsumoto. 2004. An NDPase links ADAM protease glycosylation with organ morphogenesis in C. elegans. *Nat Cell Biol.* 6:31-7.

Nordberg, A. 1994. Human nicotinic receptors--their role in aging and dementia. *Neurochem Int.* 25:93-7.

Odorizzi, G., M. Babst, and S.D. Emr. 1998. Fab1p PtdIns(3)P 5-kinase function essential for protein sorting in the multivesicular body. *Cell.* 95:847-58.

Oka, T., D. Ungar, F.M. Hughson, and M. Krieger. 2004. The COG and COPI complexes interact to control the abundance of GEARs, a subset of Golgi integral membrane proteins. *Mol Biol Cell.* 15:2423-35.

Owen, D.J., B.M. Collins, and P.R. Evans. 2004. Adaptors for clathrin coats: structure and function. *Annu Rev Cell Dev Biol.* 20:153-91.

Pan, C.L., P.D. Baum, M. Gu, E.M. Jorgensen, S.G. Clark, and G. Garriga. 2008. C. elegans AP-2 and retromer control Wnt signaling by regulating mig-14/Wntless. *Dev Cell*. 14:132-9.

Panic, B., J.R. Whyte, and S. Munro. 2003. The ARF-like GTPases Arl1p and Arl3p act in a pathway that interacts with vesicle-tethering factors at the Golgi apparatus. *Curr Biol*. 13:405-10.

Patton, A., S. Knuth, B. Schaheen, H. Dang, I. Greenwald, and H. Fares. 2005. Endocytosis function of a ligand-gated ion channel homolog in Caenorhabditis elegans. *Curr Biol*. 15:1045-50.

Pelham, H.R. 1998. Getting through the Golgi complex. *Trends Cell Biol*. 8:45-9.

Peng, H.B., L.P. Baker, and Z. Dai. 1993. A role of tyrosine phosphorylation in the formation of acetylcholine receptor clusters induced by electric fields in cultured Xenopus muscle cells. *J Cell Biol*. 120:197-204.

Perez-Victoria, F.J., and J.S. Bonifacino. 2009. Dual roles of the mammalian GARP complex in tethering and SNARE complex assembly at the trans-golgi network. *Mol Cell Biol*. 29:5251-63.

Perez-Victoria, F.J., G.A. Mardones, and J.S. Bonifacino. 2008. Requirement of the human GARP complex for mannose 6-phosphate-receptor-dependent sorting of cathepsin D to lysosomes. *Mol Biol Cell*. 19:2350-62.

Popoff, V., G.A. Mardones, S.K. Bai, V. Chambon, D. Tenza, P.V. Burgos, A. Shi, P. Benaroch, S. Urbe, C. Lamaze, B.D. Grant, G. Raposo, and L. Johannes. 2009. Analysis of articulation between clathrin and retromer in retrograde sorting on early endosomes. *Traffic*. 10:1868-80.

Port, F., M. Kuster, P. Herr, E. Furger, C. Banziger, G. Hausmann, and K. Basler. 2008. Wingless secretion promotes and requires retromer-dependent cycling of Wntless. *Nat Cell Biol*. 10:178-85.

Poulter, L., J.P. Earnest, R.M. Stroud, and A.L. Burlingame. 1989. Structure, oligosaccharide structures, and posttranslationally modified sites of the nicotinic acetylcholine receptor. *Proc Natl Acad Sci U S A*. 86:6645-9.

Prasad, B.C., and S.G. Clark. 2006. Wnt signaling establishes anteroposterior neuronal polarity and requires retromer in C. elegans. *Development*. 133:1757-66.

Presley, J.F., N.B. Cole, T.A. Schroer, K. Hirschberg, K.J. Zaal, and J. Lippincott-Schwartz. 1997. ER-to-Golgi transport visualized in living cells. *Nature*. 389:81-5.

Puertollano, R., R.C. Aguilar, I. Gorshkova, R.J. Crouch, and J.S. Bonifacino. 2001a. Sorting of mannose 6-phosphate receptors mediated by the GGAs. *Science*. 292:1712-6.

Puertollano, R., P.A. Randazzo, J.F. Presley, L.M. Hartnell, and J.S. Bonifacino. 2001b. The GGAs promote ARF-dependent recruitment of clathrin to the TGN. *Cell*. 105:93-102.

Putrenko, I., M. Zakikhani, and J.A. Dent. 2005. A family of acetylcholine-gated chloride channel subunits in Caenorhabditis elegans. *J Biol Chem*. 280:6392-8.

Ramanathan, V.K., and Z.W. Hall. 1999. Altered glycosylation sites of the delta subunit of the acetylcholine receptor (AChR) reduce alpha delta association and receptor assembly. *J Biol Chem*. 274:20513-20.

Reggiori, F., C.W. Wang, P.E. Stromhaug, T. Shintani, and D.J. Klionsky. 2003. Vps51 is part of the yeast Vps fifty-three tethering complex essential for retrograde traffic from the early endosome and Cvt vesicle completion. *J Biol Chem*. 278:5009-20.

Reynolds, E.S. 1963. The use of lead citrate at high pH as an electron-opaque stain in electron microscopy. *J Cell Biol*. 17:208-12.

Richmond, J.E., and E.M. Jorgensen. 1999. One GABA and two acetylcholine receptors function at the C. elegans neuromuscular junction. *Nat Neurosci*. 2:791-7.

Rink, J., E. Ghigo, Y. Kalaidzidis, and M. Zerial. 2005. Rab conversion as a mechanism of progression from early to late endosomes. *Cell*. 122:735-49.

Robinson, M.S. 2004. Adaptable adaptors for coated vesicles. *Trends Cell Biol*. 14:167-74.

Rojas, R., S. Kametaka, C.R. Haft, and J.S. Bonifacino. 2007. Interchangeable but essential functions of SNX1 and SNX2 in the association of retromer with endosomes and the trafficking of mannose 6-phosphate receptors. *Mol Cell Biol*. 27:1112-24.

Sandvig, K., and B. van Deurs. 2005. Delivery into cells: lessons learned from plant and bacterial toxins. *Gene Ther*. 12:865-72.

Scales, S.J., R. Pepperkok, and T.E. Kreis. 1997. Visualization of ER-to-Golgi transport in living cells reveals a sequential mode of action for COPII and COPI. *Cell*. 90:1137-48.

Schmidlin, F., O. Dery, K.O. DeFea, L. Slice, S. Patierno, C. Sternini, E.F. Grady, and N.W. Bunnett. 2001. Dynamin and Rab5a-dependent trafficking and signaling of the neurokinin 1 receptor. *J Biol Chem*. 276:25427-37.

Schmitt-John, T., C. Drepper, A. Mussmann, P. Hahn, M. Kuhlmann, C. Thiel, M. Hafner, A. Lengeling, P. Heimann, J.M. Jones, M.H. Meisler, and H. Jockusch. 2005. Mutation of Vps54 causes motor neuron disease and defective spermiogenesis in the wobbler mouse. *Nat Genet*. 37:1213-5.

Schwarz, D.G., C.T. Griffin, E.A. Schneider, D. Yee, and T. Magnuson. 2002. Genetic analysis of sorting nexins 1 and 2 reveals a redundant and essential function in mice. *Mol Biol Cell*. 13:3588-600.

Seachrist, J.L., P.H. Anborgh, and S.S. Ferguson. 2000. beta 2-adrenergic receptor internalization, endosomal sorting, and plasma membrane recycling are regulated by rab GTPases. *J Biol Chem*. 275:27221-8.

Seaman, M.N. 2004. Cargo-selective endosomal sorting for retrieval to the Golgi requires retromer. *J Cell Biol*. 165:111-22.

Seaman, M.N., E.G. Marcusson, J.L. Cereghino, and S.D. Emr. 1997. Endosome to Golgi retrieval of the vacuolar protein sorting receptor, Vps10p, requires the function of the VPS29, VPS30, and VPS35 gene products. *J Cell Biol*. 137:79-92.

Seaman, M.N., J.M. McCaffery, and S.D. Emr. 1998. A membrane coat complex essential for endosome-to-Golgi retrograde transport in yeast. *J Cell Biol.* 142:665-81.

Seguela, P., J. Wadiche, K. Dineley-Miller, J.A. Dani, and J.W. Patrick. 1993. Molecular cloning, functional properties, and distribution of rat brain alpha 7: a nicotinic cation channel highly permeable to calcium. *J Neurosci.* 13:596-604.

Setty, S.R., M.E. Shin, A. Yoshino, M.S. Marks, and C.G. Burd. 2003. Golgi recruitment of GRIP domain proteins by Arf-like GTPase 1 is regulated by Arf-like GTPase 3. *Curr Biol.* 13:401-4.

Setty, S.R., T.I. Strochlic, A.H. Tong, C. Boone, and C.G. Burd. 2004. Golgi targeting of ARF-like GTPase Arl3p requires its Nalpha-acetylation and the integral membrane protein Sys1p. *Nat Cell Biol.* 6:414-9.

Shestakova, A., E. Suvorova, O. Pavliv, G. Khaidakova, and V. Lupashin. 2007. Interaction of the conserved oligomeric Golgi complex with t-SNARE Syntaxin5a/Sed5 enhances intra-Golgi SNARE complex stability. *J Cell Biol.* 179:1179-92.

Shi, A., L. Sun, R. Banerjee, M. Tobin, Y. Zhang, and B.D. Grant. 2009. Regulation of endosomal clathrin and retromer-mediated endosome to Golgi retrograde transport by the J-domain protein RME-8. *EMBO J.* 28:3290-302.

Short, B., A. Haas, and F.A. Barr. 2005. Golgins and GTPases, giving identity and structure to the Golgi apparatus. *Biochim Biophys Acta.* 1744:383-95.

Simonsen, A., R. Lippe, S. Christoforidis, J.M. Gaullier, A. Brech, J. Callaghan, B.H. Toh, C. Murphy, M. Zerial, and H. Stenmark. 1998. EEA1 links PI(3)K function to Rab5 regulation of endosome fusion. *Nature.* 394:494-8.

Sine, S.M. 2002. The nicotinic receptor ligand binding domain. *J Neurobiol.* 53:431-46.

Siniossoglou, S., and H.R. Pelham. 2001. An effector of Ypt6p binds the SNARE Tlg1p and mediates selective fusion of vesicles with late Golgi membranes. *EMBO J.* 20:5991-8.

Siniossoglou, S., and H.R. Pelham. 2002. Vps51p links the VFT complex to the SNARE Tlg1p. *J Biol Chem.* 277:48318-24.

Smith, M.M., J. Lindstrom, and J.P. Merlie. 1987. Formation of the alpha-bungarotoxin binding site and assembly of the nicotinic acetylcholine receptor subunits occur in the endoplasmic reticulum. *J Biol Chem.* 262:4367-76.

Steger, K.A., and L. Avery. 2004. The GAR-3 muscarinic receptor cooperates with calcium signals to regulate muscle contraction in the Caenorhabditis elegans pharynx. *Genetics.* 167:633-43.

Su, M., D.C. Merz, M.T. Killeen, Y. Zhou, H. Zheng, J.M. Kramer, E.M. Hedgecock, and J.G. Culotti. 2000. Regulation of the UNC-5 netrin receptor initiates the first reorientation of migrating distal tip cells in Caenorhabditis elegans. *Development.* 127:585-94.

Sun, Y., A. Shestakova, L. Hunt, S. Sehgal, V. Lupashin, and B. Storrie. 2007. Rab6 regulates both ZW10/RINT-1 and conserved oligomeric Golgi

complex-dependent Golgi trafficking and homeostasis. *Mol Biol Cell.* 18:4129-42.

Takatsu, H., Y. Katoh, Y. Shiba, and K. Nakayama. 2001. Golgi-localizing, gamma-adaptin ear homology domain, ADP-ribosylation factor-binding (GGA) proteins interact with acidic dileucine sequences within the cytoplasmic domains of sorting receptors through their Vps27p/Hrs/STAM (VHS) domains. *J Biol Chem.* 276:28541-5.

Thomas, J.H. 1990. Genetic analysis of defecation in Caenorhabditis elegans. *Genetics.* 124:855-72.

Timpl, R., T. Sasaki, G. Kostka, and M.L. Chu. 2003. Fibulins: a versatile family of extracellular matrix proteins. *Nat Rev Mol Cell Biol.* 4:479-89.

Touroutine, D., R.M. Fox, S.E. Von Stetina, A. Burdina, D.M. Miller, 3rd, and J.E. Richmond. 2005. acr-16 encodes an essential subunit of the levamisole-resistant nicotinic receptor at the Caenorhabditis elegans neuromuscular junction. *J Biol Chem.* 280:27013-21.

Traub, L.M. 2009. Tickets to ride: selecting cargo for clathrin-regulated internalization. *Nat Rev Mol Cell Biol.* 10:583-96.

Treusch, S., S. Knuth, S.A. Slaugenhaupt, E. Goldin, B.D. Grant, and H. Fares. 2004. Caenorhabditis elegans functional orthologue of human protein h-mucolipin-1 is required for lysosome biogenesis. *Proc Natl Acad Sci U S A.* 101:4483-8.

Tribollet, E., D. Bertrand, A. Marguerat, and M. Raggenbass. 2004. Comparative distribution of nicotinic receptor subtypes during development, adulthood and aging: an autoradiographic study in the rat brain. *Neuroscience.* 124:405-20.

Tsukada, M., and D. Gallwitz. 1996. Isolation and characterization of SYS genes from yeast, multicopy suppressors of the functional loss of the transport GTPase Ypt6p. *J Cell Sci.* 109 ( Pt 10):2471-81.

Ungar, D., T. Oka, E.E. Brittle, E. Vasile, V.V. Lupashin, J.E. Chatterton, J.E. Heuser, M. Krieger, and M.G. Waters. 2002. Characterization of a mammalian Golgi-localized protein complex, COG, that is required for normal Golgi morphology and function. *J Cell Biol.* 157:405-15.

Unwin, N. 2005. Refined structure of the nicotinic acetylcholine receptor at 4A resolution. *J Mol Biol.* 346:967-89.

Verges, M., F. Luton, C. Gruber, F. Tiemann, L.G. Reinders, L. Huang, A.L. Burlingame, C.R. Haft, and K.E. Mostov. 2004. The mammalian retromer regulates transcytosis of the polymeric immunoglobulin receptor. *Nat Cell Biol.* 6:763-9.

Volpicelli, L.A., J.J. Lah, and A.I. Levey. 2001. Rab5-dependent trafficking of the m4 muscarinic acetylcholine receptor to the plasma membrane, early endosomes, and multivesicular bodies. *J Biol Chem.* 276:47590-8.

Wallace, B.G. 1994. Staurosporine inhibits agrin-induced acetylcholine receptor phosphorylation and aggregation. *J Cell Biol.* 125:661-8.

Walrond, J.P., and A.O. Stretton. 1985a. Excitatory and inhibitory activity in the dorsal musculature of the nematode Ascaris evoked by single dorsal excitatory motonerons. *J Neurosci.* 5:16-22.

Walrond, J.P., and A.O. Stretton. 1985b. Reciprocal inhibition in the motor nervous system of the nematode Ascaris: direct control of ventral inhibitory motoneurons by dorsal excitatory motoneurons. *J Neurosci.* 5:9-15.

Wanamaker, C.P., J.C. Christianson, and W.N. Green. 2003. Regulation of nicotinic acetylcholine receptor assembly. *Ann N Y Acad Sci.* 998:66-80.

Wang, H.Y., D.H. Lee, M.R. D'Andrea, P.A. Peterson, R.P. Shank, and A.B. Reitz. 2000a. beta-Amyloid(1-42) binds to alpha7 nicotinic acetylcholine receptor with high affinity. Implications for Alzheimer's disease pathology. *J Biol Chem.* 275:5626-32.

Wang, H.Y., D.H. Lee, C.B. Davis, and R.P. Shank. 2000b. Amyloid peptide Abeta(1-42) binds selectively and with picomolar affinity to alpha7 nicotinic acetylcholine receptors. *J Neurochem.* 75:1155-61.

Wang, H.Y., W. Li, N.J. Benedetti, and D.H. Lee. 2003. Alpha 7 nicotinic acetylcholine receptors mediate beta-amyloid peptide-induced tau protein phosphorylation. *J Biol Chem.* 278:31547-53.

Wang, J.M., L. Zhang, Y. Yao, N. Viroonchatapan, E. Rothe, and Z.Z. Wang. 2002. A transmembrane motif governs the surface trafficking of nicotinic acetylcholine receptors. *Nat Neurosci.* 5:963-70.

Wessler, I., H. Kilbinger, F. Bittinger, R. Unger, and C.J. Kirkpatrick. 2003. The non-neuronal cholinergic system in humans: expression, function and pathophysiology. *Life Sci.* 72:2055-61.

Whyte, J.R., and S. Munro. 2001. The Sec34/35 Golgi transport complex is related to the exocyst, defining a family of complexes involved in multiple steps of membrane traffic. *Dev Cell.* 1:527-37.

Whyte, J.R., and S. Munro. 2002. Vesicle tethering complexes in membrane traffic. *J Cell Sci.* 115:2627-37.

Wonnacott, S. 1997. Presynaptic nicotinic ACh receptors. *Trends Neurosci.* 20:92-8.

Yang, P.T., M.J. Lorenowicz, M. Silhankova, D.Y. Coudreuse, M.C. Betist, and H.C. Korswagen. 2008. Wnt signaling requires retromer-dependent recycling of MIG-14/Wntless in Wnt-producing cells. *Dev Cell.* 14:140-7.

Zarei, M.M., K.A. Radcliffe, D. Chen, J.W. Patrick, and J.A. Dani. 1999. Distributions of nicotinic acetylcholine receptor alpha7 and beta2 subunits on cultured hippocampal neurons. *Neuroscience.* 88:755-64.

Zhang, Y., B. Grant, and D. Hirsh. 2001. RME-8, a conserved J-domain protein, is required for endocytosis in Caenorhabditis elegans. *Mol Biol Cell.* 12:2011-21.

Zhdankina, O., N.L. Strand, J.M. Redmond, and A.L. Boman. 2001. Yeast GGA proteins interact with GTP-bound Arf and facilitate transport through the Golgi. *Yeast.* 18:1-18.

Zolov, S.N., and V.V. Lupashin. 2005. Cog3p depletion blocks vesicle-mediated Golgi retrograde trafficking in HeLa cells. *J Cell Biol.* 168:747-59.

# Supplementary materials (by Dr. Stefan Rensing)


**Initial tree**

The full alignment of the members of the PFAM Vps51 (PF08700, http://pfam.sanger.ac.uk/family?entry=PF08700 ) family was retrieved and a neighbour-joining (NJ) phylogenetic tree reconstructed. The *Caenorhabditis elegans* Vps51 (FFR_CAEEL), together with the functional orthologs from yeast (COG1_YEAST) and human (FFR_HUMAN) were found to be present in a monophyletic clade, albeit without botstrap support (Fig. 1). All other sequences annotated as FFR (fat-free homolog) were also present in that clade. To reduce the dataset to the functional Vps51 ortholog group, all member sequences from the monophyletic Vps51 clade were selected, except if they presented redundant versions of the same sequence (identical sequences from different organisms were kept). To provide a suitable outgroup, all sequences annotated as EXO (exocyst complex component) were also selected (Fig. 1).


**Detailed phylogenetic analyses**

Based on this refined dataset, in-depth phylogenetic inference was carried out. Using ProtTest (Abascal et al., 2005), the most suitable model was found to be JTT+G+F. Phylogenetic trees were inferred by NJ using quicktree_sd (Howe et al., 2002; Frickenhaus and Beszteri, 2008) with 1000 bootstrap resamplings, maximum likelihood (ML, Phyml as implemented in ProtTest) and Bayesian inference using MrBayes (Ronquist and Huelsenbeck, 2003) with eight gamma distributed rate categories, the JTT+G+F model and five million generations (not dropping below at a standard deviation of 0.07). Trees were displayed using Figtree v1.2.2 (http://tree.bio.ed.ac.uk/software/figtree/ ).

In both the NJ (Fig. 2) and BI tree, the majority of EXO sequences is present in a long-branched clade that was used to root the tree. In both cases, The *C. elegans* and *Dictyostelium discoideum* sequences are not part of that clade, but branch of basal within the Vps51 clade. The majority of nodes is not well

supported. The metazoan FFR clade has low bootstrap support in the NJ tree (Fig. 2) and contains some sequences from protists. In the BI analysis, the metazoan clade is well supported and does not contain protist sequences. However, it lacks the *C. elegans* and *C. briggsae* sequences. The high divergence of the domain makes confident phylogenetic inference impossible. The lack of support for the majority of branches is most probably due to long branch effects.

In order to overcome these problems and to analyse the metazoan FFR clade in mode detail, a full length alignment of these sequences was constructed using M.A.F.F.T. (Katoh et al., 2005), using the *D. discoideum* FFR sequence as an outgroup. Visual inspection of the alignment using Jalview (Clamp et al., 2004) demonstrated a high quality alignment with no need for manual refinement. The BI tree fulfilled the convergence criterion (average standard deviation of split frequencies < 0.01) after only 101,000 generations; the support for the majority of nodes is good (Fig. 3). In general, the tree resolves the taxonomy; the flies (Diptera) are very well supported, as are the bony vertebrates (Euteleostomi, including the mammals, frogs, birds and fishes). The clade that is monophyletic with these both groups contains Coelomata, Cnidaria and Placozoa; the *Ixodes scapularis* (Black-legged tick) sequence is apparently difficult to place, probably due to its long branch. The two basal branches contain the Pseudocoelomata (the two *Caenorhabditis* sequences) and the Acoelomata. The somewhat lesser amount of support for the lower branches is probably due to the fact that most taxonomic groups are represented by a single sequence only.

**Sequence length and domain structure**

The average length of the metazoan FFR/Vsp51 proteins is 729 residues (shortest sequence 261, longest sequence 917). It should be noted that a large proportion of the sequences are predicted (Fig. 3), lacking transcript or protein evidence, so that parts might be missing; in addition, there are two sequences annotated as being fragmentary. Prime candidates for incomplete sequences are those from *Branchiostoma floridae* (261), *Trichoplax adhaerens* (495) and *Ixodes*

*scapularis* (545)*,* especially as the sequences from the Acoelomata and Pseudocoelomata are longer. The longest sequence is from the outgroup, the Mycetozoan *D. discoideum*.

Motif discovery on the dataset was carried out using MEME v4.3.0 (Bailey et al., 2009). Settings (distribution of motif occurrences: zero or one per sequence, number of different motifs: ten, minimum motif width: six, maximum motif width: thirty) were chosen based on visual inspection of the alignment. The detected motif 1 (Fig. 4) covers positions 38-67 of the PFAM Vps51 HMM, representing the most highly conserved core of the domain. The presence of the motifs 1, 7 and 8 in the N-terminal part of all proteins is the unifying factor, this region represents the Vps51 core domain. Motif 9, N-terminal of this arrangement, is present in all but two sequences (*Nematostella vectensis* and *T. adhaerens*). Motif 4, C-terminal of the core block, is present in all sequences but the *C. elegans* Vps51. It is apparent from the motif arrangement that the exceptional length of the *D. discoideum* sequence is due to an N-terminal extension.

The middle region of the proteins contains some occurences of motifs out of their canonic place. Specifically, motif 7 in (two *Drosophila* sequences and in *D. discoideum*) has a shifted location and motifs 1 (*Caenorhabditis*), 2 (chicken), 6 (mouse) and 9 (*Aedes aegypti*) appear as duplicates within the same sequence. The obviously secondarily derived arrangements make a certain plasticity of the genes evident.

Located C-terminal of the middle region are motifs 10 (present in all but four sequences) and 3 (present in all but three sequences). The pattern of presence and absence suggests that these motifs were secondarily lost from the different lineages, including a common ancestor of the genus Caenorhabditis. Motif 7, immediately behind 3, is present in this place in mammals and amphibians only. Given the dissipate pattern described for this motif above, it appears plausible that it was transferred to this location in the last common ancestor of tetrapods and secondarily lost in birds.

The immediate C-terminus consists of the motifs 5, 2 and 6. These motifs are present in all sequences but three (*T. adhaerens*, *Ixodes scapularis* and *B.*

*floridae*), resp. motif 6 lacking from *Schistosoma mansonii*. Again, the presence/absence pattern in light of the taxonomy suggests secondary losses of these motifs from the respective lineages. However, given that the three sequences lacking all these motifs are the shortest ones present, it might also be possible that the gene prediction is incomplete.

Taken together, the presence of the conserved core domain located in the N-terminal part of the protein is expected to be crucial for ist function. The additonal motifs might be necessary for interactions or functions that are not obligatory. The C-terminal set of motifs might also be important, pending closer study of the genomic loci within those organisms that seem to lack them.
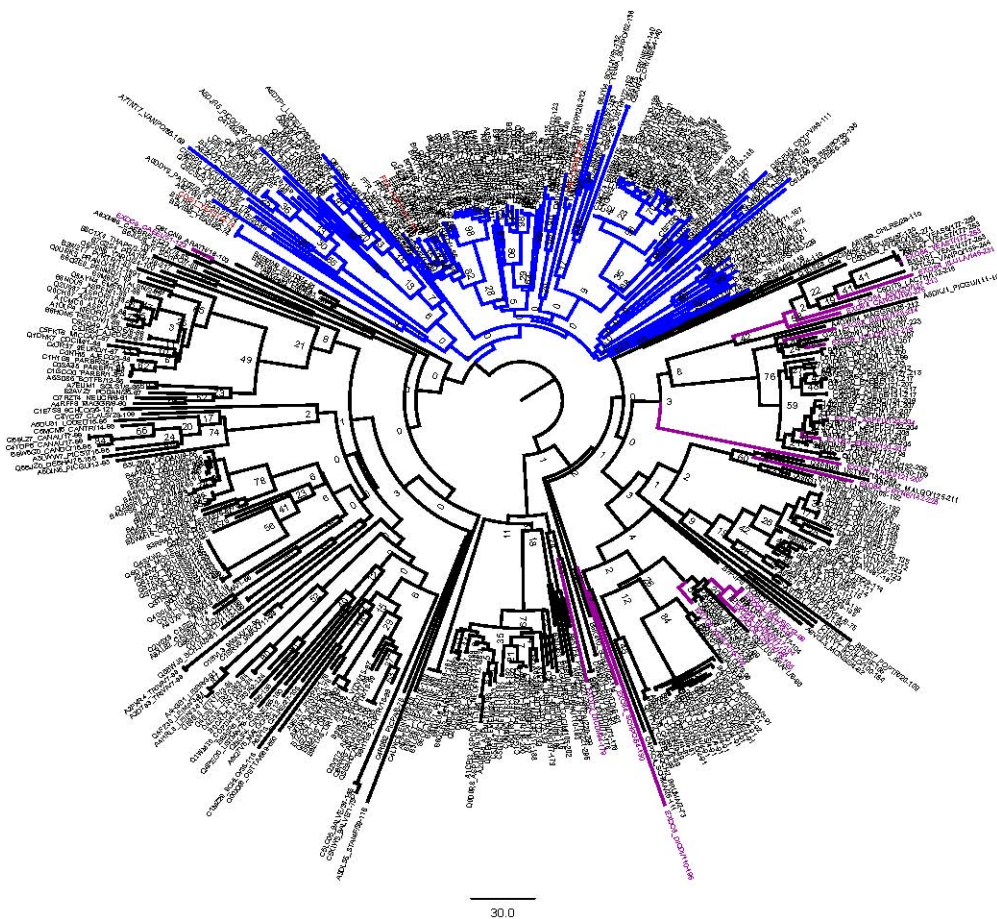


**Fig. 1: NJ tree based on the PFAM Vps51 full alignment.**
Blue: monophyletic clade containing *C. elegens* Vps51 and the functional orthologs from yeast and human (shown in red). Magenta: sequences annotated as EXO. The tree was midpoint rooted. Numbers at nodes represent results from 1000x bootstrap resampling.
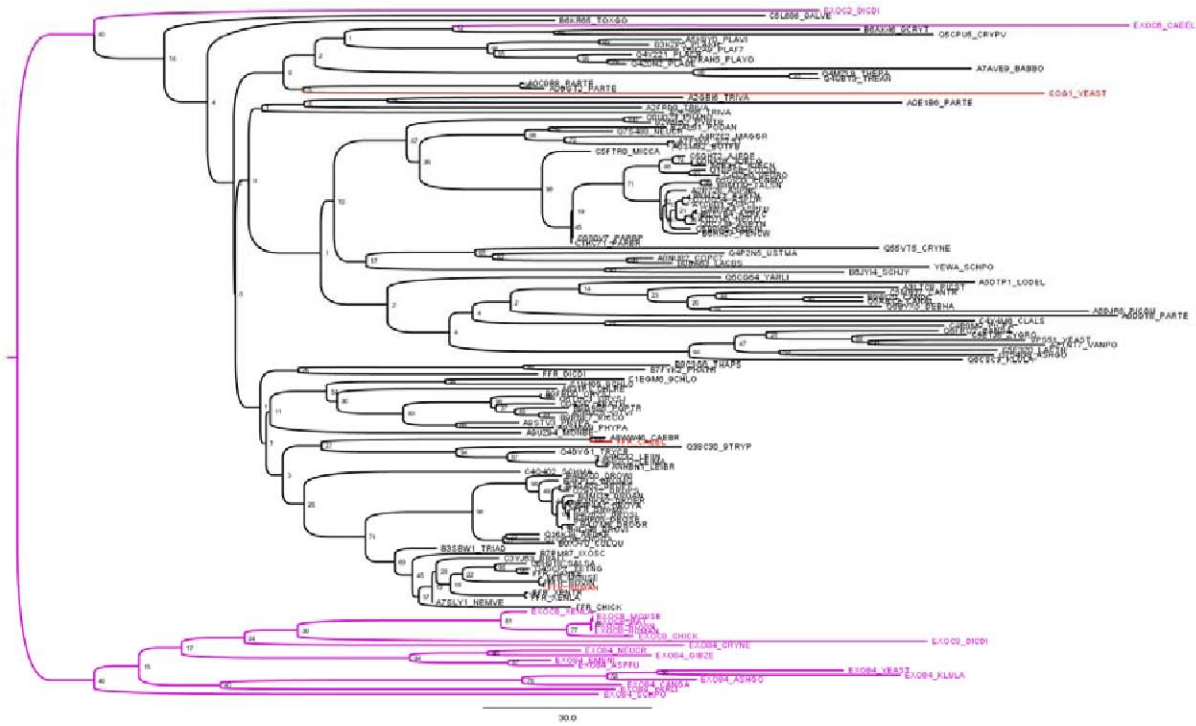
**Fig. 2: NJ tree based on the Vps51 functional ortholog group**
Red and magenta (EXO) coloring as in Fig. 1. The tree was rooted at the branch leading to the majority of EXO sequences.
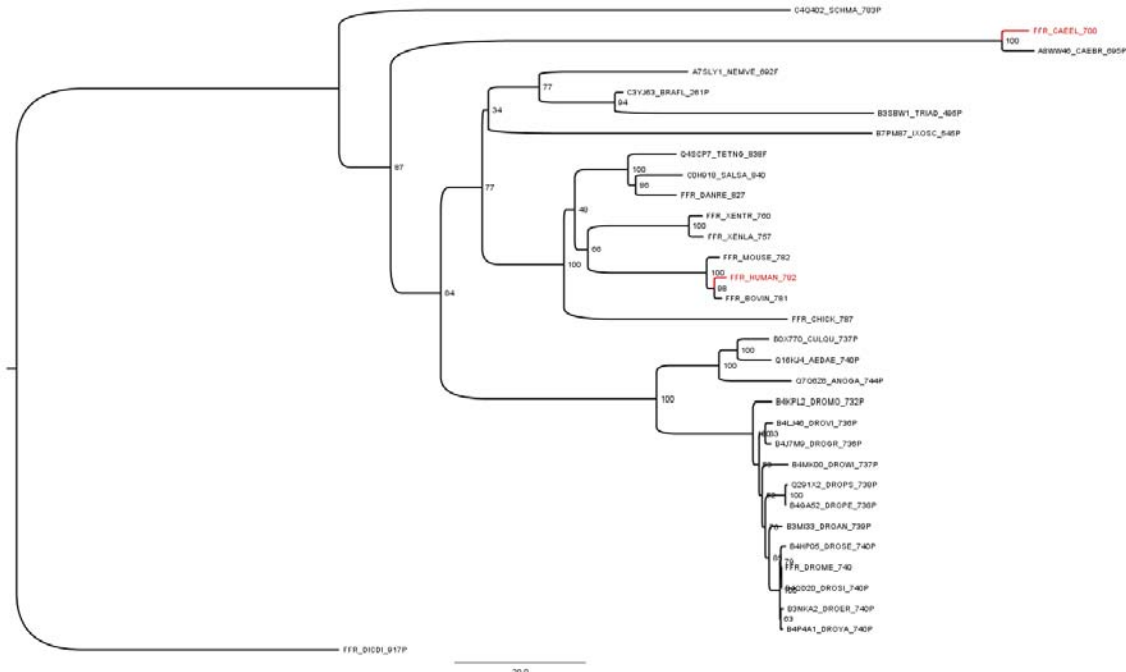


**Fig. 3: BI tree of the metazoan FFR clade**
Red coloring as in Fig. 1. The tree was rooted at the branch leading to the *D. dicoideum* FFR sequence (outgroup). Numbers at the branches are posterior probabilities. The length of each sequence is shown, separated from the accession number by an underscore. Sequences annotated as fragmentary are marked with a tailing „F", sequences annotated as predicted with a
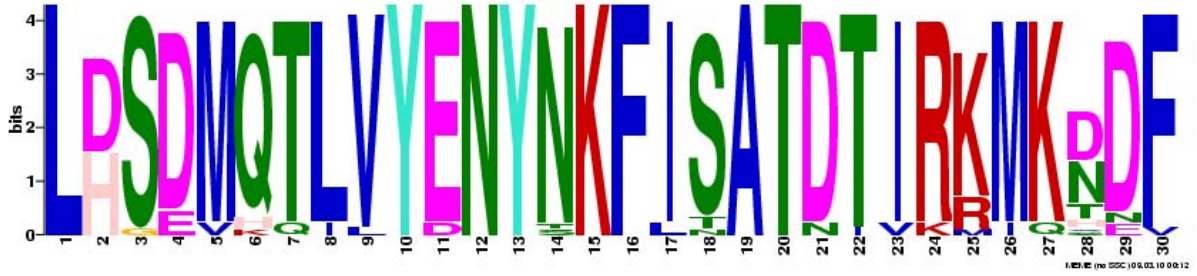
„P".



**Fig. 4: Motif covering the most conserved part of the Vps51 domain**
Sequence logo of MEME-detected motif one, overlapping with the most conserved part of the
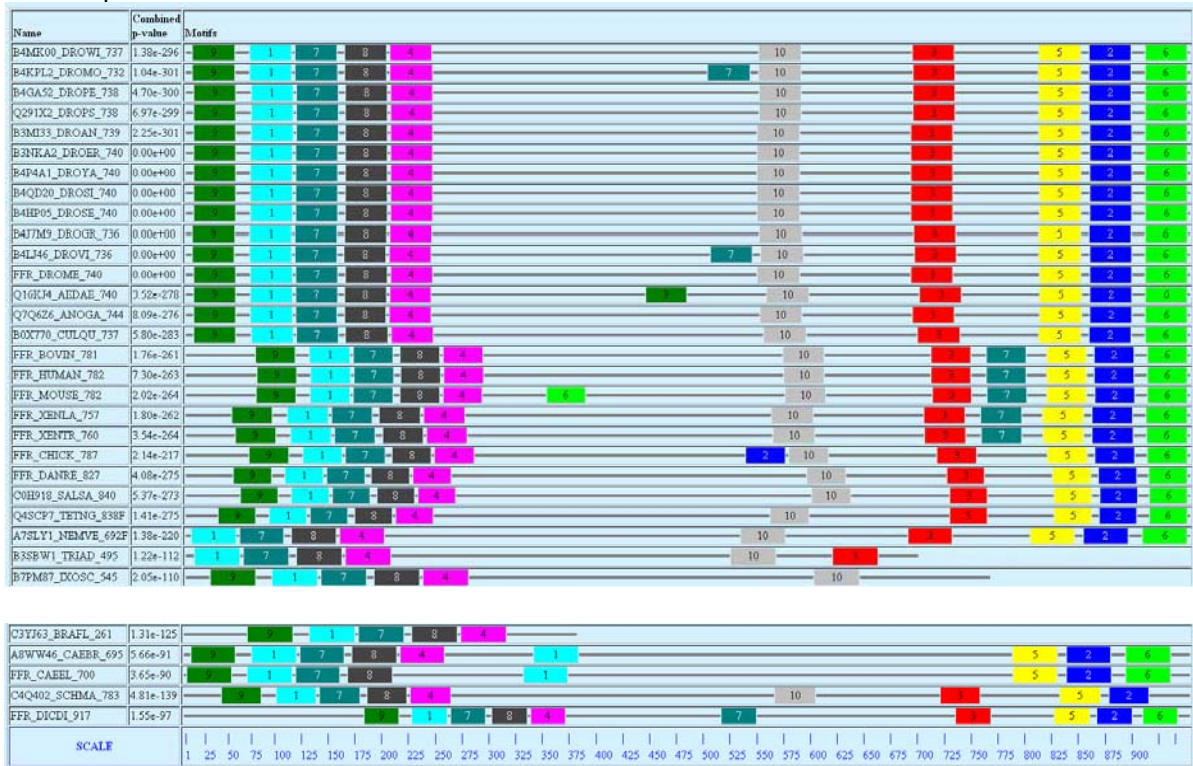PFAM Vps51 HMM.



**Fig. 5: Motifs detected in the metazoan Vps51 sequences**
MEME-detected motifs are shown as a block diagram. Sequences are ordered by phylogeny,
from top to down: flies, mammals, frogs, birds, fishes, (Coelomata, Cnidaria, Placozoa),
Pseudocoelomata, Acoelomata, Mycetozoa (outgroup).

## Literature cited

**Abascal F, Zardoya R, Posada D** (2005) ProtTest: selection of best-fit models of protein evolution. Bioinformatics **21:** 2104-2105

**Bailey TL, Boden M, Buske FA, Frith M, Grant CE, Clementi L, Ren J, Li WW, Noble WS** (2009) MEME SUITE: tools for motif discovery and searching. Nucleic Acids Res **37:** W202-208

**Clamp M, Cuff J, Searle SM, Barton GJ** (2004) The Jalview Java alignment editor. Bioinformatics **20:** 426-427

**Frickenhaus S, Beszteri B** (2008) Quicktree-SD, Software developed by AWI-Bioinformatics. *In*,

**Howe K, Bateman A, Durbin R** (2002) QuickTree: building huge Neighbour-Joining trees of protein sequences. Bioinformatics **18:** 1546-1547

**Katoh K, Kuma K, Toh H, Miyata T** (2005) MAFFT version 5: improvement in accuracy of multiple sequence alignment. Nucleic Acids Res **33:** 511-518

**Ronquist F, Huelsenbeck JP** (2003) MrBayes 3: Bayesian phylogenetic inference under mixed models. Bioinformatics **19:** 1572-1574